Titre: Title:	Solvothermal Debromination of Commercial End-of-Life Styrenic Polymer (ABS and HIPS)
Auteur: Author:	Mario Ferreiro Gonzalez
Date:	2025
Type:	Mémoire ou thèse / Dissertation or Thesis
Référence: Citation:	Ferreiro Gonzalez, M. (2025). Solvothermal Debromination of Commercial End-of-Life Styrenic Polymer (ABS and HIPS) [Ph.D. thesis, Polytechnique Montréal]. PolyPublie. https://publications.polymtl.ca/67854/

POLYTECHNIQUE MONTRÉAL
affiliée à l'Université de Montréal

Solvothermal Debromination of Commercial End-of-Life Styrenic Polymer (ABS and HIPS)

MARIO FERREIRO GONZALEZ
Département de génie chimique

Thèse présentée en vue de l'obtention du diplôme de *Philosophiæ Doctor*
Génie chimique

Août 2025

POLYTECHNIQUE MONTRÉAL
affiliée à l'Université de Montréal

Cette thèse intitulée :

Solvothermal Debromination of Commercial End-of-Life Styrenic Polymer (ABS and HIPS)

présentée par **Mario FERREIRO GONZALEZ**
en vue de l'obtention du diplôme de *Philosophiæ Doctor*
a été dûment acceptée par le jury d'examen constitué de :

Moncef CHIOUA, président
Gregory PATIENCE, membre et directeur de recherche
Oumarou SAVADOGO, membre
Charles BRUEL, membre externe

DEDICATION

Dedicated to my parents who always supported me,
to my all my friends and family,
specially those who are no longer with us,
and to Gregory, whose unwavering support made this possible.
. . . Nuk Re . . .

ACKNOWLEDGEMENTS

It has been a journey...

I have to thank Gregory again; it has been an honor to work with him at Polytechnique. I will be forever grateful for all the support and trust he has provided, especially in my worst moments, and for his encouragement and dedication, which made this thesis possible. I have the doubtful privilege of having lived through a pandemic during this adventure, which I believe taught us all an important lesson: to be grateful.

So I am grateful to all the friends that I made at Poly. It was an amazing experience. Yet, I would like to give a special thanks to Tugce for being a real friend and suffering with me through transport phenomena; this adventure would not have been the same without you. To Olivier, a great friend who is missed, but one of those instant friendships seeded in random conversations about games and history with local beers. I also would like to thank all the team at Poly, from the technicians to administrative staff, who made Polytechnique a great place to study and work. Outside of Poly, my Canadian adventure brought great people into my life. In particular, Yacine and Christelle, you made my life there great. I would like to express my deepest gratitude to my parents, who have always been supportive and caring; I am incredibly lucky to have them. This is also extended to the rest of my family (Soler, Gonzalez y Ferreiro). My thoughts are also with my uncle Antonio, who would have been very proud and who is a constant inspiration to me as a person. To all my friends who made me who I am and who have been there for me, Ignacio, I nigo, Dani, Elvira, Lucia, Chercho, Harmario, Carlota, Balbu, Lolo, Manu (que bien lo pasamos por aquí jaja), Nano, etc., so many to name all of them, but all important. Finally, to Diegoncho. Chamaco, I hope this inspires you to great things in life and that you appreciate it fully. Special thanks to Marta and Elena for being incredible and a part of this Montreal adventure.

...Thanks to you all

RÉSUMÉ

L'inquiétude croissante concernant les retardateurs de flamme bromés (RFB) s'accroît. Leur efficacité en tant qu'inhibiteurs de flamme, leur stabilité thermique et leur compatibilité avec les polymères en ont fait le principal retardateur de flamme dans de nombreuses applications . Les RFB ont été utilisés dans les plastiques des équipements électriques et électroniques (EEE) depuis le début des années 1970, avec les bisphénols polybromés (PBB). Les PBB ont été progressivement éliminés (volontairement par l'industrie) peu après en raison de l'incident survenu sur les Grands Lacs, où du bétail et des personnes ont été empoisonnés après avoir confondu le retardateur de flamme avec un additif alimentaire pour animaux. Cependant, la nécessité de se conformer aux réglementations anti-incendie a poussé à développer d'autres composés bromés tels que les polybromobiphényles (PBB), les polybromodiphényléthers (PBDE) et le tétrabromobisphénol A (TBBPA). Ces composés ont dominé le marché et ont été ajoutés à la plupart des thermoplastiques utilisés dans l'industrie des EEE. Malheureusement, ces nouveaux RFB sont également considérés comme des polluants persistants (POP), toxiques et perturbateurs du système endocrinien. Actuellement, ils sont progressivement éliminés et leur utilisation est limitée, de nombreuses réglementations dans le monde entier tentant de réduire leur présence dans les plastiques. Les équipements EEE ayant une durée de vie moyenne de 8 ans, de nombreux plastiques mis sur le marché arrivent actuellement en fin de vie. Il existe donc un stock important (13 500 kt de WEEE en 2021, selon l'UE) de plastique qu'il n'est pas possible de recycler en raison de la forte concentration de RFB. Pour aggraver la situation, la Chine et la Malaisie ont interdit l'importation de DEEE, perturbant ainsi le flux de résidus plastiques présents. L'élimination de ces RFB de ce plastique en fin de vie permettrait aux entreprises de recyclage de valoriser ce déchet au lieu de l'enfouir et de réduire ainsi son impact sur l'environnement. L'intérêt pour l'utilisation de ces plastiques a conduit à une étude croissante des stratégies de débromation possibles. L'hétérogénéité des plastiques concernés, des types de retardateurs de flamme et des méthodes d'incorporation a fait de la récupération d'énergie l'objectif principal de la recherche.

Comme le Groupe Lavergne, notre partenaire industriel, est une entreprise qui se consacre au recyclage mécanique des plastiques, notre approche consistait à obtenir une méthode de débromation aussi proche que possible des méthodes conventionnelles. Nous avons décidé qu'une méthode solvothermique de débromation serait la meilleure option, car elle nécessitera moins de traitement chimique et de gestion que le recyclage chimique pur. En outre, cette méthode permet d'adapter facilement les équipements déjà utilisés pour le recyclage mécanique. Dans un premier temps, nous nous sommes efforcés de nous assurer que la

détermination de la teneur en Br par fluorescence X (XRF) était fiable. Nous avons certifié la précision à l'aide d'étalons et les avons comparés aux résultats obtenus par l'analyse par activation neutronique (ANA). L'analyse par activation neutronique a confirmé que nos résultats étaient exacts et que la fluorescence X est une technique fiable pour déterminer la teneur en brome, même dans une matrice polymère de quelques millimètres d'épaisseur. Nous nous sommes concentrés sur les deux principaux polymères présents dans les WEEE, l'acrylonitrile-butadiène-styrène (ABS) et le polystyrène/polystyrène à haut impact (PS/HIPS). Pour le traitement, nous avons sélectionné deux milieux, l'éthylène glycol (EG) et le triéthylène glycol (TEG).

Ces solvants ont des points d'ébullition élevés, ce qui permet de travailler à des températures élevées sans devoir recourir à la pression (qui endommage les chaînes de polymères), et peuvent dissoudre soit KOH soit NaOH, les réactifs. Le procédé a fonctionné entre 160 et 230 °C pour le HIPS et entre 160 et 190 °C pour l'ABS. Le traitement du HIPS a permis d'obtenir une débromation de 99 %. Au lieu de broyer le polymère en fines particules, nous l'avons extrudé en un filament fin pour le comparer à des morceaux de déchets plastiques typiques. Les morceaux de plastique de 60 mm ont mis entre 4 et 24 h pour réagir, alors que lorsque le polymère a été transformé en filaments d'environ 3 mm de diamètre, il a réagi en moins de 5 min. Le traitement solvothermique à l'ABS a également permis d'obtenir une débromation de plus de 95 %. Nous avons constaté que la dénitrification se produit, jusqu'à 30 %, au cours de ce traitement, mais que les propriétés du polymère restent largement inchangées. Une augmentation de la température de transition vitreuse d'environ 10 °C est associée à la dénitrification du polymère. Le XRF détecte la présence de Br et Sb dans le solvant après le traitement, mais aucun composé organique provenant du backbe de FR n'a été détecté lors de l'analyse GC-MS. Nous démontrons donc la viabilité de cette méthode pour débromer l'ABS et le HIPS, en récupérant Br et Sb sans générer de sous-produits et avec un impact minimal sur la structure du polymère (en particulier sur le HIPS/PS).

ABSTRACT

The increasing concern regarding brominated fire retardant (BFr) is growing. Their efficacy as flame inhibitors, thermal stability, and compatibility with polymers made them the main fire retardant in multiple applications. BFRs were used in electric and electronic equipment (EEE) plastics since the beginning of the 1970s, with the polybrominated bisphenols (PBBs). The PBBs were phased out (voluntarily by the industry) soon after due to the incident on the Great Lakes, where livestock and people were poisoned when they confused the fire retardant with an animal food additive. However, the need to comply with fire regulations pushed the development of other brominated compounds such as polybrominated biphenyls (PBBs), polybrominated diphenyl ethers (PBDEs), and tetrabromobisphenol A (TBBPA). These compounds dominated the market and were added to most of the thermoplastics used in the EEE industry. Unfortunately, these new BFRs are also considered persistent pollutants (POPs), toxic, and disrupt endocrine systems. Currently, they are being phased out and their use is being limited, with multiple regulations around the world trying to reduce their presence in plastics. With EEE equipment having an average market life of 8 years, many of the plastics released to the market are currently reaching their end-of-life. Thus, there is a large stock (13,500 kt of WEEE in 2021, according to the EU) of plastic that is not possible to recycle due to the high concentration of BFRs. To worsen the situation, China and Malaysia have banned the importation of WEEE, disrupting the flow of plastic residue present. Removing these BFRs from this end-of-life plastic would allow recycling companies to valorize this waste instead of land-filling and thus reduce its environmental impact. The interest in using these plastics has led to an increasing study of possible debromination strategies. The heterogeneity of the plastics involved and the fire retardant types and incorporation methods made energy recovery the main target of the research.

Since Lavergne Group Inc., our industrial partner, is a company focused on mechanically recycling plastics, our approach was to obtain a debromination method as close as possible to conventional methods. We decided that a solvothermal method to debrominate would be the best option, since it will require lower chemical treatment and management than pure chemical recycling. Additionally, this method allows an easy adaptation of equipment already in use in mechanical recycling. In an initial stance, we worked to ensure that the determination of the Br content using X-ray fluorescence (XRF) is reliable. We certified the accuracy with standards and compared them with the results obtained by neutron activation analysis (NAA). NAA confirmed that our results were accurate and that XRF is a reliable

technique to determine bromine content, even in a polymeric matrix of a few millimeters thick. We focused on the two main polymers present in WEEE, acrylonitrile-butadiene-styrene (ABS) and polystyrene/high impact polystyrene (PS/HIPS). For the treatment, we selected two media, ethylene glycol (EG) and triethylene glycol (TEG).

These solvents have high boiling points, allowing work at high temperatures without the need to use pressure (that damages the polymer chains), and can dissolve either KOH or NaOH, the reactants. The process operated between 160 to 230 °C for HIPS and 160 to 190 °C for ABS. HIPS treatment achieved a debromination of 99%. Instead of grinding the polymer to fine particles, we extruded it into a thin filament to compare with typical plastic scrap pieces. 60 mm plastic chunks took up to between 4 to 24 h to react, while when the polymer was transformed into filaments of around 3 mm in diameter, it reacted in less than 5 min. ABS solvothermal treatment also achieved more than 95% debromination. We found that denitrification happens, up to 30%, during this treatment, but the thermochemical polymer properties remain largely unchanged. An increase in the glass transition temperature of approximately 10 °C is associated with the polymer denitrification. XRF detects the presence of Br and Sb in the solvent after the treatment, but no organic compounds from FR's backbone were detected with GC-MS analysis. We, therefore, demonstrate the viability of this method to debrominate ABS and HIPS, recovering Br and Sb without the generation of by-products and with minimal impact to the polymer structure (especially to HIPS/PS).

TABLE OF CONTENTS

LIST OF TABLES

LIST OF FIGURES

LIST OF SYMBOLS AND ACRONYMS

ABS	Acrylonitrile Butadiene Styrene
BFR	Brominated Flame/Fire Retardant
Br-HIPS	Brominated High Impact Polystyrene
Br-ABS	Brominated Acrylonitrile Butadiene Styrene
Br-PC/ABS	Brominated Polycarbonate/Acrylonitrile Butadiene Styrene Blend
CAGR	Compound Annual Growth Rate
FTIR	Fourier-Transform Infrared Spectroscopy
GPPS	General-Purpose Polystyrene
GC	Gas Chromatography
HIPS	High Impact Polystyrene
HPLC	High Performance Liquid Chromatography
IC	Ion Chromatography
MS	Mass Spectrometer
PS	Polystyrene
PC	Polycarbonate
PBBs	Polybrominated Biphenyls
TBBPA	Tetrabromobisphenol A
PBDEs	Polybrominated Diphenyl Ethers
TGA	Thermogravimetric Analysis
XRF	X-Ray Fluorescent
WEEE	Waste Electric and Electronic Equipment
EEE	Electric and Electronic Equipment

LIST OF APPENDICES

CHAPTER 1 INTRODUCTION

1.1 Background and problem identification

When, in the second half of the nineteenth century, Parkes and then Hyatt produced the first thermoplastic by adding camphor to cellulose nitrate (in this case modifying a natural polymer), it was difficult to unveil the revolution that was about to happen. The first thermoset synthetic polymer, known as Bakelite—a phenol-formaldehyde—was synthesized in 1907. Styrene was first synthesized in 1831, but it was almost a hundred years later, in 1911, when practical uses for it started to be considered [15]. Shortly before the Second World War, the expansion of knowledge in chemistry, physics, and engineering merged to create the chemical engineering discipline in synergy with accessible and cheap oil, boosted the petrochemical industry and its derivatives, polymers among them [16].

Steadily, polymers spread to all areas of our lives. Fueled by an increased number of synthetic polymers with a wide range of properties, economical compared with traditional alternatives, and improved manufacturing processes, plastics became the perfect material for many applications and created new ones (plastics can be sprayed, molded, used as paint, glue, etc.) [16, 17].

Plastic success is indisputable, to the extent that many scholars refer to our time as "The plastic age". With more than 20 groups of plastics, with grades, sub-grades, blends, and additives, plastics are a fundamental part of our industrial society. But its success comes with a price: the environmental burden. Their excellent properties and chemical stability also made them persistent pollutants due to their low biodegradability. Waste management and recycling of plastics started to be a concern in the middle of the 20th century, and by the end of the century, legislators started to pass laws to control plastic waste and promote recycling. Nowadays, plastic pollution is among one of the main environmental concerns with worldwide initiatives to track it, improve its management, and find more sustainable alternatives such as biopolymers [16, 17].

The combustible nature of polymers, their spread in modern societies, and their integration in almost any electric and electronic equipment (EEE) resulted in a fire hazard. To remove or reduce the risk, several regulations were forced requiring these plastics to possess some type of fire resistance depending on their final application. Fire safety standards for EEE thermoplastics focus on material flammability and fire hazard testing. UL 94 classifies plastics by their burning characteristics (HB, V-0, V-1, V-2). Glow-wire tests (IEC 60695-2-10/–2-12)

simulate ignition by overheated conductors. Flame-impingement (IEC 60695-11-5) and cable propagation (IEC 60332-1-2) methods to determine flame spread, complemented by smoke density (EN 61034-2) and oxygen-index (ASTM D2863) measurements. Polymeric material evaluations (UL 746C) and consolidated safety requirements in IEC 62368-1 and the EU Low Voltage Directive (2014/35/EU) ensure that design and construction limit fire risk [18–24].

To comply with all these new regulations and tests, most of the polymers used in EEE are additivated with fire retardants. Of these fire retardants, the brominated ones are the predominant ones due to their efficacy, economy, and polymer compatibility. In 2023, the brominated fire retardant BFR market was 2.18 billion USD. and it is predicted to grow at 6% per year to reach 3.77 billion USD[25].

Brominated flame retardants are organic compounds with varying numbers of bromine atoms bonded to an organic compound. The most extensively produced are polybrominated biphenyls (PBBs), polybrominated diphenyl ethers (PBDEs), and tetrabromobisphenol A (TBBPA). They form by substituting hydrogen atoms on the organic backbone with three to ten bromine atoms. However, owing to ecological concerns, PBBs are being phased out and being supplanted by PBDEs and TBBPA [26]. New regulations limit the presence of these brominated compounds in plastics, impeding the use of a large plastic feedstock to be recycled. Currently, most of these plastics are being landfilled or, when possible, used as fuel[1]. With increasing numbers of brominated EEE plastic reaching their end-of-life, it is crucial to develop a process able to remove bromine and produce a clean feedstock to recycle, thus solving two problems at the same time. Removing brominated fire retardants from the environment and increasing recycling ratios. The debromination process should, ideally, be able to pair with traditional mechanical recycling, so The Lavergne Group Inc., our industrial partner and origin of this research project, could implement it on their facilities. The Lavergne Group Inc., a Quebecois plastic recycling company, specializes in selling resins from end-of-life plastics. The company currently has several kilotons of brominated plastic, mostly acrylonitrile butadiene styrene (ABS) and high impact polystyrene (HIPS) that cannot be recycled due to their bromine content. To overcome this situation, we identified a feasible approach That would merge some advantages of the chemical recycling processes But without their main limitations. An alkaline solvothermal process that removes bromine from the polymers. With independence of the BFR and the addition type (bonded or not to the polymer chain), using non-toxic, available, and inexpensive chemicals such as ethylene glycol and potassium hydroxide. This method can recover bromine and antimony from the polymers and allow further mechanical recycling with minimal impact on the polymer properties.

1.2 Research Objectives

The main goal of this project is to develop and characterize a process to safely remove bromine from end-of-life styrenic polymer (HIPS and ABS) while ensuring their further recyclability. We set three main scientific objectives that are published or in the process of being published in scientific journals. Additionally, this work has produced a declaration of invention with a patent in progress.

1. Demonstrate that X-ray fluorescence spectroscopy as a reliable and fast method to analyze bromine content in WEEE HIPS and ABS, while describing the elemental composition of these plastics. The results are published in The Canadian Journal of Chemical Engineering (CJCE). To this day (July 2025), this article has been included in the Top 15 articles published in the CJCE in 2024 ([27]), and in a virtual issue: "Exploring themes: Top-viewed articles from across chemical engineering," and is currently the third most-read paper of the last two years.

    - Prove the reliability of XRF measuring plastics of different sizes.
    - Define the best sample preparation, analytical method for analysis.
    - Determine elemental content of end-of-life plastics, determining the content of metals and other elements (rather than Br or Sb)

2. Perform a solvothermal debromination of commercial end-of-life polystyrene/high impact polystyrene. The results are published in Recycling (MDPI) a journal with a Current Impact Factor of 4.6.

    - Determine the best debromination conditions.
    - Characterization of the polymer before and after the treatment to ensure its further recyclability.
    - Study kinetics, diffusion and thermal degradation models.

3. Solvothermal debromination of commercial end-of-life acrylonitrile butadiene styrene polymer. The results are being review in Chemical Engineering Journal Advances (ELSEVIER) a journal with a Current Impact Factor of 7.1. The article is currently on preprint format at SSNN

    - Determine the best debromination conditions.
    - Characterization of the polymer before and after the treatment to ensure its further recyclability.

- Study denitrification of the nitrite group, its implications and possible limitations for the process.
- Analyze the solvent to determine if there are reaction by-products.

1.3 Thesis Outline

A short description of the chapters and the coherence between them:

Chapter 1 This section describes the origin and evolution of the current environmental challenges that plastics and fire retardant poses. Here is briefly described our research objectives and how this must be aligned with our industrial partner objectives.

Chapter 2 This chapter covers the basics related to electronic waste. The principal characteristics of our target polymers (ABS and HIPS/PS), and brominated fire retardant: types and action mechanisms. It also dives into the denitrification of ABS, an important topic in this research, and overall, all scientific bases that are needed to understand this work. Finally, the chapter covers briefly the basics of diffusion and thermal analysis.

Chapter 3 This chapter covers the basics of X-ray fluorescence and its use to perform elemental analysis in plastics. Additionally, the chapter describes the validation of our XRF results and provides a case study. This was an important step since bromine determination in plastics with other techniques is expensive and not really available for us. Thus, the use of XRF allowed us to carry out more tests and to obtain more results. Finally, validating the date obtained with the method is crucial to produce reliable results. The results are published in **The Canadian Journal of Chemical Engineering (CJCE)**, in the Top 15 articles published in the CJCE in 2024 ([27]), and in a virtual issue: "Exploring themes: Top-viewed articles from across chemical engineering.

Chapter 4 This chapter 4 corresponds with the second article of this thesis. Here we debrominated HIPS/PS with an alkali solvothermal treatment. The polymer is successfully debrominated at temperatures of about 230 °C in 4 h. We also demonstrate that by transforming the polymer into filaments of around 1 mm it is possible to achieve almost full debromination without the need to grind the polymer into fine powder, protecting its chemical integrity. The results are published in **Recycling (MDPI) a journal with a Current Impact Factor of 4.6**.

Chapter 5 Corresponding with the third and last article of this thesis, Chapter 5 covers the solvothermal debromination of commercial ABS. Like in our previous article we reported debromination higher than 90% at 190 °C and 4 h. Furthermore, we dug into the denitrification process and quantification, polymer cross-linking and other possible effects of the treatment

to the ABS

Chapter 6 Summary of the work, conclusions and future work recommendations.

CHAPTER 2 LITERATURE REVIEW

The modern world's electronification and digitization, combined with a culture of disposable gadgets and devices, have led to a continuously growing amount of waste electrical and electronic equipment (WEEE). Since collection and recycling still lag behind our e-waste production, new techniques and processes are expected to be promoted to address this increasing concern. Being able to remove brominated fire retardants from this not-yet-feedstock could impact the recyclability of a significant portion of the WEEE produced. [1, 28]

This chapter is divided into four main sections. First, a brief introduction to the main components in WEEE: non-polymeric components and typical polymers found in WEEE, with a focus on styrenic polymers such as acrylonitrile butadiene styrene (ABS) and polystyrene (PS). The second section will cover brominated fire retardants (focused on EEE components) and the detection methods available for their determination. The third section will address techniques for polymer characterization. And finally, the last section will discuss the debromination of WEEE.

2.1 WEEE

Electrical and electronic equipment are manufactured using several components, both polymeric and non-polymeric. The majority of the non-plastic fraction is composed of metals, and due to their higher scrap value, they are often separated from the plastic fractions (when possible) at early stages. [29, 30] Table 2.1 shows the amount of metals present in WEEE and their percentage of recovery. The majority of these metals are part of electronic components (circuits, wires, etc.), but some are also incorporated into the polymer matrix. TiO_2 is widely used as a white pigment and UV stabilizer due to its stability, availability, and non-toxicity (for example: Ti-Pure™ from Chemours).[31] Sb is another metal used as a polymer additive (as synergist agent with the brominated fire retardants), in this case as antimony trioxide Sb_2O_3.[32, 33]

Table 2.1 Metal fraction in E-waste. [1]

Metal	**Amount**	**Category**
Fe	24 billion kg	Total Metals
Al	4 billion kg	Total Metals
Cu	2 billion kg	Total Metals
Ni	0.52 billion kg	Total Metals
Other	0.46 billion kg	Total Metals
Recovered: 60%		
Zn	280 million kg	Other Metals
Pb	70 million kg	Other Metals
Sn	44 million kg	Other Metals
Co	34 million kg	Other Metals
Sb	28 million kg	Other Metals
Other	2 million kg	Other Metals
Recovered: 4%		
Ag	1,200 thousand kg	Precious Metals
Au	270 thousand kg	Precious Metals
Pd	120 thousand kg	Precious Metals
Pt, Rh, Ru	9 thousand kg	Precious Metals
Recovered: 20%		

Of the 62 billion kg of e-waste produced in 2022, 17 billion kg were plastic. 31 billion kg metals and the rest correspond to other components. Wager et al. (2009), in a study of e-waste in Switzerland, found that ABS and HIPS account for one third of all the plastic used in EEEE (Table 2.2). [2] Currently, Europe leads the recycling effort with 42.8% of e-waste collected and recycling followed by Oceania (41.4%) and the Americas (30%).

Table 2.2 Amounts and relative polymer presence in E-waste found in a Swiss Study. [2]

Material	**Amount** ($\mathrm{t\,y^{-1}}$)	**Relative %**
ABS	$6600\,\mathrm{t\,y^{-1}}$	14.8 %
HIPS	$5200\,\mathrm{t\,y^{-1}}$	11.7 %
PP	$4400\,\mathrm{t\,y^{-1}}$	9.9%
PC	$3000\,\mathrm{t\,y^{-1}}$	6.7%
EPS	$2300\,\mathrm{t\,y^{-1}}$	5.2%
PE	$2000\,\mathrm{t\,y^{-1}}$	4.5%
PUR	$1800\,\mathrm{t\,y^{-1}}$	4.0%
PA	$1400\,\mathrm{t\,y^{-1}}$	3.1%
PMMA	$1200\,\mathrm{t\,y^{-1}}$	2.7%
PBT	$1100\,\mathrm{t\,y^{-1}}$	2.5%
PS	$900\,\mathrm{t\,y^{-1}}$	2.0%
PPO/PPS	$850\,\mathrm{t\,y^{-1}}$	1.9%
ABS/PC	$700\,\mathrm{t\,y^{-1}}$	1.6%
PP-O	$500\,\mathrm{t\,y^{-1}}$	1.1%
PVC	$300\,\mathrm{t\,y^{-1}}$	0.7%
ABS/PVC	$250\,\mathrm{t\,y^{-1}}$	0.6%
Total	$44\,500\,\mathrm{t\,y^{-1}}$	**100 %**

Therefore, ABS and PS (HIPS) represent two of the main polymers in WEEE, even more significantly when considering polymeric blends such as ABS/PVC or ABS/PC. Moreover, Stenvall et al. (2013) reported that HIPS (42%), ABS. (38%), and polypropylene (10%) are the main polymers found in WEEE samples collected in Sweden. [30]

2.1.1 Acrylonitrile Butadiene Styrene – ABS

ABS is a thermoplastic commonly manufactured by suspension, mass, and emulsion polymerization. Styrene-acrylonitrile (SAN) chains are chemically grafted onto the polybutadiene (PB) backbone, creating long chains of PB crisscrossed with shorter ones of poly(styrene-co-

acrylonitrile). [2, 34, 35]

Figure 2.1 presents the chemical structure of ABS; however, the presence of each monomer in the chain is not constant, with values varying depending on which properties of the polymer are being promoted. Typical ratios for each monomer are: acrylonitrile: 15–50%; butadiene: 5–30%; styrene: 40–60%.

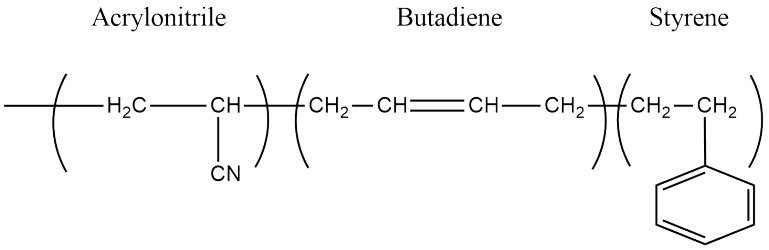

Figure 2.1 Chemical structure of ABS

The PB fraction improves impact resistance and fracture toughness. Styrene provides good processing behaviour, strength, and gloss. Hardness, rigidity, and chemical resistance are contributed by the acrylonitrile group. [36] Table 2.3 provides a summary of the main thermal properties of ABS.

Table 2.3 Main properties of ABS polymer. [3]

Property	**Value**
Density at 20 °C	1.03 to 1.09 $\mathrm{g\,cm^{-3}}$
Density (melt)	0.93 $\mathrm{g\,cm^{-3}}$
Glass Transition Temperature	102 to 107 °C
Melting Temperature (DSC)	220 to 260 °C
Thermal Conductivity	0.1 $\mathrm{W\,m^{-1}\,K^{-1}}$
Chemical Resistance	Excellent to acids, alkalis, oils
UV Resistance	Poor without stabilizers
Number Average Molecular Weight, M_n	3×10^4 $\mathrm{g\,mol^{-1}}$ to 2×10^5 $\mathrm{g\,mol^{-1}}$

2.1.2 High Impact Polystyrene – PS

Polystyrene typical manufacturing process implies, free radical polymerization in the presence of initiator (peroxide) and a solvent. This process is commonly paired with chain transfer

agents (mecaptans). HIPS is the impact modified version of the PS, and consist in the addition of polybutadiene rubber (PB) to the PS to increase the impact resistance.

Table 2.4 Main properties of PS polymer. [3]

Property	**Value**
Density at 20 °C	1.04 to 1.06 $\mathrm{g\,cm^{-3}}$
Density (melt)	0.945 $\mathrm{g\,cm^{-3}}$
Glass Transition Temperature	85 to 102 °C
Melting Temperature (DSC)	275 °C
Thermal Conductivity	0.155 $\mathrm{W\,m^{-1}\,K^{-1}}$
Chemical Resistance	Excellent to Alcohols, alkalis
UV Resistance	Poor without stabilizers
Number Average Molecular Weight, M_n	3×10^4 $\mathrm{g\,mol^{-1}}$ to 2×10^5 $\mathrm{g\,mol^{-1}}$

2.2 Brominated Fire Retardant – BFRs

Polymers can decompose and become combustible if exposed to a heat source, making them a fire hazard in certain situations. Especially, since polymers constituting EEE components may be exposed to potential heat sources from the electrical parts, lawmakers passed a series of fire-protection regulations, such as UL94 V0 and V2 requirements for electrical applications. For the past decades, brominated fire retardants have been the main additives used to comply with such regulations. Brominated fire retardants are not the only ones available on the market (alternatives based on phosphorous are present in the market), but they were the primary additives for thermoplastics.

Since FRs tend to reduce certain polymeric properties, the industry has always sought compounds with higher efficiency, thus requiring lower amounts of FR. Brominated compounds are highly efficient, especially when used together with antimony trioxide as a synergist, but still represent between 10 to 20% of the plastic weight. BFRs can be introduced into plastic resins either as direct additives, without any chemical bond, or as reactants in the polymer chain. The latter is achieved by adding brominated monomers during the polymerization step, incorporating these compounds into the polymer structure (e.g., the use of brominated styrene as a co-monomer in ABS and HIPS). [37–39]

Flame retardants must have the thermal stability to resist processing temperatures of the thermoplastics without being stable in excess, thus preventing their main function as fire

retardants. [37, 38]

The proposed action mechanism for flame inhibition is the reactions of HBr (from brominated compounds) released in the flame with $OH\cdot$ and $H\cdot$ radicals, which are the most reactive radicals in the propagation step of the oxidative reactions in the combustion, thus acting primarily in the gas phase as radical scavengers, reducing partial pressure of O_2 near the flame, and by the endothermic nature of the debromination reaction to form HBr [40]:

$$OH\cdot + HBr \rightarrow H_2O + Br\cdot \tag{2.1}$$

$$H\cdot + HBr \rightarrow H_2 + Br\cdot \tag{2.2}$$

The overall rate of propagation decreases owing to the lower reactivity of radicals, which regenerate HBr by reaction with volatile products of polymer degradation: The lower reactivity of $Br\cdot$ radicals reduce the rate of propagation, which then will form HBr again by reacting with volatile products from the plastic decomposition.

$$RH + Br\cdot \rightarrow HBr + R\cdot \tag{2.3}$$

The previous mechanism competes with the branching step from which the oxygen is consumed in hydrocarbon's flames, making it very suitable for inhibition of flames feed with oxygen (as is expected in normal uses).

$$O_2 + H\cdot \rightarrow OH\cdot + O\cdot \tag{2.4}$$

Sb_2O_3 volatilize bromine as $SnBr_3$ and HBr at lower temperatures to produce $SbBr_3$ and H_2O, in an endothermic reaction that occupies part of the total partial pressure reducing the O_2 partial pressure, and therefore, improving the flame-inhibition of this elements, acting at earlier moments of the burning process. [37, 40, 41]

2.2.1 X-ray fluorescence for Br content determination

BFRs are considered persistent organic pollutants (POPs), toxic and a human health hazard, and thus, Canada, the European Union (EU), and other countries are setting laws to control and reduce the presence of PBDEs in plastics and monitoring their presence in the environment. [4, 42]

The EU defines a few options to treat plastic fractions containing POPs. Over the levels legally established. The permitted treatments are those considered to destroy or transform irreversibly the POPs: If a plastic fraction contains persistent organic pollutants (POP) At concentrations higher than regulatory limits, the only authorized treatments are: physico-chemical treatment. Incineration on land, or use as a fuel or other means to produce energy. Excluding waste containing PCBs.

Table 2.5 EU Scenarios for Restricted PBDEs and Total Bromine [4]

Scenario	**Analysis Type**	**Limit Values**	**Compliance Notes**
Option 1	Two analyses: - Total Bromine - Restricted PBDEs	- Total Br: 2000 ppm (CLC/TS 50625-3-1) - Restricted PBDEs: • 500 mg/kg (from 10 Jun 2023) • 350 mg/kg (from 30 Dec 2025) • 200 mg/kg (from 30 Dec 2027)	Most robust. Ensures clear traceability and full regulatory compliance.
Option 2	One analysis: - Restricted PBDEs only	- Same PBDE thresholds as Option 1 with same valid dates	If below threshold, assumed compliant with CLC/TS 50625-3-1 since its goal is PBDE removal.
Option 3	One analysis: - Total Bromine only	- Provisional thresholds (no new WEEELABEX values): • 500 ppm (from 10 Jun 2023) • 350 ppm (from 30 Dec 2025) • 200 ppm (from 30 Dec 2027)	If below threshold: compliance assumed. If above: PBDE analysis required. Data collection advised to validate assumption.

Note: Restricted PBDEs include tetra-, penta-, hexa-, hepta-, and deca-BDEs, per REGULATION (EU) 2019/1021.

To enforce these regulations, Br determination and WEEE plastic sorting are therefore required. In the EU, waste management companies are required to separate the polymers

between those over and below $2000\,\mathrm{mg\,kg^{-1}}$. with those under the $2000\,\mathrm{mg\,kg^{-1}}$ being considered meeting the de-pollution regulation. [43]

Several studies used X-ray fluorescence (XRF) to determine Br content in the plastic. This non-destructive technique allows a fast elemental bromine determination, with little sample preparation and high accuracy. This determination is used to estimate the total BFR (in contrast to determining the specific compound) content in the sample. Gallen et al.(2014), found that XRF can achieve a determination of BFRs of up to 92% in different plastic samples, when compared with typical destructive analytical methods such as GC-MS. Beccaguttiet al. (2016) used X-ray fluorescence spectroscopy (XRF), ion chromatography (IC), and ion-selective electrodes (ISEs) to determine the content of Br and Cl in real WEEE samples. They found that XRF offers the best accuracy and repeatability when properly calibrated. Sharkey et al. (2018), however, report that due to the matrix effect portable (XRF Gun) XRF is not suitable to determine concentrations of BFRs [44, 45]. Yet, Sharkey et al. (2022) findings are that portable XRF is able to screen BFRs content to legal limits in 90% of the plastics collected during a 5-year study [46]. Additional studies further demonstrated the capabilities of XRF and portable XRFs to accurately determine bromine content in plastics[47–50].

2.2.2 Debromination Processes

Recent research has focused on developing, scalable, and environmentally friendly methods to remove bromine from these plastics, for a safer recycling.

Pyrolysis

Pyrolysis consists of thermally degrading the organic compounds (in this case, polymers) in the absence of oxygen, typically yielding as main products a mixture of molecules, such as oils (liquids), waxes (solids) and gases. The yield is dependent on the conditions used, the catalyst, etc., and the recovered products are then refined as chemicals or used for energy recovery as fuels. Pyrolysis is the preferred method for polymer chemical recycling. This method can process plastic mixtures without previous sorting (as happens with mechanical recycling) and composite materials that are challenging to recycle with other methods.[51, 52] Pyrolitic debromination, however, is not a straightforward process. Blazsó et al. (2002) carried out a pyrolysis of brominated epoxy from electronic scrap and only achieved a partial debromination of the BFRs present. They observed a bromine rearrangement by substituting the hydrogen on phenolic rings and a cyclic rearrangement. [51] These findings are consistent with those reported by Jakab et al.(2003) [53]. They studied the thermal decomposition of HIPS added with decabromodiphenyl ether and decabromodibenzyl. Although each BFR de-

composed via a different pathway, both formed organobrominated compounds that remained in the oil. A two-step pyrolysis of TV cases made of brominated HIPS removed the Br in an initial isothermal pyrolysis at 300 °C under vacuum, to then decompose the rest of the plastic to produce an oil Br free. [54] Catalytic-pyrolysis solves the problem of the remaining brominated compounds in the oil. Bhaskar et al.(2003) achieved a 99% debromination of the pyrolysis oils with the presence of iron oxide carbon composite catalyst (Fe-C) [55]. Antimony trioxide Sb_2O_3 decreased the degradation temperature and reduced the production of hydrogen bromide HBr and brominated compounds by the formation of $SbBr_3$.

Supercritical and Solvent Debromination

Supercritical fluids, particularly supercritical CO_2 offer an alternative path for debrominating electronic and polymeric waste by extracting brominated flame retardants (BFRs). Studies have optimized process parameters, incorporated co-solvent effects, and mapped phase behavior to maximize BFR removal. Complementary hydrothermal–alkaline treatments further convert residual bromine to soluble ions, offering integrated debromination pathways. Supercritical CO_2 extraction experiments were conducted on polybutylene terephthalate (PBT) containing brominated flame retardants (BFRs). Pure CO_2 treatment achieved 100% debromination at 50 MPa and 100 °C. By adding other solvents (methanol, isopropyl alcohol, toluene) to the reaction media, it was possible to reduce the required pressure to achieve complete debromination to 20 MPa[56]. Onwudili et al [57]. Explored the fate of bromine and antimony during alkaline hydrothermal treatment of BFR-containing plastics. Showed that under mild sub-critical water conditions with NaOH, most bromine is converted into bromide ions. However, antimony oxide remains largely in the solid residue. Suggesting a need for downstream recovery steps. In a study comparing the extraction of BFRs with traditional organic solvents (toluene, acetone) versus supercritical CO_2. CO_2 with a small percentage of co-solvent (ethanol) achieved comparable results. Extraction yields toluene with lower residual solvent in the polymer. The recommended process conditions (25 MPa, 60 °C, 5% ethanol) for optimal throughput and minimal polymer degradation. The results for the sample of HIPS with Hexabromocyclododecane (HBCD) reach less than 10% regardless of the method used (supercritical or solvent) [58]. Vilaplana et al. compared ultrasonication andisopropanol/*n*-hexane as solvent, microwave-assisted extraction (MAE) and *n*-hexane/isopropanol, and pressurized liquid extraction (PLE) and methanol/isopropanol as debromination mechanisms. MAE and PLE achieved the highest efficiencies in all cases, but debromination ratios vary greatly depending on the fire retardant (from 100% to 10% debromination)[59].

Solvothermal treatment

With a boiling point of 190 °C for ethylene glycol (EG) and 230 °C for triethylene glycol (TEG), these solvents allow working at high temperatures without the need for high pressure, which would damage the polymer [60]. In a process treating PS with a solution of water/TEG as solvent, with 1 M of KOH and under microwave irradiation at 250 °C for 30 min led to the removal of 85% bromine from the polymer matrix. Additionally, Bhaskar et al(2008). reported that the glycol acts as a hydrogen source in the substitution reaction [60]. Grause et al. (2015) successfully debrominated HIPS using EG and NaOH at different concentrations (from 0.5 to 2 M) using a flask and improvised ball mill. Ball mill experiments reach 100% debromination at 190 °C whereas flask ones reach 40% with the same conditions[6].

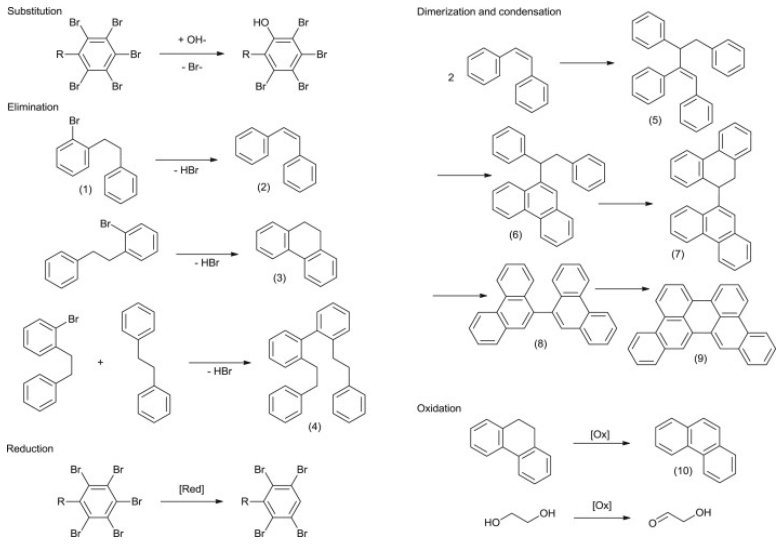

Figure 2.2 Grause et al (2015) proposed pathways of DBDPE degradation.[6]

Zhang et al. (2012) reported a similar solvothermal research. In this case, however, they focus on methanol, isopropanol, and ethanol as solvents. The brominated ABS was extracted by the solvent at temperatures ranging from 70 to 170 °C, 90 °C as the ideal condition. Time and temperature are the main factors affecting the extraction of the brominated compound. The solvent containing the brominated compound is then mixed with copper to remove and recover the bromine. It is important to note here that the plastic was ground to a 14–20 mesh in liquid nitrogen [61].

Another solvothermal treatment (180 °C and 10 h) with polyethylene glycol and sodium hydroxide removed up to 98% bromine from brominated epoxy resins collected from printed circuit boards, and removed it from the metallic residue. This study reports that the main importance of temperature and time is to achieve higher debromination ratios. The proposed

debromination mechanism is a catalytic dehydrohalogenation of poly(ethylene glycol)/sodium hydroxide system. Where the organobrominated compound will lose both a Br and a H atom to form a double carbon bond (alkene).

Interestingly, there is little more literature in this sense and none with this approach. Kameda et al. (2009), dehalogenated automobile shredder residue (ASR) with a ball mill and a solution of NaOH/ethylene glycol (EG) at 196 °C. This mechanochemical treatment increases the contact of the OH^- and ASR, reaching 100% dechlorination in less than 4 h. An activation energy of 50 kJ mol^{-1} is reported from this study [62]. More recently, Lu et al (2020). With a scaled-up system of the previous work from Kameda et al (2009). Fully dehalogenated 1000 g of ASR in a ball mill, including solvent recovery and salt separation [62].

Gilman et al (1951). reported the following reactions to describe process for the reductive debromination of aromatic bromides using a glycol–alkali system [63].

1.Formation of Glycolate Salt

$$HOCH_2(CH_2OCH_2)_2CH_2OH + 2NaOH \rightarrow NaOCH_2(CH_2OCH_2)_2CH_2ONa + 2H_2O \quad (2.5)$$

2.Internal Rearrangement (Hydride Generation)

$$NaOCH_2(CH_2OCH_2)_2CH_2ONa \rightarrow NaOCH(CH_2OCH_2)_2CHONa + 2H^- \quad (2.6)$$

3. Reductive Debromination of Aromatic Compound

$$ArBr + 2H^- \rightarrow ArH + Br^- \quad (2.7)$$

4. Formation of Aldehyde By-product

$$2Br^- + NaOCH(CH_2OCH_2)_2CHONa \rightarrow 2NaBr + CHO(CH_2OCH_2)_2CHO \quad (2.8)$$

In contrast with the suggested debromination mechanism of Grause et al (2015) [6], Gilman et al (1951) reports that the bromine atoms are easily replaced with by H^-, and then the bromine reacts with the Na^+ Although the process is different the final products remain the same in both situations. Besides the debromination pathway and the lower prevalence of this process over other debromination techniques it is clear that alkaline solvothermal effectively removed halogenated compounds from polymeric matrix.

ABS Denitrification

The solvothermal treatment using glycols and alkali as reagent dies has a limitation when used on ABS polymers. Few studies had used this combination (EG +alkali) to denitrogenate the polymer, especially as a pre-step of the pyrolysis. The nitrile group of ABS provides chemical resistance and heat stability to the polymer. However, this group becomes a problem in valorizing the polymer, especially as energy. The nitrile, when treated through pyrolysis, leads to nitrogen oxide, HCN emissions, and heavy residues (organonitrogenated compounds), reducing oil quality.

Zhou et al. (2009), report the denitrification of waste ABS plastics as part of an initial step prior to its pyrolysis of the modified polymer under an inert atmosphere. They perform an alkaline denitrogenation of an ABS solution of dioxane (ABS/DOA) in the presence of poly(ethylene glycol) -PEG600- and sodium hydroxide at 160 °C. PEG enhances the conversion of nitrile ($-$CN) groups into carboxyl ($-$COOH) and amide ($-CONH_2$), effectively removing a large fraction of nitrogen before thermal cracking. Thermogravimetric analysis shows that denitrogenated ABS (DABS) begins to decompose at around 330 °C, compared with 372.5 °C for untreated ABS, reflecting changes in the polymer´s thermal stability. DABS pyrolysis yields nearly ten times fewer heavy fractions and substantially lower nitrogen content when compared with untreated ABS. These findings demonstrate that PEG-enhanced alkaline denitrogenation [64]. Following the same principles, Du et al.(2011) implemented a chemical method for nitrogen removal from ABS plastics to make them cleaner and more suitable for fuel recovery. PEG, trahydrofuran (THF) solvent combined with NaOH at 160 °C for 2 h was used to hydrolyze the nitrogen-containing nitrile groups. Under these conditions, they achieved 93 % denitrification. PEG alone seems to have lower denitrification capability, removing just 35 %. The chemical transformation from nitrile groups to amide and carboxyl groups was confirmed with IR and NMR analyses. All these results are, however, based on the use of other organic solvents to enhance denitrification [14].

Other key findings were:

- THF was the best solvent, with better compatibility with ABS than dioxane or toluene.
- PEG/NaOH outperformed PEG/KOH, possibly due to better molecular fit with ABS.
- PEG600 gave the highest nitrogen removal compared to other PEG variants.

Du et al.(2011): proposed the following reaction pathways for ABS denitrificaiton[14].

$$\breve{}\mathrm{C} \equiv \mathrm{N} \; + \; H_2O \; \xrightarrow[\mathrm{PEG/NaOH}]{\Delta} \; \breve{}\mathrm{CONH_2} \tag{2.9}$$

$$\breve{}\mathrm{CONH_2} \; + \; H_2O \; \xrightarrow[\mathrm{PEG/NaOH}]{\Delta} \; \breve{}\mathrm{COOH} \; + \; NH_3 \tag{2.10}$$

Partial ABS denitrification, while originally non-desirable, could bring some benefits to the global process. In a study, polypropylene-thermoplastic starch (PP/TPS, 70/30 w/w) blends were compatibilized with 30% of three carboxylic acids (myristic C14, palmitic C16, stearic C18) and compared to a blend containing 10% maleic-anhydride-grafted PP (PPgMA). PP/TPS and compatibilizers were co-extruded at 160 °C, pelletized, injection-molded, and characterized. All carboxylic acids significantly improved interfacial adhesion—via hydrogen bonding with starch and van der Waals interactions with PP—yielding 10–25% increases in tensile strength, while at 180 - 260 °C, an increase is up to 54 % higher impact energy (myristic acid), while DSC showed enhanced PP crystallinity [65]. Polat et al. (2024): researches the effects of carboxylic groups on polyacrylate latices. Polyacrylate latices bearing 0–10% acrylic acid were synthesized. Latex viscosity, gel fraction, dynamic mechanical properties, and FTIR of cast films were monitored over 14 days. As acrylic acid content increases, interpolymer hydrogen bonding and acid–acid condensation drive gradual crosslinking. Latices with 4–6% acid remain pumpable yet develop 20–35% gel fraction and a rise in film hardness after one week. FTIR shows the emergence of anhydride/carboxylate bands while DMA reveals a stiffened network [66].

The effects of carboxylic groups were studied in poly(propylene terephthalate) (PPT) samples with low (16 m ≡/kg), medium (25 m ≡/kg) and high (56 m ≡/kg) carboxyl end-group concentrations were prepared. Raising –COOH content did not change T_g (67 °C to 69 °C) or T_m (223 °C to 224 °C) or overall crystallinity, but accelerated thermal degradation (30 % mass loss in air fell from 65 min for 16 m ≡/kg to 58 min for 56 m ≡/kg) and slowed non-isothermal crystallization (peak exotherm T_cc dropped from 181 °C to 166 °C). Above T_g, conductivity followed an Arrhenius dependence ($E_\mathrm{a} \approx 180\,\mathrm{kJ\,mol^{-1}}$) and scaled with –COOH concentration, consistent with proton-driven ionic transport; below T_g, polarization dominated. Thus, increased carboxyl end-groups degrade thermal stability, retard crystallization kinetics and enhance high-temperature ionic conductivity [67].

Activation Energy Calculation from TGA Data

The Coats–Redfern method applies a general integral approximation and requires specifying a reaction model $f(\alpha)$ to compute $g(\alpha)$. This method is applied to the full conversion range and can, in principle, accommodate any reaction order or mechanism. Extraction of E_a and A follows from a linear fit of $\ln[g(\alpha)/T^2]$ versus $1/T$. Its main limitation is that it has

a high dependence of $g(\alpha)$, which could lead to misleading parameters, and multi-step or mechanism-shifting processes break the assumed linearity.

On the other hand the Horowitz–Metzger method assumes first-order kinetics and focuses on the temperature region around the derivative thermogravimetry (DTG) peak T_s, where $\alpha \approx 0.632$. Defining $\theta = T - T_s$ yields a simple linear relation for $\log[-\ln(1-\alpha)]$ versus θ. This approach is mathematically less demanding and quick to implement, but it cannot be extended to other reaction orders or to reactions whose rate law deviates from first order.

In summary, Coats–Redfern gives broader applicability at the expense of model selection and mathematical complexity, while Horowitz–Metzger delivers a straight route to E_a for pure first-order decompositions around the DTG maximum. Neither method is optimal for multi-step mechanisms, so researchers often turn to iso-conversional techniques to overcome these limitations [68, 69].

- Coats–Redfern Method

$$g(\alpha) = \frac{A}{\beta} \int_{T_0}^{T} \exp\!\Big(-\frac{E_a}{R\,T'}\Big)\, dT' \tag{2.11}$$

$$\ln\!\Big[\frac{g(\alpha)}{T^2}\Big] = \ln\!\Big(\frac{A\,R}{\beta\,E_a}\Big) - \frac{E_a}{R\,T} \tag{2.12}$$

- Horowitz–Metzger Method

$$\theta = T - T_s, \quad \log\!\big[-\ln(1-\alpha)\big] = \frac{E_a}{2.303\,R\,T_s^2}\,\theta \tag{2.13}$$

CHAPTER 3 ARTICLE 1: EXPERIMENTAL METHODS IN CHEMICAL ENGINEERING:X-RAY FLUORESCENCE—XRF

Mario Ferreiro Gonzalez, Nooshin Saadatkhah and Gregory S. Patience

Published in The Canadian Journal of Chemical Engineering, Published: 27 February 2024

3.1 X-ray fluorescence (XRF) is a non-destructive spectrometric technique to detect elements with an atomic number from 11 (sodium) and beyond 92 (uranium). When X-rays or gamma rays eject tightly bound inner core electrons, an electron from an outer shell will fill the empty orbital and fluoresce. Every element has a characteristic fluorescence, which depends on the element and the electrons in the orbitals that are ejected and those that fill the orbital. With the characteristic energy of the fluorescence, we determine elemental composition and concentration when adequately calibrated. Typical run times range from a second to a few minutes with an sensitivity to as low as $1\,\mu g\,g^{-1}$ (ppm). XRF guns are portable devices that produce qualitative data while libraries loaded to laboratory instruments are capable of producing quantitative data. A broad range of scientists and engineers apply XRF in research—140 of the 250 scientific categories in the Web of Science (WoS) cite XRF analyses. Of the 10,000 articles indexed in WoS since 2018, chemical engineering ranks 5th with the most articles. The focus of the research in this category includes adsorption and waste water, combustion and pyrolysis, catalysis and zeolites, and nanoparticles and oxidation.

3.1.1 keywords

XRF, spectroscopy, fluorescence, elemental analysis, non-destructive, X-ray, WEEE, polymers

3.2 INTRODUCTION

X-ray fluorescence (XRF) determines the chemical composition of solids, liquids, and powders, together with their thickness and the composition of overlapping layers as in coatings.

This method is fast and non-destructive with a concentration range from $> 1\,\mu g\,g^{-1}$ (ppm) to 100 %. The measurement and analysis time depends on the number of elements and accuracy required, and varies between seconds to an hour. The detection range is higher for elements with higher atomic numbers. Application of XRF includes metal, cement, oil, polymer, plastic and food industry, mining, mineralogy, geology, water and waste materials, and pharmacy.

In 1895, Rontgen discovered X-rays when he saw cathode rays (an incandescent green light) pass through a glass tube and project onto a fluorescent screen.[70, 71] Roentgen named them X, meaning unknown. The discovery of X-rays initiated the theory of the atomic structure that was further developed after Thomson introduced electrons in 1897.[72] Thomson directed cathode rays between two aluminum plates in a vacuum tube to observe luminescence on a glass at the end of the tube. The rays travelled downwards along the tube when the upper plate was negatively charged, and travelled upward when it was positively charged. They concluded that cathode rays were negatively charged particles (electrons).[73] In 1909, Barkla correlated the X-rays radiating from a sample to its atomic weight.[74] Coolidge with twenty other research chemists and a large body of assistants produced ductile tungsten (filament) by reducing impurities in 1910.[75] In 1913, Moseley developed the primary XRF theory by numbering elements. Moseley revised the periodic tables from atomic weight to atomic number and proved the relationship between frequency (energy) and the atomic number (Moseley's Law), which is the principle of X-ray spectrometry.[76] He observed in an X-ray spectrum that the K line transitions moved the same amount each time the atomic number increased by one.[77] In 1925, Coster and Nishina were the first to use primary X-rays instead of electrons to excite a sample.[78] After that, Glocker and Schreiber were the first to quantitatively analyze materials with XRF.[79] Detector technology had to catch up in order to make the technique practical, which began after the 1940s. The 1950s saw the first commercially produced X-ray spectrometers. In 1970, the lithium drifted silicon detector was developed, which is still in use today.

XRF belongs mostly to the domain of material scientists and spectroscopy, as these two fields account for 25 % of the >16 000 articles Web of Science (WoS) has indexed. Chemical engineers have contributed > 1100.[10] The first article in the database was from 1967, and it took almost 30 years to reach 100 articles per year. In 2018, another 20 years later, WoS logged 1000 articles in a year. XRF is related to X-ray photoelectron spectroscopy (XPS),[80], X-ray diffraction (XRD),[81] and inductively coupled plasma (ICP) as it identifies and assesses the elemental composition and oxidation state. In terms of performance, it assesses bulk properties somewhat like XRD and Fourier transform infrared spectroscopy (FTIR), but the latter two report structural information.[82] XRF detects concentrations to

less than 1 ppm while XRD is rarely capable of detecting species below 1 % and FTIR goes to 100 ppm. This article belongs to a series on experimental methods and instrumentation most often applied by chemical engineers, which already includes such techniques as Raman, XPS, and XRD.[83] Instrumentation technology continues to advance in terms of both spatial resolution and detection limits of the elemental composition (Figure 3.1). XRF is a bulk technique with a lower detection limit compared to XRD and FTIR but analyzes over a larger area. μ-XRF, on the other hand, overlaps more with XPS and Raman as it samples a much smaller area (on the order of 10–100 µm but it detects elements with a senstivity three orders of magnitude greater.

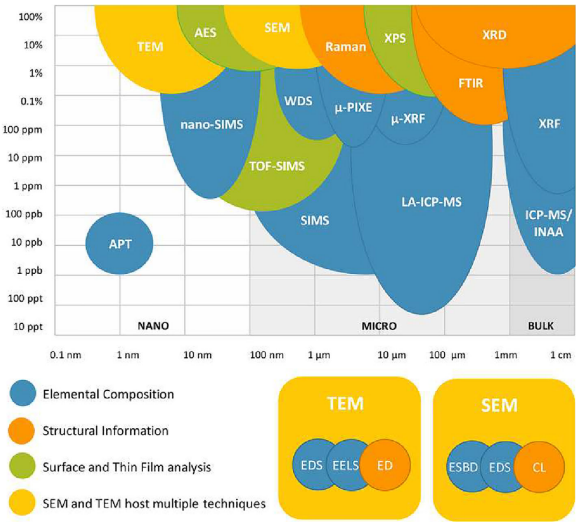

Figure 3.1 Diagram of microanalytical methods arranged according to spatial resolution and chemical sensitivity. APT: atom-probe tomography. TEM: transmission electron microscopy. AES: Auger electron spectroscopy. SEM: scanning electron microscopy. TOF-SIMS: time-of-flight secondary ion mass spectroscopy. WDS: wavelength dispersive spectroscopy. XPS: X-ray photoelectron spectroscopy. μ-PIXE: micro particle-induced X-ray emission. μ-XRF: micro X-ray fluorescence. LA-ICP-MS: laser ablation inductively coupled mass spectrometry. XRD: X-ray diffraction. FTIR: Fourier transform infrared spectroscopy. ICP-MS/INAA: inductively coupled plasma mass spectrometry and instrumental neutron activation analysis. (Copied from the work of Braidy et al.,[7] which was adapted from https://myscope.training/legacy/analysis/introduction/.)

The target audience for the series includes students and experienced engineers that are less familiar with the specifics of each analytical instrument. Thus, we cover the theory and equipment only briefly but detail the applications and the limitations of the instrument—detection limits, repeatability, and uncertainty.

3.3 THEORY

X-ray sources that irradiate samples include X-ray tubes, synchrotrons (an enormous particle accelerator that measures several kilometres in diameter) , and radioactive material. X-rays were described as electromagnetic waves or beams of photons with a wavelength (or energy) between gamma-rays and ultraviolet light: 0.01–10 nm (or 0.125–125 keV).

XRF instruments bombard samples with X-ray radiation to remove electrons from the inner orbitals via the Compton or photoelectric effect—when the electron absorbs all of the photon energy, whereas in the Compton effect only part of the energy is taken by the electron. (Figure 3.2).

Once the the electron is ejected, other electrons from an outer orbital fill the empty space almost instantaneously (1×10^{-15} s). Due to the quantum nature of these interactions (when an electron absorbs or releases energy, it is a fixed amount of energy —photon—that depends on the atomic element and the transition), the transition to a lower energy state releases an element-specific energy, in this case, in the form of X-rays (fluorescence photon) that are measured by a detector. The element-specific fluorescence wavelength permits a qualitative determination while the intensity of the emission provides a quantitative analysis. The characteristic energy depends on the orbital from which the electron is removed and the filling electron orbital (Figure 3.3).

Table 3.1 K and L shell emission lines in keV.

Element	$\mathbf{K}\alpha_1$	$\mathbf{K}\alpha_2$	$\mathbf{K}\beta_1$	$\mathbf{L}\alpha_1$	$\mathbf{L}\alpha_2$	$\mathbf{K}\beta_1$
Br	11.92	11.87	13.29	1.48	1.48	1.52
Sb	26.35	26.11	29.72	3.60	3.59	3.84
Ti	4.51	4.50	4.93	0.45	0.45	0.48
Fe	6.40	6.39	7.057	0.70	0.70	0.71

However, when a sample is bombarded with X-rays, it not only fluoresces, but it also produces an electron cascade (partially due to the Auger effect), bremsstrahlung X-rays (X-rays emitted when a charged particle "decelerates"), and backscattered X-rays (characteristic or fluorescence X-ray emission from underlying materials like air).[84, 85]

Irradiating an atom with X-ray photons expels an electron with an energy level characteristic of the shell—L, K, M (and element). The atom that expels an electron leaves an empty orbital (initial vacancy) that places it in an unstable excited state (Figure 3.3). Siegbahn nomenclature follows the electron transition. For transitions from $n = 2$ to $n = 1$, the corresponding letter will be K; from $n = 3$ to $n = 2$, it is L; from $n = 4$ to $n = 3$ it is M; and

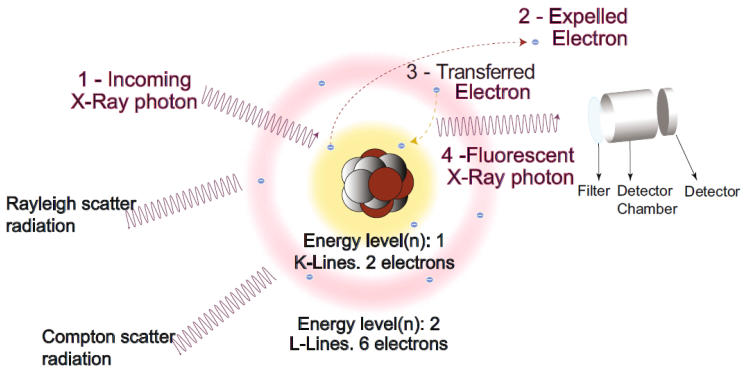

Figure 3.2 X-ray fluorescence (XRF) basics. When an X-ray photon collides and expels an electron from an inner shell, it leaves a hole in the shell. To recover nuclear stability, an electron from an outer shell drops into the lower shell to fill the hole. The drop from outer (higher energy) to inner layer (lower energy) fluoresces and each element/shell has a characteristic emission of this energy difference. Compton and Rayleigh scattering also result when an electron is ejected.

so on (Table 3.2).

Table 3.2 A compilation of the possible quantum number for the first 3 energy levels of an atom: n is the energy levels, l is angular quantum number, m is the magnetic quantum number.

Notation	$\boldsymbol{n}$	$\boldsymbol{l}$	$\boldsymbol{m}$	$\boldsymbol{j = l \pm \frac{1}{2}}$
K	1	0	0	$\frac{1}{2}$
L1, L2, L3	2	0, 1	0, 1, -1	$\frac{1}{2}$, $\frac{1}{2}$, $\frac{3}{2}$
M1, M2, M3, M4, M5	3	0, 1, 2	0, 1, -1, 2, -2	$\frac{1}{2}$, $-\frac{1}{2}$, $\frac{3}{2}$, $-\frac{3}{2}$, $\frac{5}{2}$

The emitted X-rays appear as peaks over a given energy spectrum. The intensity of each peak reflects the concentration of an element in the sample compared to regression line standards (Figure 3.5). Fluorescence and scatter depends on both the X-ray energy and the material characteristics (thickness, density, and composition).

Additionally to electronic transitions, the light–matter interaction and how the latter deposit energy in the former will dictate other parameters in XRF analysis such as penetration and analysis depth. This is not only relevant to perform elemental studies but also when talking about radiation exposure and safety. A beam of photons passing through an element will lose its energy proportionally to their initial intensity, material depth, and density. [86] This effect is defined as the mass attenuation coefficient (μ/ρ), and is proportional to is Avogadro's

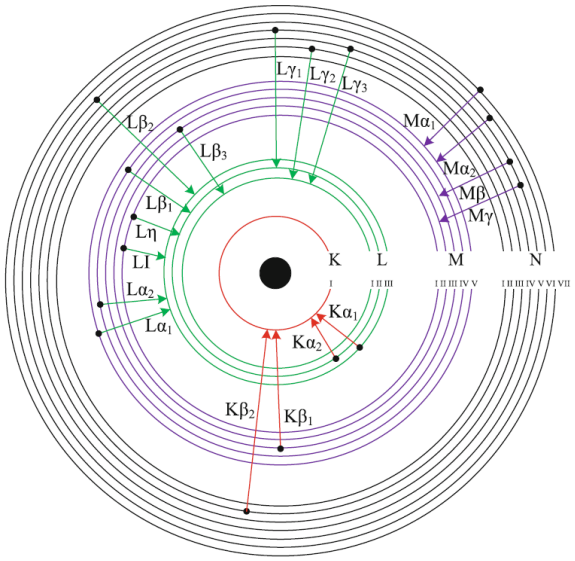

Figure 3.3 Not all transitions are permitted due to quantum reasons. The characteristic emission energy depends on the line and transition (Tables 3.1 and 3.2). Each line represent a different quantum coordinate (quantum number) of the expelled electron and the filling one. L lines for example represent the electrons situated on the energy level 2 and with defined n, l, m, and j values. For example, Kα_1 represents the transition from L3 to a K line.[8]

Table 3.3 Operational parameters for all detectable elements applied to the brominated polymer.

Run	**Element lines**		***V*** (kV)	***I*** (µA)	**Filter**	**He atmosphere**
	K lines	**L lines**				
5	F–Si		5	60	None	Yes
4	P–Cl		9	30	Ti	Yes
3	K–V	Te–Ba	12	25	Al, 50 µm	No
2	Cr–Co	Pr–Tm	20	15	Al, 200 µm	No
0	Ni–Mo	Yb–Am	50	6	Ag	No
1	Tc–Sb		50	6	Cu, 500 µm	No

number, N_A and the sum of the principal photon interactions, σ_tot, and inversely proportional to the atomic mass unit, μ, and the relative atomic mass of a determined element, A.

$$\mu/\rho = \frac{\sigma_\mathrm{tot} N_\mathrm{A}}{\mu A} \tag{3.1}$$

where

$$\sigma_\mathrm{tot} = \sigma_\mathrm{pe} + \sigma_\mathrm{coh} + \sigma_\mathrm{incoh} + \sigma_\mathrm{pair} + \sigma_\mathrm{trip} + \sigma_\mathrm{ph.n.} \tag{3.2}$$

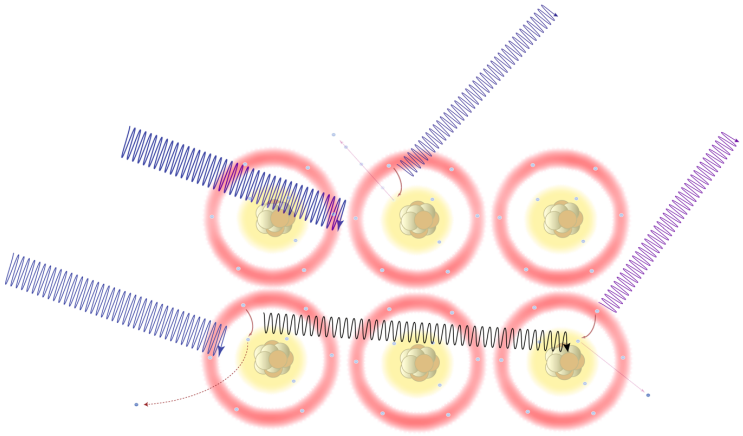

Figure 3.4 Primary fluorescence is the one directly induced by the X-ray source. Secondary fluorescence is created by the fluorescence X-ray from the sample itself acting as an X-ray source.

and

σ_{pe}	photoelectric effect contribution
σ_{coh}	coherent scattering contribution
σ_{incoh}	incoherent scattering contribution
σ_{pair}	electron-positron production contribution
σ_{trip}	atomic electrons contribution
$\sigma_{\text{ph.n.}}$	photonuclear contribution

Some of these contributions, like $\sigma_{\text{ph.n.}}$ and σ_{pair}, only occur at very high energies over 5 MeV. However, the attenuation coefficient, photon interaction cross sections, and related quantities depend on the photon energy. [86]

3.3.1 Rayleigh and Compton scatter

In addition to XRF, elastic and inelastic interactions produce scattered photons. When a photon interacts inelastically with an electron, part of the photon energy transfers to the electron. The scattered photon will have a lower energy and therefore longer wavelength than the incoming photon and is known as Compton scatter or incoherent scatter. The energy lost by the photon depends of the collision angle. The intensity of the scattered radiation is inversely proportional to the mass attenuation coefficient of an element (Figure 3.6). The mass attenuation factor is the ratio of the linear attenuation coefficient, measured in cm^{-1} μ, to the material density in $\text{g}\,\text{mL}^{-1}$, ρ. By measuring the mass attenuation coefficient of different elements, it is possible to use the Compton effect for quantitative analysis.[87]

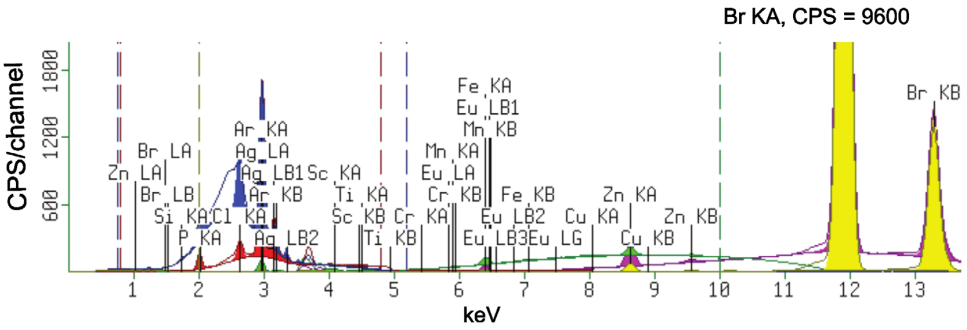

Figure 3.5 Standard X-ray fluorescence (XRF) trace for a plastic sample containing brominated fire retardant. The y-axis represents the number of counts (counts per second, CPS) of light (X-ray photons) accumulated per detector channel. Each channel represents an energy range (keV). The x-axis represents the energy of the detected photon, in kilo electron volts (keV). The CPS is proportional to the element concentration, thus higher CPS means higher concentrations. If the resolution is high the peak will narrow the energy's value (x-axis) of the element's characteristic energy (Table 3.2, Figure 3.3). XRF spectrum details elements and transitions. The most noticeable peak corresponds to Br Kα_1 with 9600 counts while the second peak with the most counts was Br Kβ_1. In this case, Br is the element whereas Kα_1, Kβ_1 are the transitions. Zn Kα_1 is also well defined. Many element's traces are present and several overlap that have similar characteristics energies. The colour of the different peaks refer to the measuring conditions, who are optimized for a certain range of elements. In this case, using an Epsilon 4 from Malvern Panalytical coupled with Omnian Scan Parameters (Table 3.3). The yellow configuration is set to detect elements from Ni to Mo using K lines, and Yb to Am with L lines. The instrument applies a voltage of 50 kV and 6 µA to generate the X-rays. Additionally, this method use Ag filter and air atmosphere (for lighter elements, it is possible to use He).

$$\Delta\lambda = \frac{h}{m_e c}(1 - \cos\theta) \tag{3.3}$$

where:

$\Delta\lambda$ is the change in wavelength (Compton shift),

h is Planck's constant ($6.63 \times 10^{-34}\,\mathrm{J\,s^{-1}}$),

m_e is the electron mass,

c is the speed of light ($3 \times 10^{8}\,\mathrm{m\,s^{-1}}$), and

θ is the scattering angle.

Strongly bound electrons resonate at the same frequency as incident photons and then emit scattered photons at that frequency—elastic scattering. This is known as Rayleigh or coher-

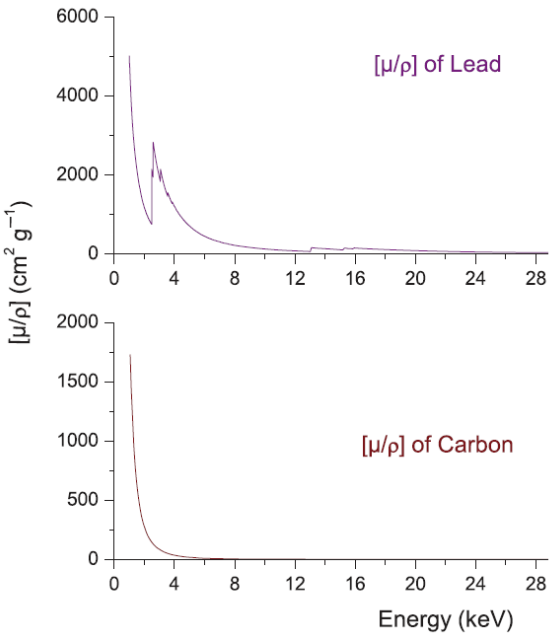

Figure 3.6 Mass attenuation (μ/ρ) for C (light element) and Pb (heavy element) and its variation with the incident radiation energy.

ent scattering and the energy loss in the process approaches zero as photons scatter with the same energy as the incident photons.[87, 88]

3.3.2 Polarization

X-rays, as any electromagnetic wave, are transversal and thus the wave is perpendicular to the direction of transmission. They have both an electrical (E) and a magnetic component (B). A filter that polarizes X-rays rotates only one component of the electrical field (E). The polarization effect contemplated here affect both components, but in the explanation, we are considering only the electric component (E). When a wave is polarized, it means that all the electrical components of E are in the same plane.

Any electrical component of the electromagnetic wave is the vectorial sum of its horizontal and vertical components (E_z and E_x) (Figure 3.7). When non-polarized X-rays are reflected at a 90° angle, the resulting X-rays are polarized because the vertical components are not reflected in the new direction of propagation. Adding a second 90° reflection will eliminate all the original X-rays and thus reduce the background noise and improve the quality of the signal. Secondary targets are partially used for this purpose.

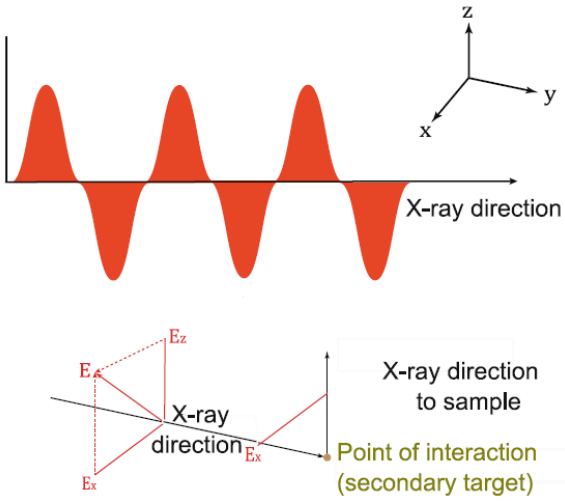

Figure 3.7 Polarization: As electromagnetic waves travel, the electrical component of the wave is perpendicular to direction of the motion. When the wave diffracts at 90°, the electrical component that was perpendicular and disappears. Repeating this operation two times removes the background.

3.3.3 X-ray tubes

X-ray tubes includes a filament (cathode) and an anode in a vacuum chamber (Figure 3.8). [89] An electrical current heats up the filament, which then emits electrons. A high voltage (20–150 kV) across the filament and the anode accelerates electrons to the anodes.[90] Electrons hit the anode and decelerate, which makes the anode emit characteristic radiation (X-rays) and bremsstrahlung radiation in a continuous spectrum of energy (continuum). The energy of this radiation depends on the anode material (gadolinium, tungsten, rhenium, molybdenum, aluminum, chromium, palladium, gold, and graphite). Tungsten, because of its high atomic number ($Z = 74$), produces bremsstrahlung radiation more efficiently compared to other target materials with lower atomic number.[91] Molybdenum ($Z = 42$) and rhodium ($Z = 45$) with intermediate atomic number produce characteristic X-rays with intermediate energies for medical purposes.[92] Detection of light elements requires a high intensity of low energy radiation (1–10 keV), while heavy elements require excitation energies up to 50 keV.[93]

X-rays leave the end of the tube through a beryllium window or through side-windows (Figure 3.8).[94]

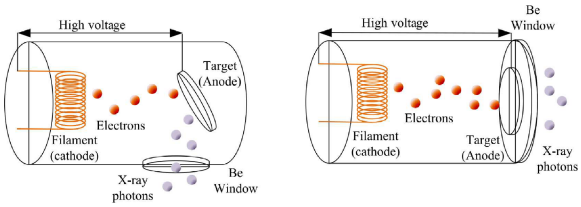

Figure 3.8 X-ray tube arrangement: Side window (left), target transmission (right).

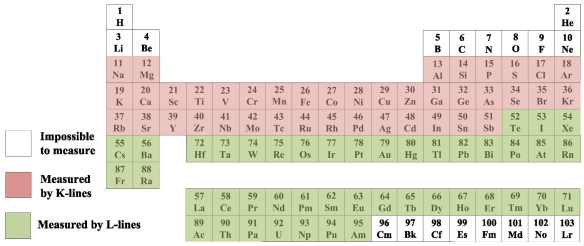

Figure 3.9 The measurability of the elements.

3.3.4 Secondary targets

X-rays illuminate secondary targets (fluorescent, Barkla, and Bragg) producing characteristic radiation to irradiate samples. Secondary targets have multiple advantages; they: (1) polarize the radiation; (2) reduce or remove background noise; (3) generate specific emission spectrum; (4) produce a wider energy distribution of the irradiating photons; and (5) improve detection limits.

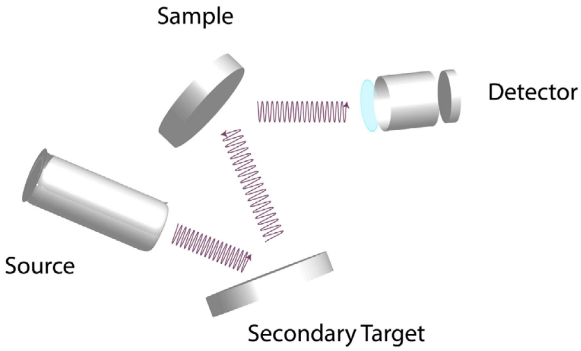

Figure 3.10 Secondary target configuration.

Fluorescent targets include heavy elements like tungsten that fluoresce when irradiated by an X-ray source. Scattering is reduced but the the energy of the fluorescent radiation of the target must be greater than the bond energy of the electrons of the sample. Some instruments are equipped with several secondary targets allowing the selection of the desire

fluorescent emission. **Barkla targets** consist of light elements to scatter photons. Some of the targets fluoresce, but the intensity is lower than the bond energy of the electrons of the sample. Barkla targets produce a wide energy spectrum and are best for heavy elements. **Bragg targets** are generally crystals that selectively reflect a specific energy in a desired direction, which improves the detection limits by reducing background levels.

Detectors

XFR spectrometers comprise either energy dispersive (EDXRF) or wavelength dispersive (WDXRF) detectors. The former measures the energy of the characteristic radiation from the sample and separates it into elements in the sample (dispersion). The latter disperses the wavelengths by channelling all the radiation from the sample to crystal, like a prism, that diffracts the energies in several directions. EDXRF operates with a fraction of a Watt with high detection efficiencies while WDXRF requires several kilowatts.[95] Ultimately, the energy of the electromagnetic wave, E, and wavelength, λ, are equivalent

$$E = hf = \frac{hc}{\lambda} \tag{3.4}$$

EDXRF has solid-state detectors that measure elements from Na up to U. When an X-ray photon enters the detector, it produces an electrical pulse with a height proportional to its energy. A multi channel analyzer counts the amplified pulses. The area of the peaks gives the intensity.

WDXRF includes gas-filled and scintillation detectors. The former measures from Be to Cu, and the latter measures from Cu to U. The height of the peak gives the intensity. In WDXRF, the majority of the power is dissipated as heat so it requires liquid cooling for the X-ray tube.[95]

3.3.5 The fundamental coefficient method

The fundamental coefficient method is a combination between fundamental parameters and the statistical formulation of Lachance-Traill. This method addresses the difficulty of XRF to perform a precise matrix correction. The method requires standards and a series of calculations for the coefficients that must satisfy the Lachance-Traill equations and Tertian's identities. The theoretical parameters include mass absorption, excitation factors, and instrumental factors. Nowadays, all XRF software include such considerations. However, a specific method for the sample and calibration is still required. [96]

Thus, the effective coefficients for a given composition C_i, C_z,C_k, and so forth are as follows:

$$C_i = R_i(1 + \alpha_{iz}C_z + \alpha_{ik}C_k + \ldots) \tag{3.5}$$

where:

i represents a fluorescent element;

$C_{i,z,k\ldots}$ is the relative concentration of element i,z,k ...;

R_i is the relative intensity; and

α_{iz}, α_{ik} ...are the effective coefficients for the given composition C_i, C_k, and so forth.

The Tertian's identities are expressed by the following:

$$a_{ij} = \alpha'_{ij} - h_{ij}\frac{C_i}{R_i} \tag{3.6}$$

Followed by similar expressions for α_{ik}, α_{iz} ....[96]

3.3.6 Total reflection XRF (TXRF)

Total reflection X-ray fluorescence (TXRF) is used for the analysis of trace elements in small sample volumes, typically in the microlitre (μL) range. TXRF use the principle of total reflection of X-rays at a very shallow angle of incidence on a flat substrate. The incident X-rays excite the atoms, causing them to emit characteristic photons. These photons are then detected by a detector placed at a fixed angle.[97] The TXRF detects trace elements in the parts per billion (ppb, $\mathrm{ng\,g^{-1}}$) range. It also offers excellent precision and accuracy, with relative standard deviations typically below 5 %.

3.4 APPLICATIONS

XRF is applied broadly in the sciences: 140 of the 250 Web of Science scientific categories cite it two times or more. Journals assigned to multidisciplinary materials science published 1510 of the 9000 published since 2018, and the other top categories are environmental sciences (1080 articles), multidisciplinary geosciences (930 articles), physical chemistry (884 articles), and then chemical engineering (717 articles). The journal *Fuel* in the chemical engineering category cites XRF most, with 81 articles. The other most prolific journals are *Journal of*

Environmental Chemical Engineering (60), *Catalysis Today* (35), *Minerals Engineering* (33), *Energy & Fuels* (31), and *Desalination and Water Treatment* (30).

VOSViewer is a web-based software that generates maps of bibliographic data—keywords, authors, countries, and journals—from databases like Scopus and Web of Science. The keyword map for chemical engineering has 4 clusters of research centred on zeolite, catalyst, and mechanism with the most keywords, followed by temperature (T), combustion, pyrolysis, biomass, then adsorption (ads'n), kinetics, aqueous solution (aq sol'n), and finally oxidation (oxid'n), nanoparticles (NP), degradation. These clusters correlate broadly with the journals that publish the most work applying XRF: *Catalysis Today* belongs in the red cluster, *Fuel* and *Energy & Fuels* would be in the green cluster, *Desalination and Water Treatment* is in the blue cluster, while *Journal of Environmental Chemical Engineering* would belong in the yellow cluster. Although these journals have published the most with XRF, the top 3 cited articles are in *Applied Catalysis B-Environmental* and *Journal of Water Process Engineering*. The articles are entitled: "Enhanced photocatalytic removal of phenol from aqueous solutions using ZnO modified with Ag" (239 citations since 2018),[98] "Synthesis of CeaMnOx hollow microsphere with hierarchical structure and its excellent catalytic performance for toluene combustion" (163 citations since 2019),[99] and "Development of synthetic zeolites from bio-slag for cesium adsorption: Kinetic, isotherm and thermodynamic studies" (147 citations since 2020).[100]

The cjche has published 10 articles that mention XRF since 2017. The major research themes have been $LiFePO_4$ and batteries,[101] metals,[102, 103] sewage sludge[104] and adsorption, and bitumen,[105] bed coke,[106] and coal.[107]

XRF and X-ray spectroscopy is versatile non-destructive and for this reason it is applied in almost all human technological and research areas. Its practical industrial applications are often uncited, as they constitute a standard for steel alloy quality control, pharmaceuticals to assess potential contamination, and petroleum to measure sulphur and metal content in crude oil and lubricants. More recent applications could be directed at measuring the capability of regenerated biochar at removing Hg.[108] In archeology, it is used to determine silver content, and its evolution over time, in ancient coins like for Greek coins in a small colony on the Iberian Peninsula minted from 4 to 1 B.C.[109] This technique can be used to determine different alloy grades such as gold purity in jewellery,[110] and to determine heavy metals presence in medicinal plants, cosmetics, and ethnic spices.[111, 112] Soil pollution is commonly analyzed using portable and desktop XRF.[113]

Archaeology Researchers analyze silver content in coins, coatings, and other objects with XRF. In geoarchaeology they examine target compounds like basalt in artifacts. The

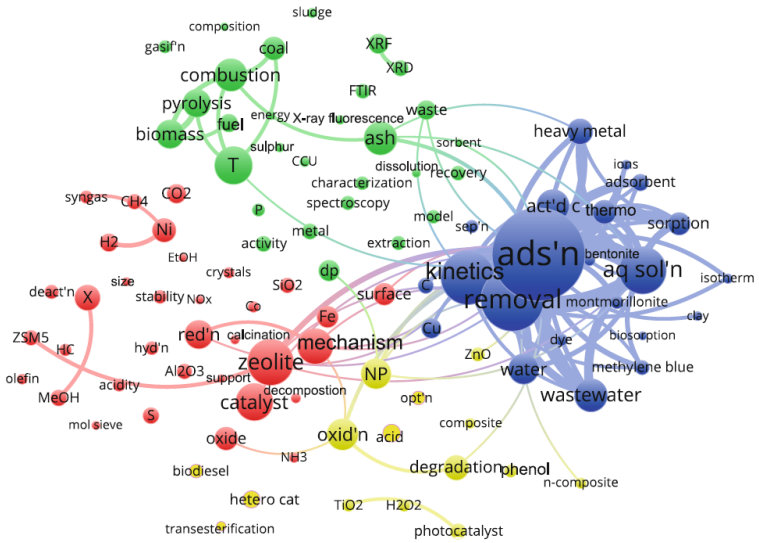

Figure 3.11 XRF bibliometric map of the 102 most cited keywords of articles from journals indexed by Web of Science from 2000 to 2022 in the chemical engineering category.[9, 10] The size of each node and font-size correlate with the number of times the keywords occur in the database. ads'n is the largest node with 252 occurrences, and the smallest nodes correspond to 22 occurrences. The VOSViewer on-line software groups the keywords into 4 clusters: red cluster with 34 keywords, green (30), blue (22), and yellow (15). The largest nodes of each cluster are: zeolite (125 articles), T (102), ads'n (252), and oxid'n (86). The lines represent citation links. Abbreviations: act'd c—activated carbon, ads'n—adsorption, aq sol'n—aqueous solution, CCU—carbon capture utilization, deact'n—deactivation, decomp'n—decompostion, EtOH—ethanol, gasif'n—gasification, HC—hydrocarbon, hetero cat—heterogeneous catalysis, hyd'n—hydrodynamics, MeOH—methanol, mol sieve—molecular sieve, n-composite—nano-composite, opt'n—optimization, oxid'n—oxidation, P—pressure, red'n—reduction, sep'n—separation, T—temperature, X—conversion.

trace compounds detected by XRF relate to the artifacts' origins.[114]

Environment XRF detects pollutants in various environments like soils, waste, materials, and sediments, like those near a crude oil facilities in the Niger Delta.[115]

Medicine XRF is used for the detection of elements in blood, heavy metals in tattoo ink, and non-radioactive iodine assimilation. [116]

Industry Industrially, XRF determines the compositions of minerals and rock. It measures the concentration of P,S,Cl,K, and Ca in phosphate rock, for example, which is necessary for phosphate processing. [117] XRF was used to determine potassium content of illite in Canadian oil sands. It proved more reliable with a better tolerance to surface contamination compared with other techniques such as methylene blue titration.[81]

In the chemical engineering research, we apply the technique to determine the success of slime coal particle separation and then to validate a computational fluid dynamics (CFD) method (green cluster).[107] XRF also determined the copper content after a novel bioleaching process to selectively recover precious metals from waste of electrical and electronic equipment (WEEE) (blue cluster). [103] These examples demonstrate the reach and versatility of the XRF spectroscopy technique.

3.5 UNCERTAINTY AND ERRORS

Portable XRF (PXRF) units are popular because they cost less then desktop units and are easy to transport from one site to another. However, laboratory/desktop XRF instruments detect more elements than portable systems (Na to U) and are more precise and accurate. Industries and miners apply PXRF mostly for qualitative analysis (blue cluster).[118]

3.5.1 Error sources and limitations

Limitations of XRF include the following:

1. Interference effect: Interference errors are linked to the background and other characteristic emissions lines. Background interference can be removed by a fine measuring of the background and subtracting it from the measurement. This is especially critical when background peaks are close to the elements in the sample.[119]
   Spectral interference—overlapping fluorescent (emission) lines. The tail of one peak overlaps the centre of an adjacent element to increase the intensity of this peak, which

then overestimates the concentration. To account for this phenomenon requires standards to determine the real element contribution. Alternatively, we use secondary emission lines on the spectrum where there is no overlap.[119, 120]

2. Matrix effect: The intensity of the emission line depends on the composition and morphology of the sample, which compromises the relationship between fluorescence X-ray and concentration: [119, 121]

   (a) Absorption effect: Fluorescent photons are partially absorbed by the sample before reaching the detector. This underestimates element concentration because it attenuates the signal intensity.

   (b) Enhancement effect: Contrary to the absorption effect, fluorescent photons from the sample excite other elements, increasing X-ray emission. This overestimates concentration.[119]

   We mitigate the matrix effect with calibration, mathematical models, or introducing empirical values. [121, 122] Usually, XRF software corrects for these, but require data.

3. Depth resolution: While it is possible to increase X-ray penetration by increasing the beam energy, different atoms will return fluorescent X-ray at different depths. Silica will only return photons from 20 pm, while zirconium fluoresces from 3.4 mm Therefore, some elements are more identifiable at low concentrations. [123]
   Penetration depth, x, varies with the the following [123]:

$$x = -\ln \frac{I}{I_0} \left(\frac{\rho}{\mu} \right) \tag{3.7}$$

   where I is the intensity of photons returning from the sample, I_0 is the number of photons entering the sample, $\frac{\mu}{\rho}$ is the mass attenuation coefficient of a given element for a particular matrix, and ρ is the object density.

4. Sensitivity: Factors that limit sensitivity include sample composition, sample preparation, and conditions of measurement. It is defined by the number of photons counted by the detector versus the number of photons that pass through it. Thin detectors might allow the photons to pass without triggering a signal. In the range of the X-rays, the photo-effect predominates with respect to photon detection, and thus a 10 mm thickness for the scintillator is sufficient.

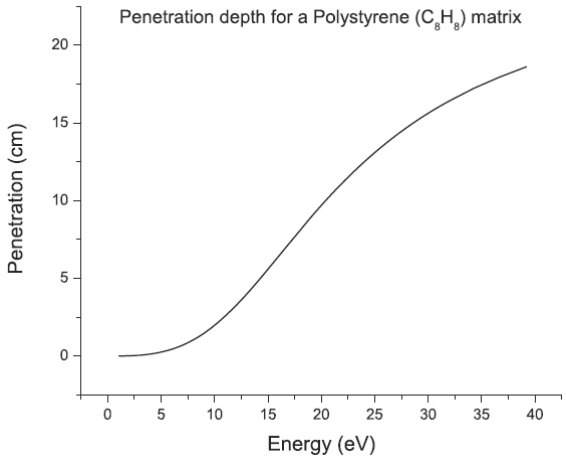

Figure 3.12 X-ray penetration in a polystyrene C_8H_8 (PS) matrix assuming a density of $1.04\,\mathrm{g\,cm^{-3}}$. Photons penetration at 40 kV reach 200 mm.

5. Lowest limit of detection: X-rays generated and detected are random and the the intensity depends on the dwell time, and so follow a statistical distribution forming a Gaussian distribution.

Table 3.4 International recommendations and nomenclature on analytical detection and quantification on concepts. [62]

Concept	**Symbol**	**Definition**
Critical Level	LC	Minimum signal an instrument may reliably recognized as 'detected'
DetectionLimit	LD	The net signal level that can beexpected to lead to detection
DeterminationLimit	LQ	The signal level over which thesignal could be quantified

Abbreviations: LC, critical level; LD, detection limit; LQ, determination limit.

XRF is a mass analyzer and requires a substantial sample: diameter above 10 mm thickness greater than 2.5 mm for ED-XRF. [114] For smaller samples, laser ablated inductively coupled plasma spectrometry (LA-ICP-MS) is better suited. [124] The sample depth depends on the incident radiation and the element of interest (Table 3.5).

3.6 Experimental procedure

1. Sample preparation: This is a critical step as it impacts both accuracy and precision.[125] The size and shape of the sample depends on the instrument being used.

2. Instrument setup: Set the measurement conditions, such as known element present in

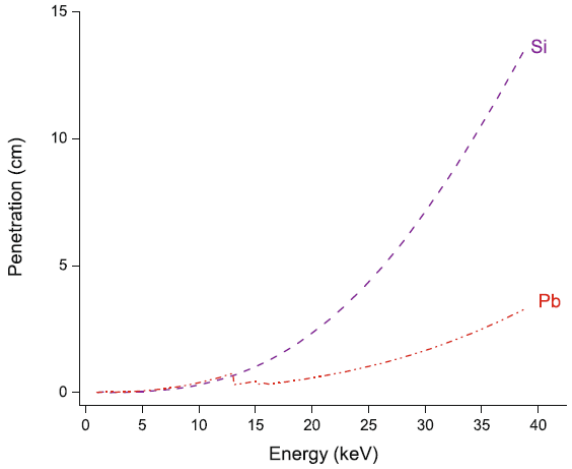

Figure 3.13 X-ray penetration comparison between Si and Pb.

Table 3.5 Analysis depth.

Material	**Mg Kα μm**	**Cr Kα**	**Sn Kα**
Lead	0.7	4.5	55
Iron	1	35	290
SiO_2	8	110	9000
$Li_2B_4O_7$	13	900	46000
H_2O	16	1000	53000

the sample, elements that are absent, voltage, filters, sample mass, dimensions when possible, and measurement time. A calibration might be needed occasionally to improve sensitivity togther with an element library, which is usually included with the instrument.

3. Sample analysis: The samples is then placed in the instrument according to the sample preparation and analysis method selected. A safety procedure to ensure that the XRF analysis chamber is well closed is recommended (usually the instrument has safety protocols).

4. Data analysis: The results reported by the instrument software.

5. Quality control: We recommend repeating the measurements multiple times to evaluate the repeatability. Introducing standards to calibrate the signal increases the confidence in the accuracy.

3.6.1 Sample preparation

A sample diameter greater than 10 mm and thicker than 2.5 mm are optimal for ED-XRF analyses.[114] An accurate analysis requires a sample surface layer that is homogeneous and representative of the bulk sample. For solid samples or metals that are coated or oxidized in air, grinding and polishing removes the rust and coating layers. For powders, both a supporting film to place under the sample or pressing the sample into a tablet works well.

3.6.2 Case of study

In the plastic industry, XRF has several advantages:

1. It identifies elemental composition rapidly (from seconds to minutes) and accurately quantifies elemental composition of contaminants and additives such as pigments, fillers, stabilizers, or flame retardants for quality control and environmental compliance.[126]

2. It is a non-destructive technique so we can apply other spectroscopic or mechanical measurements, which is particularly important for research when only small quantities are available and for expensive or irreplaceable parts.[127]

3. Its high sensitivity and accuracy in determining concentrations of trace elements—impurities or contaminants—to evaluate their impact on material properties and quality.[128].

4. Compared to most other methods (like mass spectrometry), it is cost effective, more accessible to a wider range of users, and apt for quality control with frequent analyses.

Plastic pollution and its impact on the environment is a growing concern as micro-plastics form when it degrades. Besides the increase in micro-plastics in bodies of water, additives are also a concern. Brominated fire retardant additives (BFRs) (piolybrominated diphebyl ethers [PBDEs] and polybrominated byphenyls [PBBs]) were the preferred class of compounds to meet fire safety norms for electric and electronic plastics. These fire retardants are currently banned because of their impact on the environment and their health hazards—endocrine disruption, neurotoxicity, and developmental toxicity. [4, 129–132] As of July 21, 2023, Australian authorities require importers to apply for a special authorization to import decabromodiphenyl ether (decaBDE). [133] These compounds limit recyclability. Companies that want to use WEEE plastics as a feed-stock for, among others, recycling or waste-to-energy must remove BFRs. XRF instruments are a prime means to pre-sort polymers to minimize contamination. However, companies must certify material composition with more

detailed analyses (GC-MS, for example) of the extracted BFRs to meet international norms like IEC 62321-6.

Table 3.6 XRF elemental analyses of a WEEE HIPS sample (PS-FR(17) code). Note the very high concentration of Br and Sb. Each of the four rows of data are XRF measurements from different pieces of the same WEEE plastic part that had been ground down For each row represents at least 4 measurements to calculate $\pm s$ ($n \geq 4$)

	Ca (ppm)	Fe (ppm)	Ni (ppm)	Zn (ppm)	Se (ppm)	Br (ppm)	Sb (ppm)
Sample 1	241 ± 8	91 ± 5	10 ± 9	96 ± 3	190 ± 4	62 000 ± 46	2800 ± 6
Sample 2	205 ± 2.2	24 ± 1.4	0 ± 1	100 ± 3	230 ± 5	100 000 ± 74	5000 ± 7
Sample 3	247 ± 8	164 ± 7	16 ± 6	112 ± 4	150 ± 4	77 000 ± 62	3300 ± 7
Sample 4	189 ± 6	19 ± 4	9 ± 5	122 ± 4	340 ± 5	76 000 ± 69	5100 ± 9

As part of the project to debrominate electronic plastics, we analyzed several waste samples. The analyses detected Br and other elements in the plastics of WEEE devices (Table 3.6) with Br concentrations reaching 10 % of the total mass and Sb up 0.5 %. The accuracy of the measurement is quite good with a standard deviation of < 0.1 % of the Br and high concentration and < 5 % for the all the other elements except Ni. The distribution of Br in the sample varies by 40 %! Industry detects bromine in plastics with XRF guns and the results are comparable to GC-MS. [48] XRF and XRF guns have many advantages compared to GC such as portability, speed, and ease of sample preparation. However, matrix effects and peak overlapping compromise accuracy when neglected. The type of sample and its preparation is a key factor to maximize the repeatability. In 3.7, we demonstrated the accuracy and reliability of XRF guns to analyze polymers, and for this reason industry uses the instrument so readily. We do, however, recommend repeating measurements as many as 5 times, and as demonstrated above, when the elements are distributed unevenly, multiple samples must be taken from different areas to ensure that it is representative of the whole piece (Table 3.6): the standard deviation of the Br measurement was less than 1 % but differences between samples from different areas of the piece were up to 40 000 ppm The heterogeneous distribution could also be due to the manufacturing.

Here, we compare the concentration of 10 samples from a Bruker S1 TITANXRF gun with a neutron activation analysis (NAA) (Table 3.7). Although the standard deviation of the error is 22 %, the range of concentration varies over four orders of magnitude (10 to $> 100\,000$). Presumably, the NAA data best represent the actual concentration of BFR in the sample, so the gun overestimates the true value.

XRF produces both qualitative and quantitative data. Quantitative analyses require mass,

Table 3.7 A validation table comparing the bromine concentration measured by a Bruker XRF TITAN S1 gun and neutron activation analysis (NAA) (Slowpoke reactor at Polytechnique Montreal).

Sample	m g	x_{Bruker} µg g^{-1}	x_{NAA} µg g^{-1}	% error $\frac{x_{\text{Bruker}}-x_{\text{NAA}}}{(x_{\text{Bruker}}+x_{\text{NAA}})/2}$
1	0.55	282	208	30 %
2	0.68	61	36	51 %
3	0.41	20	20.5	-2 %
4	0.91	92 000	97 400	-6 %
5	0.68	100 000	93 000	7 %
6	0.39	32	17	62 %
7	0.64	392	333	16 %
8	0.59	113 000	99 000	13 %
9	0.39	140 000	94 500	39 %
10	0.27	119 000	97 800	20 %

density, suspected elements in the sample, dwell time, and calibration standards for the software. The elemental concentration is ultimately calculated statistically based on both measurement and input parameters. Qualitative analyses require less input data and report sample composition to a lesser degree of accuracy. XRF qualitative analyses are fast and relativity easy to interpret. [121] The spectra present a series of peaks representing the detected photons per second (cps) at a specific energy (y-axis represents intensity, whereas x-axis is energy).

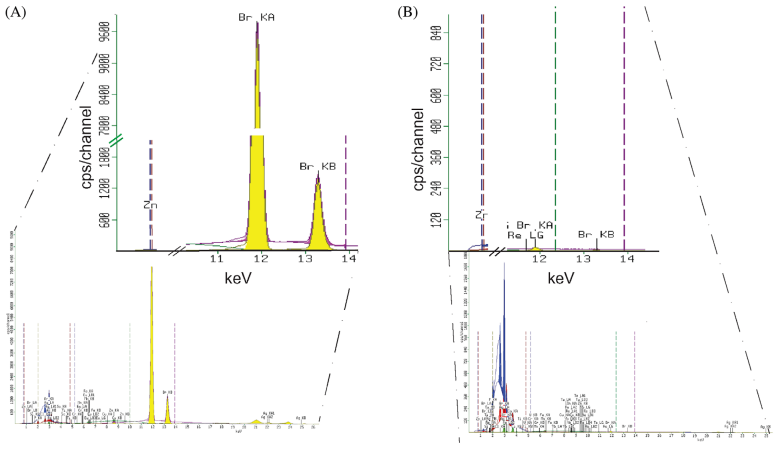

Figure 3.14 XRF results from a plastic sample containing brominated fire retardant before and after treatment. The peak difference relative to the bromine energy lines at 12 kV are clearly evident.

The Br KA peak height of a WEEE plastic approaches 10 000 cps before treatment (Figure 3.14 left panel). After the debromination treatment of these end-of-life plastics, the Br KA peak virtually disappeared, barely reaching 12 cps (Figure 3.14 right panel). With this spectrum, we deduce that that the treatment method is very efficient, although we are incapable of assigning a final Br concentration or the scavenging efficiency as it is only a qualitative analysis. This approach is suitable to quickly determine some results, or to find elements and their relative abundance in the sample when the sample's composition is unknown.

3.7 CONCLUSIONS

XRF spectroscopy detects species composition from concentrations of 1 ppm to 100 % of any element from Na to U, without destroying the sample. Portable XRF guns are versatile and report Br concentration within about 25 % of neutron activation analysis. To achieve higher accuracy requires a detailed calibration with a precise sample preparation procedure, which depends on the matrix, the elements of interest, and the sample state (solid, liquid, powder...). Furthermore, quantitative analyses require some knowledge of the sample to be able to account for the limitations of the technique. However, even without prior knowledge of the sample composition, XRF analysis is capable of qualitative analysis. Many instruments, like the Epsilon 4 from Malvern Panalytical, come with a pre-calibration routine for all elements that facilitates quantitative analysis.

CHAPTER 4 ARTICLE 2: ALKALINE SOLVOTHERMAL DEBROMINATION OF COMMERCIAL BROMINATED POLYSTYRENE

Mario Ferreiro Gonzalez, Fernanda Cabañas-Gac, Gregory S. Patience

Article published in the journal Recycling from MDPI editorial, Published: 1 June 2025

4.1 Government regulations required consumer products—electrical and electronic components, toys, furniture, clothing, and cars— to meet ever increasing flame resistance standards, and industry met these norms by adding brominated fire retardants. However, end-of-life treatment and up-cylcing of these plastics is challenging as the brominated compounds are endocrine disruptors, bioaccumulators, and persist in the environment. Pyrolysis, catalytic cracking, or combustion, to recover its fuel value, produces toxic brominated dibenzodioxins and dibenzofurans Here, we demonstrated the efficacy of a solvothermal treatment that extracts up to 99 % of the bromine from high impact polystyrene (HIPS) and polystyrene (PS) in electrical and electronic waste—e-waste. The process operated between 160 °C to 230 °C with ethylene-glycol or triethylene-glycol as solvent and NaOH or KOH as extraction agents (0.5 M to 2 M). Reaction rates depended on the particle size: 60 mm plastic chunks took up to between 4–24 h to react while fibres 3 mm in diameter reacted in less than 5 min.

4.1.1 keywords

Fire retardants, Polymers, Recycling, Solvothermal treatment, Alkali debromination, HIPS, High Impact Polystyrene, PS, Polystyrene Brominated fire retardants

4.2 Introduction

The spread of electronic devices and the world's disposable culture plague the planet with an enormous and continuously growing amount of waste electrical and electronic equipment (WEEE). According the European Union (EU), 13 500 kt of WEEE were sold in 2021 (Table 4.1). Of these, roughly 4900 kt were collected and 4800 kt were treated. More than 90 %

was recycled or recovered as energy (4400 kt). Finally, over 90 % (4000 kt) was reused. The average WEEE production per EU citizen for the period 2018-2020 was $12\,\mathrm{kg\,y^{-1}}$, whereas the recovery for 2021 was estimated at $5.5\,\mathrm{kg\,y^{-1}}$. The EU (Directive 2012/19/EU) target was 65 % recovery by 2019, however only Bulgaria and Slovakia reached this target.[5]

Table 4.1 Electrical and electronic equipment (EEE) put on the market and waste of electrical and electronic equipment (WEEE) collected, treated, recovered, and recycled in the EU in the period of 2012 to 2021. Values given in thousand of tonnes.[5]

	2012	2013	2014	2015	2016	2017	2018	2019	2020	2021
Sold on the market	7.6	7.2	7.5	8.0	8.5	9.0	10.2	11.2	12.4	13.5
Collected	2.9	3.0	2.9	3.2	3.5	3.7	3.9	4.5	4.7	4.9
Treated	3.1	3.1	2.9	3.1	3.5	3.7	3.9	4.4	4.6	4.7
Recovered (recycling, energy recovery, ...)	2.5	2.7	2.6	2.8	3.2	3.4	3.5	4.0	4.3	4.4
Reused and recycled	2.4	2.5	2.4	2.6	3.0	3.1	3.2	3.6	3.9	4.0

Despite falling short of the EU target, collection of WEEE has increased steadily over the last several years (Table 4.1). The content of metals (including precious metals), rare elements and other compounds such as plastic, make WEEE a great source of secondary raw materials; in 2016 alone, raw materials from WEEE were valued at 55 billion Euros. The potential value of some materials available from WEEE are: 16 000 kt of iron valued at 3600 million Euro, 2200 kt of Cu at 9500 million Euro, and 12 000 kt of plastics are valued at 15 000 million Euro [134]. High-impact polystyrene (HIPS) comprises 25 % of the plastic in WEEE and 20 % of the WEEE is plastic.

Charitopoulou et al. estimated that 7 % of WEEE plastics contain brominated fire retardants (BFR). [135] Recovering these materials with poor infrastructure may bring more harm than benefit, releasing toxic compounds (affecting primarily those handing it) and generating greenhouse gases. Finding alternatives to close the loop has become a primary objective for sustainable development, which can be addressed by increased recyclability (e.g. designed for disassembling), development of recovery processes, refurbishing, etc. Toxic compounds confound recycling plastic from e-waste because of the extra process steps and it requires dedicated management systems. Moreover, PS waste that ends up in the ocean break into micro particles potentially releasing the additives, which further increases societies concern about these polymers. [136] Unfortunately, handling and stricter environmental regulations have increased cost, making recycling of WEEE less attractive. Developed countries have opted to land-fill or export their WEEE to developing countries where handling and recycling regulations are less onerous and the labour forces is less costly. [57] The recovery and recyclability problems are compounded when taking into account that most of WEEE plastic have a life span of around 10 years: most of the plastic reaching recovery facilities currently

was fabricated 10 years ago. Therefore there is a gap of 10 years before these additives are out of the end-of-life polymers if we ban all BFR now. [11]

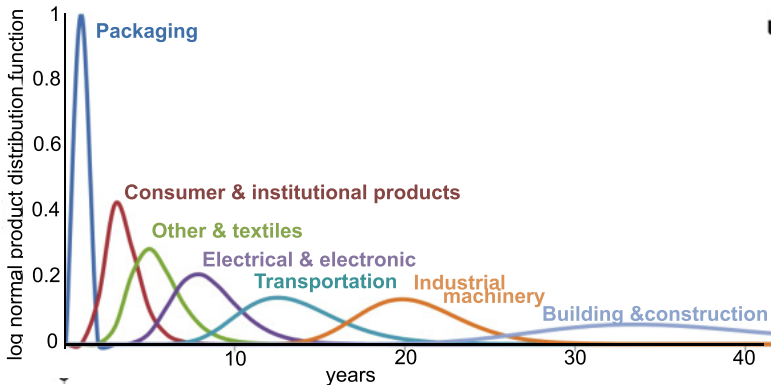

Figure 4.1 Average market life from industrial products from fabrication to end-of-life. [11]

BFR are defined as organic molecules with various configurations of bromine atoms bonded to the molecular backbone.[137] The most abundant are polybrominated biphenyls (PBBs), polybrominated diphenyl ethers (PBDEs), and tetrabromobisphenol A (TBBPA). BRFs are manufactured by replacing hydrogen atoms of the diphenyl oxide structure with bromine atoms. The number of bromine atoms varies from 3 to 10 atoms depending on the reaction chemistry. Commercially BFRs comprise a range of PBB, PBDE, and TBBA. PBBs were discontinued voluntarily in the US after the 1973–1974 agriculture contamination crisis in Michigan.[138] Thus, the current extent of PBB in consumer products is low since manufacturers replaced it by the two alternatives. Metal synergistic additives like antimony oxide (Sb_2O_3) accompany BFR.[26, 37]

This research focuses solely on brominated fire retardants. Currently, most technology to debrominate WEEE degrades the polymer and produces unrecoverable byproducts and monomer whose remaining value is a fuel.[139] However, combusting and pyrolyzing (thermal degradation on the absence of oxygen) these compounds and mixtures produces toxic brominated dibenzodioxins and dibenzofurans. [140] Besides toxic compounds, pyrolysis generates char, oil, and syngas. Conventional pyrolysis, fast pyrolysis and slow pyrolysis have been tested for Br-HIPS: Fast and slow pyrolysis yields the highest amount of fuel and chemicals.[141] In a fixed bed reactor, pyrolysing Br-HIPS at 430 °C produced an oil with 12 % Br (76 % of the bromine in the plastic). [142] When Br-HIPS was pyrolyzed in a fluidized bed reactor from 450 °C to 550 °C, the oil contained more than 90 % of the bromine.[143] Further treatment is required, either before or after pyrolysis to extract all of the bromine from the oil. Catalytic cracking has several advantages compared to a strictly thermal treatment:

It reduces the reaction time and temperature while improving product quality and reducing the percentage of undesirable by-products. Silica-alumina, zeolites, metal based catalysts, and minerals have been developed. [141] Oil yield with BaO as a catalyst exceeded 93 %, with 76 % styrene monomer, and 18 % dimer. [144] However, a second step was required to remove the Br to repolymerize the styrene. BFR and antimony interfere with the catalytic reaction due to the modified thermal behavior compared to pure polymers. Sodium zeolite effectively release the Br from the WEEE, however, it remains with the oil [140, 145]. Hydrothermal treatment degrades polymer at lower tempeature than pyrolysis. In situ treatments remove bromine and antimony from the produced oil. Researches have reported 96 % debromination of Br-HIPS at 280 °C polypropylene as a reductive agent; also, supercritical CO_2 debrominated 97 % of a HIPS sample reducing the concetration of Br below 0.1 %. The low Br concentration in the oil comes at the expense of energy to achieve supercritical conditions.[141] Bromine was also extracted from Br-HIPS with an autoclave at 280 °C, with the addition of polypropylene as H_2 source. The product oil contained 1.2 % of the original Br, while the water retained the rest of the Br as a HBr.[146] Co-pyrolysis, pyrolysis of two or more compounds simultaneously, improved oil yield without catalyst, solvent or chemicals. Polypropylene and polyethylene react synergistically with the HIPS to achieve high debromination rates. The quality and quantiy of the wax and oil depends on the source of Br-HIPS and how much PP is added. Co-pyrolysis Br-HIPS has also been tested with biomass/coal yielding 62 % of oil compared to 53 % oil of pyrolysis of Br-HIPS alone with bromine staying with the char rather than in the oil.[141] Alkali compounds, calcium, sodium, and potassium, capture bromine in situ when it is released during thermal and supercritical decomposition. [141, 146] Similarly, an ammonia quench traps Br after it is released and becomes volatile. [147] Since ammonia can trap HBr, it can convert more than 90 % of the mass fraction of bromine to inorganic ammonium bromine. Grause, et al. (2015) extracted bromine from HIPS without destroying the polymer matrix: Decabromodiphenyl ethane reacted in a ball mill charged with a solution of ethylene glycol (EG) and 0.5 M NaOH at 190 °C for 24 h to recover 98 % of the Br.

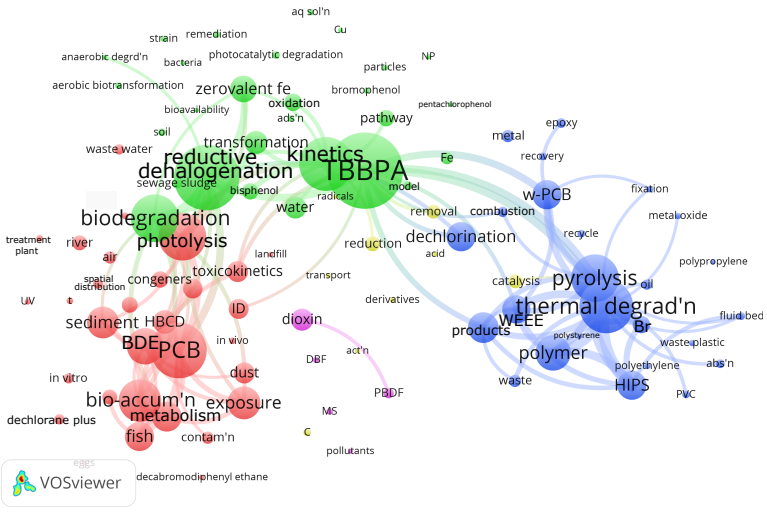

Figure 4.2 Plastic/flame retardant debromination bibliometric map of >100 most mentioned keywords in the 561 articles indexed by Web of Science.[9, 10] The size of the nodes correlates with the number of articles the keyword appears in the database. The smallest nodes represent 6 articles, while the largest node (TBBPA) represents 86 articles. The keywords that appears most in each of the clusters are: red: PCB (polychlorinated biphenyl (in 63 articles with 33 keywords in the cluster), green: TBBPA (tetrabromobisphenol) (in 86 articles with 29 keywords in the cluster), blue: thermal degradation (in 61 articles with 25 keywords in the cluster) yellow: reduction, (in 17 articles with 11 keywords in the cluster), and magenta: dioxin (in 25 articles with 5 keywords in the cluster). The 100 lines drawn in the maps connect articles that cross-reference each other. We excluded several keywords because they were either redundant or the nodes were too big and would overlap other keywords too much: red, PBDE (polybrominated diphenyl ether) —233 occurences, blue, debromination —224, red, BFR (brominated flame retardant) — 208, blue, degradation — 127, red, decabromodiphenyl ether — 116, blue, fire retardant — 96. Abbreviations: abs'n—absorption, act'n—activation, ads'n—adsorption, aq sol'n—aqueous solution, BDE—brominated diphenyl ether, C—carbon, contam'n—contamination, DBF—dibenzofuran, HBCD—hexabromocyclododecane, HIPS—high impact polystyrene, MS—mass spectrometer, NP—nanoparticle, PAH—polycyclic aromatic hydrocarbons, PBDF–,-olybrominated dibenzofuran, PCB—polychlorinated biphenyls, PVC—polyvinyl chloride, reductive dehalogen'n—reductive dehalogenation, spatial dist'n—spatial distribution, t—time, TBBPA—tetrabromobisphenol, thermal degrad'n—thermal degradation, UV—ultraviolet irradiation, and WEEE—waste electrical and electronic equipment.

We generated a bibliographic map based on VOSViewer open software and the Web of Science reference data base to assess the research focus around debromination of flame retardants in plastic. Web of Science has indexed 2320 articles with debromination as the keyword in the "All Fields" search field. We manually searched for articles in this selection with keywords "retardant" OR "suppressant" and "flame" OR "fire", and "polymer" OR "plastic", which

reduced the number of articles to 561. VOSViewer grouped the 110 most often mentioned keywords into 5 clusters. The red cluster has 33 keywords including PCB (polychlorinated biphenyl), photolysis, bioaccumulation. VOSViewer assigned 29 keywords to the green cluster centred on TBBPA (tetrabromobisphenol), reductive halogenation, biodegradation. The blue cluster with 25 keywords is dedicated to thermal degradation, pyrolysis, polymers including HIPS, polystyrene, polyethylene, and polypropylene. The yellow and magenta clusters have 11 and 5 keywords respectively.

In this work, we test solvothermal methods to extract Br from commercial brominated-HIPS — waste electrical and electronic equipment (specifically from printers). Our focus has been to test glycols with a reasonably high boiling point to accelerate the reaction kinetics and diffusion of alkali (reacting species) and glycol. We show that reaction rates in filamentous HIPS is orders of magnitude higher than for bulk HIPS.

4.3 Results and discussion

Unlike experiment-design blends of polymers and brominated fire retardants, end-of-life plastic contains various additives; antimonium oxide added with halogenated fire retardants, for example.[148] Commercial plastics have carbon black, TiO_2, and glass fiber, all of which impact debromination rates. Strong alkalis scavenge bromine atoms from fire retardant compounds.

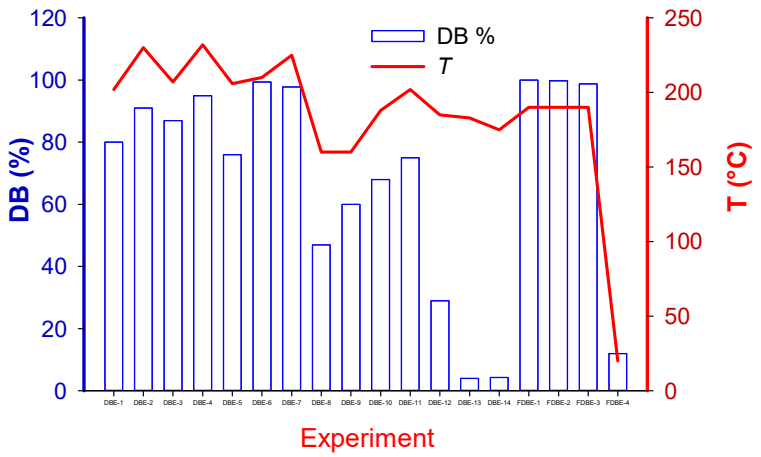

Figure 4.3 Debromination achieved in each experiment and its temperature correlation.

The final element of the reaction sequence is expected to be either NaBr or KBr. Antimony trioxide Sb_2O_3 appears to be inert in this reaction and remains with the polymeric matrix or

in the solvent. To account for the contribution of each factor to the extent Br was extracted from the sample (Figure 4.3), X, we assumed a completely backmixed reactor model with a first order reaction rate, $-r_{\mathrm{Br}} = kC_{\mathrm{Br}}$, where k is the rate constant, t is time, and V is volume:

Variable Descriptions

C_{Br}: Concentration of brominated species.

E_a: Activation energy.

k': Rate constant.

k: Regression rate constant accounting for contributions from factors in Design of Experiments (DOE) .

k_0: Rate constant at T_0.

$r_{C_{\mathrm{Br}}}$: Reaction rate of brominated species.

R: Universal gas constant.

t: Time.

T: Temperature.

T_0: Reference temperature (150 °C).

TEG: Factor representing the use of TEG as solvent (2 for TEG, 1 for EG).

V: Volume of solvent.

d_{pellet}: Pellet morphology factor (1 for large pellets, 2 for filament).

X: Conversion factor.

ω: Agitation rate.

$\beta_1, \beta_2, \beta_3, \beta_4, \beta_5$: Exponents for reaction rate dependencies.

$$\frac{\mathrm{d}C_{\mathrm{Br}}}{\mathrm{d}t} = -r_{C_{\mathrm{Br}}} = kC_{\mathrm{Br}} \tag{4.1}$$

$$\frac{\mathrm{d}X}{\mathrm{d}t} = k(1 - X) \tag{4.2}$$

$$X = 1 - \exp\left(-kt\right) \tag{4.3}$$

where the reference temperature, T_o, is 150 °C

$$k' = k_o \exp\left[\frac{E_a}{R}\left(\frac{1}{T} - \frac{1}{T_o}\right)\right] \tag{4.4}$$

Standard statistical models assume a linear relationship to characterize the relationship between the primary variables and factors, but they often miss the fact that the relationships are related to power laws.[149]

Therefore, we introduced power law expressions to account for how the reaction rate, k, varies with the factors—V (volume of solvent), TEG (=2 with TEG as solvent, 1 with EG as solvent), KOH (=2 with KOH as an extracant, 1 with NaOH as extractant), ω (agitation rate), d_{pellet}, (pellet morphology: 1 = large pellets, 2 = filament).

$$k = k'V^{\beta_1} \cdot [\text{NaOH}]^{\beta_2} \cdot \text{TEG}^{\beta_3} \cdot d_{\text{pellet}}^{\beta_4} \cdot \omega^{\beta_5} \tag{4.5}$$

Assigning a value of 1 or 2 to the stochastic factor accounts for how the reaction rate depends on them quantitatively. For example, the best fit exponent for NaOH is 0.8, so the reaction rate constant is greater by $2^{0.8} = 1.7$ with NaOH versus KOH. The best fit expression that fit the experimental data for k becomes.

$$k = 0.15 \exp\left[\frac{71000}{R}\left(\frac{1}{T} - \frac{1}{T_o}\right)\right] \cdot V^{0.5} \cdot [\text{NaOH}]^{0.8} \cdot \text{TEG}^3 \cdot d_{\text{pellet}}^{10} \tag{4.6}$$

The exponent for d_{pellet} ($\beta_4 = 10$) translates to a kinetic rate constant $1000 \times (2^{10})$ higher for the filaments compared to the pellets. This would indicate that mass transfer in the plastic matrix limits reaction rates. The TEG solvent is 8 times more effective than EG, but this might also be due to the possibility of working at higher temperatures, i.e. solvent and temperature as factors might be confounded. Unsurprisingly, the stirring rate has no substantial contribution to reaction rate as mass transfer across the matrix must be limiting. The model — Eqs. 4.4,4.6—accounts accounts for 92 % of the variance in the data (Figure 4.4).

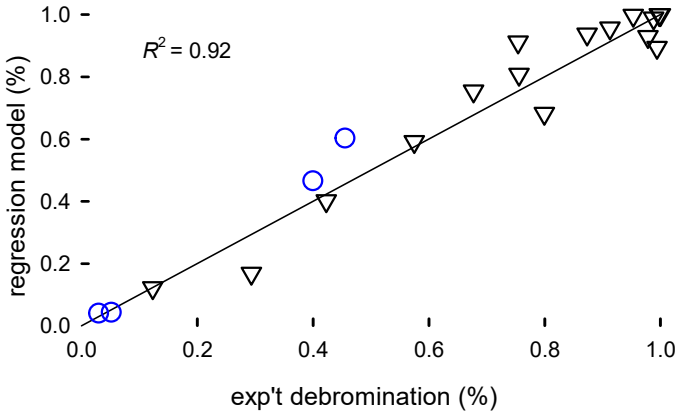

Figure 4.4 Parity plot of the model fit of the extent of bromine extracted from the HIPS, X (Eq. 4.6), versus the experimental data. The correlation was based on the experimental data represented by the black inverted triangles. The blue circles are predicted values from the model that were excluded from the fitting.

This statistical model estimates the energy of activation (E_a) is equal $71\,\mathrm{kJ\,mol^{-1}}$, which is higher than expectation since mass transfer is limiting the rate. To fully characterize the reaction, we coupled the effluent gas to an on-line mass spectrometer to monitor the concentration of non-condensable gases. The MS detected a low level of methane after 3 h of reaction. (Figure 4.5).

Scale-up of statistical models for scale-up are hazardous but this psuedo-engineering model advocates micronizing pellets to increase surface area, using NaOH, higher temperature, and TEG. A more focussed experimental design would better substantiate how the reaction rate changes with concentration, pellet size/morphology, and temperature. While building the model, we excluded four data points to later assess how well it predicts conversion. The model fits two of the data points at very low conversion (< 5 %) surprisingly well. At higher conversion, the model is less accurate but reasonably good considering the breadth of the conditions in the screening design.

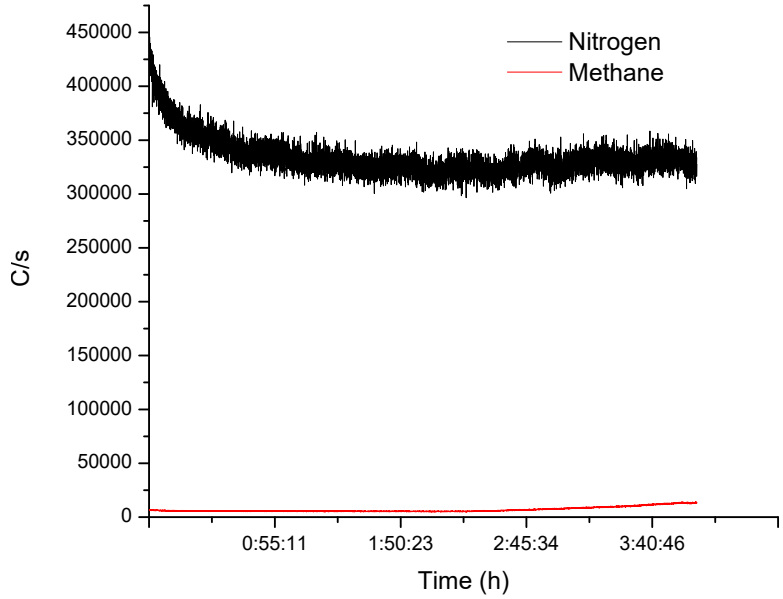

Figure 4.5 MS signal measure at the exit of the reflux column while debrominating HIPS. After 3 h on stream, the MS detected methane. Although the increment was small compared to the N_2 carrying gas: it increased with time and plateaued after 4 h.

4.3.1 XRF

XRF was used to determine Br content in the plastic samples and the solvent (Table 4.2). XRF has proven to be a fast and reliable technique to measure Br.[150] Because it is a non-destructive analysis the same sample could be characterized with complementary techniques such as FTIR and TGA.[82, 151] Additionally, the instrument results were validated regularly with RoHS standards to guarantee its fidelity. Table 4.3 represent the main transition energies for the most common elements present within polymeric matrix. These transition energies of the elements correspond to the peaks present on the XRF spectra (Figure 4.6)

Although XRF is a superficial analytical technique it is suitable for our application. Penetration depth in the polymeric matrix is higher than in other materials and bromine is heavy enough to be easily detectable by this technique. There are articles already comparing the results of XRF capability to quantify Br elemental concentration on different polymeric samples reaching precision of GC-MS techniques. [48, 152, 153] We did make the needed measures to improve the representativity of the measurements by measuring each piece at least 5 times, different pieces from each bath were measured and the thickness was never higher than 2mm. It is reasonable to assume that the concentration would be homogeneous throughout the polymer. Other techniques such as ICP analysis would have been an ideal complement to this study, However, as we were aware of the limitations of the XRF, and we

wanted to ensure that our results are trustworthy, our equipment was calibrated and checked periodically with RoHS calibration standards. Finally, to elevate our confidence even more, we analyze different polymeric samples with different Br content and then send them to the neutron activation analysis (NAA) laboratory at Polytechnique Montreal, proving the validity of the method. [150] (results are shown on table 7) The equipment used was specifically calibrated by its use on the plastic industry, with specific mode to target RoHS compounds, primarily Br.

All the samples were measured 5 times before and after reaction. The reaction media leached some of the metal additives and contaminants.

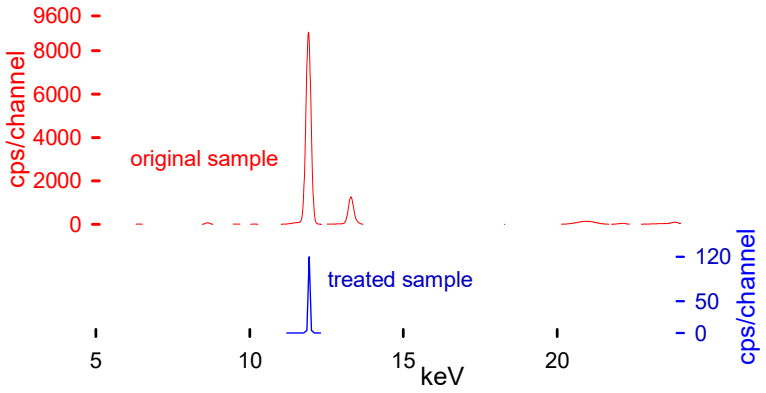

Figure 4.6 XRF spectra before (upper plot in red) and after treatment (lower plot in blue). An Epsilon4 instrument measured the Br concentration operating with an Ag 50 anode tube, SDD10P detector, Ag 100 filter, at 50 000 kV, and 0.2 mA in air.

4.3.2 FTIR

FTIR shows (Figure 4.7) that the treatment removes the polybutadiene fraction of HIPS, since its characteristic peaks are no longer presents on the FTIR. It is unclear if its being removed or undergoing a side reaction (hydrolysis of double bonds from PB as suggested by Grause et al. [6]) or undergoes cross-linking. Other studies claim that OH radicals bind to the superficial aromatic rings without opening it. This hydroxyl radical additionally increases the hydrophilicity of the polymer. Since we used an alcohol and a strong base, there is enough OH radicals to react with the polymer surface. This could explain, at least partially, the persistence of the OH peak in the FTIR spectra even after thoroughly drying the polymer. The same study also shows that at high concentrations, OH and O radicals react with the

Table 4.2 Representative debromination results in 50 mL of tri-ethylene glycol (TEG) and 1 M of alkali. DBE is the code to represent debromination experiment with chunks of plastic while FDBE are filamentous samples. On average, each sample has 64 000 ppm Br.

Code	Mass g	Alkali	T °C	t min	Debromination %
DBE-1	1.02	KOH	202	240	80
DBE-2	1.06	KOH	230	240	91
DBE-3	1.20	KOH	207	480	87
DBE-4	1.06	NaOH	232	240	95[†]
DBE-5	24.96[*]	NaOH	206	240	76
DBE-6	1.03	NaOH	210	240	99.4
DBE-7	1.13	KOH	225	100	97.8
DBE-8	1	KOH	>160	1440	47[‡]
DBE-9	1.01	NaOH	>160	1440	60[‡]
DBE-10	25.23	KOH	188	720	68
DBE-11	25.17	KOH	202	720	75
DBE-12	100.52	KOH	185	240	29
DBE-13	1.11	KOH	183	240	4[‡]
DBE-14	1.08	KOH	175	240	4.3[‡]
FDBE-1	0.0053	NaOH	190	2	99.97
FDBE-2	0.0064	NaOH	190	2	99.79
FDBE-3	0.095	NaOH	190	5	98.81
FDBE-4	0.14	KOH	20	1440	12

[†] All tests were conducted with agitation except this test.
[*] 100 mL TEG.
[‡] Tests excluded from the parameter estimation.

Table 4.3 Photon energies of principal K, L, and M-shell emission lines (in keV)

Element	**K**α_1	**K**α_2	**K**β_1	**L**α_1	**L**α_2	**L**β_1
Cl	2.62	2.62	2.81			
Ar	2.95	2.95	3.19			
K	3.31	3.31	3.58			
Ca	3.69	3.68	4.01			
Ti	4.51	4.50	4.93	0.45	0.45	0.45
V	4.95	4.94	5.42	0.51	0.51	0.51
Cr	5.41	5.40	5.94	0.57	0.57	0.58
Mn	5.89	5.88	6.49	0.63	0.63	0.64
Fe	6.40	6.39	7.05	0.70	0.70	0.71
Co	6.93	6.91	7.64	0.77	0.77	0.79
Ni	7.47	7.46	8.26	0.85	0.85	0.86
Cu	8.04	8.02	8.90	0.92	0.92	0.94
Zn	8.63	8.61	9.57	1.01	1.01	1.03
Br	11.92	11.87	13.29	1.48	1.48	1.52
Sb	26.35	26.11	29.72	3.60	3.59	3.84
Te	27.47	27.20	30.99	3.76	3.75	4.02
I	28.61	28.31	32.29	3.93	3.92	4.22

ring, opening it and leading to some cross-linking. [154] It remains unclear if these reactions even happen under our condition, and in case that they do the extent of them. None of the other analysis presents indications of a noticeable change of the polymeric properties after the treatment.

The OH vibrations at around 3500 cm^{-1} were absent in some samples. This could be due to an incomplete reaction or due to a better drying that eliminated the solvent or it could be due to a substitution reaction.[6] The fire-retardant backbone could remain inside the polymer and because its aromatic structure will be masked by the polystyrene spectra. The FTIR analysis (Figure 4.8) shows a consistent PS-like spectra, indicating that the base polymer remains unchanged by the reaction.

Selecting two points of each spectrum (one for the peak changing and one to the Aliphatic C-H Stretching that we assume remains unchanged during the process) we can normalize the results. Then, by comparing the ratios, we can determine the absolute variation.

The absorbance ratio for HIPS and DBE at different wavenumbers can be written as:

$$\mathrm{Ratio}_{\mathrm{HIPS}} = \frac{\text{Absorbance at } 2919\,\mathrm{cm}^{-1}}{\text{Absorbance at } 1539\,\mathrm{cm}^{-1}} = \frac{0.0636}{0.0439} = 1.45 \tag{4.7}$$

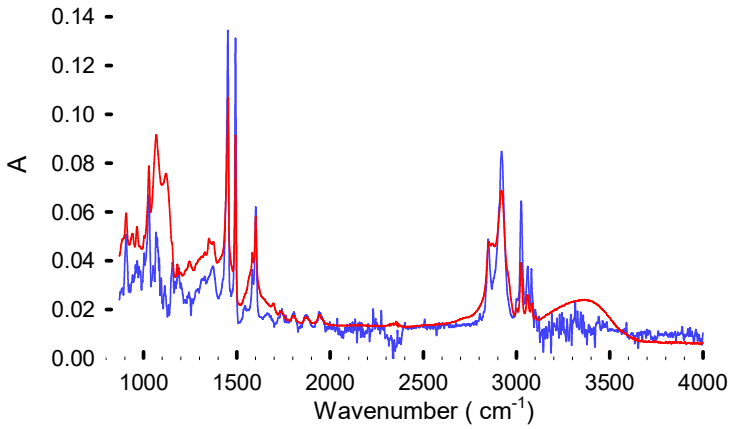

Figure 4.7 FTIR spectra from virgin polystyrene from Sigma Aldrich (in blue) the sample DBE-8 (in red) achieving 99.5 % debromination. Residual solvent is absorbed by the polymer due to the presence OH groups at 3500 cm^{-1} from the triethylene glycol

. The plot illustrates that even in the samples with the highest Br extraction, the structure remains essentially intact.

$$\text{Ratio}_{\text{DBE}} = \frac{\text{Absorbance at } 2919\,\mathrm{cm}^{-1}}{\text{Absorbance at } 1539\,\mathrm{cm}^{-1}} = \frac{0.0688}{0.0252} = 2.73 \tag{4.8}$$

where: 1539 cm^{-1} peak (associated with polybutadiene) is decreasing relative to the 2919 cm^{-1} peak (Aliphatic C-H Stretching)

- For HIPS, the ratio is approx 1.45, indicating higher presence of the polybutadiene-related peak.
- For DBE-8, the ratio is approx 2.73, indicating a less prominent polybutadiene-related peak.

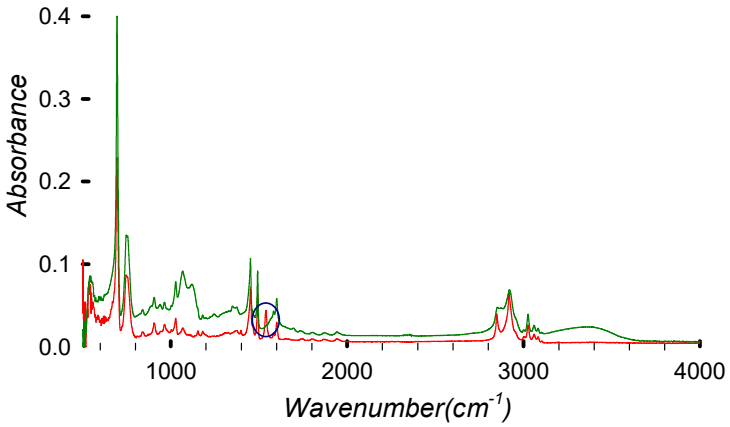

Figure 4.8 FTIR spectra of virgin HIPS (in red) compared with the debrominated (99.5 %) sample DBE-8 (in green).

Additionally, the HIPS FTIR spectra clearly show a peak at 1537 cm^{-1} related to the carbon double bond of polybutadiene. This peak disappears after the treatment, indicating the removal or degradation of polybutadiene. It is, however, possible that the polybutadiene is losing the double bond due to temperature, which could induce a cross-linking reaction and double bond loss.[155]

4.3.3 TGA and DCS

TGA results give a consistent PS-like decomposition pattern (Figure 4.9). However, the decomposition starts at a higher temperature for the debrominated polymer (HIPS 8) compared with virgin PS (green line) and and brominated HIPS (black line). This may be explained by a partial cross-linking of the polymer during the treatment, due to the presence of other components providing an increased stability, and by lower decomposition temperatures of the brominated fire retardant.[6, 156]

Sb_2O_3 shifts the curve towards lower temperature because of its synergy with brominated fire retardant. [53] The decomposition of most of the Br-FR and Sb_2O_3 in this first step also means that the remaining pattern is the polymer (HIPS) itself (Figure 4.10).

Finally, due to the high viscosity of ethylene and triethyleneglycol, they remained in the polymeric matrix, even after washing with water and drying at 60 °C for several days. The presence of EG or TEG was obvious due to their specific boiling point appearing on the TGA trace.

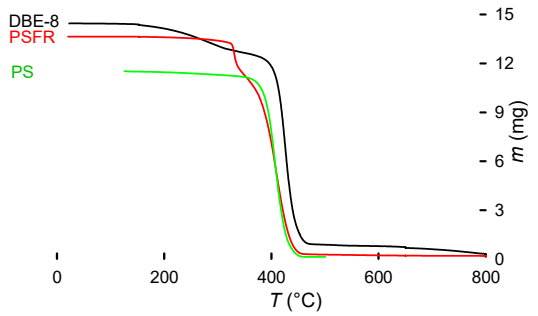

Figure 4.9 TGA of debrominated (DBE-8) compared with a brominated HIPS sample before treatment and a virgin PS sample. Is is noticeable the characteristic mass loss from the fire retardant that trigger a early decomposition of the polymer. Additionally, as stated on the FTIR section, DBE-8 sample retains part of the triethylene glycol swallowed. The TGE with a boiling point of 285 °C is slowly released from the polymer. From approximately 300 °C the decomposition curve remains PS-like.

Figure 4.10 presents the characteristic two-step decomposition of a brominated fire retardant plus Sb_2O_3 synergyst. The first occurring at about 330 °C, due to the fire retardant and Sb_2O_3 synergyst action. According E. Jakab et al [53], this is the moment when the fire-retardant mechanism starts. By scavenging radicals from the decomposing polymer (the primary function of the fire retardant), the Br coupled with Sb_2O_3 react to form $SbBr_3$. This reaction also removes some hydrogen from the polymeric chain, to then, take part in an intermediate reaction to form BrH. This hydrogen bromide reacts later with the oxygen from the Sb_2O_3 to form H_2O. Removing H from the main chain induces a beta-scission initiating the polymer decomposition (explaining the earlier decomposition when compared with not brominated equivalents). Radical scavenge increase the energy required to induce oxidation and therefore the combustion of the polymer. [53, 140, 157, 158] The last peak starting at 360 °C until 470 °C represent the normal polymeric decomposition.

Figure 4.9 additionally shows a decrease of the remaining mass at 800 °C there is a change to oxygen atmosphere to clean the pan and remove any organic remnants, providing additional information about possible additives and decomposition pathways.

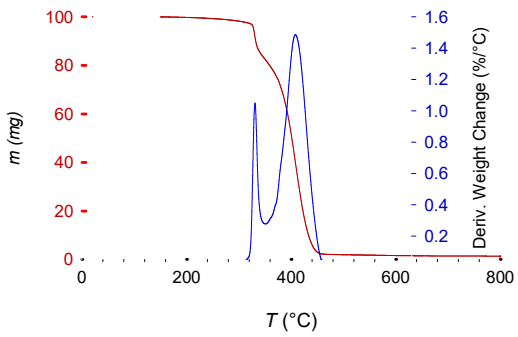

Figure 4.10 Characteristic decomposition curve of brominated fire retardant HIPS (in red, coupled with Sb_2O_3 as synergy agent). The blue line represent the derivative weigh change showing two main decomposition steps. .

DSC analysis (Figure 4.11) confirmed further the chemical resistance of the polymer to the treatment.[159] With a glass transition temperature of 101.2 °C fitting within the values for this polymer 85 °C to 102 °C. [3] Siregar et al. report a HIPS glass transition temperature of 105 °C. [160]. Another study comparing virgin PS with others containing clay particles report a glass transition temperature of 94 °C for the virgin polymer and 106 °C for the clay-filled. The end-of-life polymer in this study, includes fire retardants fillers and colorants, which modify the T_g but its value is consistent with reported literature.

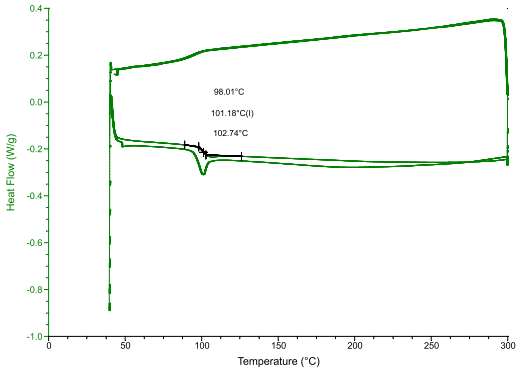

Figure 4.11 DSC Results from the DBE-9 treatment. 25 g treated at 206 °C for 240 min

4.3.4 Activation Energy Calculation from TGA Data.

There are many kinetic methods to determine the E_a from TGA data. For this analysis which pretends to compare such as energies for the polymer before and after determination, we have decided to follow the approach used by Turk et al.[161]

They assumed that there is only one decomposition mechanism with an activation energy specific to it, and that the polymer decomposition will follow the following basic rate equation:

$$\frac{d\alpha}{dt} = k\,(1-\alpha)^n \tag{4.9}$$

where:

α : Fractional mass loss , $(0 \leq \alpha \leq 1)$.

t : Time.

k : Reaction rate constant

For our compaction we have decided to use two different calculation methods:

Coats-Redfern Method

The Coats-Redfern method which assumes a first-order reaction using the following equation to calculate the activation energy (E_a)

$$\ln\left(\frac{\alpha}{T^2}\right) = \ln\left(\frac{AR}{aE_a}\right)\left[1-\frac{2RT}{E_a}\right] - \frac{E_a}{RT} \tag{4.10}$$

where:

α is the fractional mass loss

T is the temperature in K

A is the pre-exponential factor

R is the gas constant ($0.008\,314\,5\,\mathrm{kJ\,mol^{-1}\,K^{-1}}$)

E_a is the activation energy in $\mathrm{kJ\,mol^{-1}}$

The activation energy is then obtained by plotting

$$\ln\left(\frac{\alpha}{T^2}\right) \text{ vs. } \frac{1}{T} \tag{4.11}$$

where the activatin energy is obtained from the slope of the plott that correspond with: $-\frac{E_\mathrm{a}}{R}$

Horowitz-Metzger Method

The Horowitz-Metzger method obtains the activation energy (E_a) using the following expression:

$$\ln\left(\ln\frac{W_0}{W}\right) = \frac{E_\mathrm{a}\theta}{RT_s^2} \tag{4.12}$$

where:

W_0 is the initial weight of the sample

W is the weight of the sample at temperature T

T_s is the temperature at which $\frac{W}{W_0} = e^{-1}$

$\theta = T - T_s$

R is the gas constant ($0.008\,314\,5\,\mathrm{kJ\,mol^{-1}\,K^{-1}}$)

E_a is the activation energy in $\mathrm{kJ\,mol^{-1}}$

Again the activation energy is obtained by plotting

$$\ln\left(\ln\left(\frac{W_0}{W}\right)\right) \text{ vs. } \theta \tag{4.13}$$

where the activation energy is obtained from the slope of the linear plot that is given by $\frac{E_\mathrm{a}}{RT_s^2}$
The results obtained on this initial thermoanalytical study are consistent with the results found in the literature fro thermoplastics of numbers ranging from about $50\,\mathrm{kJ\,mol^{-1}}$ to $150\,\mathrm{kJ\,mol^{-1}}$. [69, 161, 162] As expected the Coats-Redfern method yields lower values. However, the Horowitz-Metzger Method gives higher values but more variability (Table 4.4). Besides the theoretical fitness of this method to analyze polymers the arbitrary temperature selection might be a cause of imprecision when studying the decomposition of additivated polymers. [69, 161, 162]

Table 4.4 Activation energy values (E_a, $\mathrm{kJ\,mol^{-1}}$) calculated using the Coats-Redfern and Horowitz-Metzger Method.

Sample	**Coats-Redfern** E_a	**Horowitz-Metzger** E_a
PS-FR1	50	81
PS-FR2	48	128
DB-8 (99.4%)	34	61
DB-9 (97.8%)	59	87
PS (Pure)	53	79

Unfortunately, this initial results did not provide any clear information in relation to the debromination, brominated or pure polystyrene. It is possible that more precise studies on the different steps of the decomposition together with methods that study more advanced reaction orders could provide better insight of the process.

4.3.5 Diffusion Calculations

Due to the nature of the process studied, we considered that solvent-polymer diffusion is the main limitation for the debromination, in this case the ethylene glycol/triethylene-glycol into the HIPS/PS polymeric matrix. [6, 163] Diffusion is a process primarily controlled by temperature with an activation energy of $71\,\mathrm{kJ\,mol^{-1}}$, followed by the chemical nature of the diffusing species, and the diffusion matrix. Once the polymer reach the glass transition temperature, diffusion is mostly defined by Flick's Law. There are several models and theories that characterize solvent diffusion in polymers. The model of Petit et al.[164] considers diffusion in both polymeric solutions and gels. Since the treatment temperatures in this work exceed the glass transition and the solvent is absorbed by the polymer, we assume it behaves as a gel and for this reason we have adopted their model. The model shows that the solvent diffusivity correlates with the jump frequency (k_{jf}):

$$kjf = F_p \exp\left(-\frac{\delta_E}{k_\mathrm{B} T_\mathrm{K}}\right) \tag{4.14}$$

where:

F_p = frequency pre-factor

δ_E = height of the potential barrier (in J)

k_B = Boltzmann constant ($1.38 \times 10^{-23}\,\mathrm{J\,K^{-1}}$)

T_{K} = temperature in Kelvin

$$D = k_{jf}\,\beta^2\,c^{-2\nu} \tag{4.15}$$

where:

D = diffusion coefficient

β = pre-factor for the concentration term

c= polymer concentration

ν = parameter depending on polymer concentration

First, we calculate the rate constant k with the equation and data from our statistical model. We decided to use a temperature of 190 °C because is the temperature in which we obtain the highest debromination ratio. Also, we assumed the use one solvent (EG) for the modeling and the ideal shape of the polymer of 1 mm^2 and 2 mm thickness.

$$k = b_0 \cdot \exp\left(\frac{-b_1}{8.314} \cdot \left(\frac{1}{T} - 0.00216\right)\right) \tag{4.16}$$

where:

$b_0 = 0.15$

$b_1 = 71000\,\mathrm{J/mol}$

$T = 463.15\,\mathrm{K}$

Substituting the values into the equation:

$$k = 0.15 \cdot \exp\left(\frac{-71000}{8.314} \cdot \left(\frac{1}{463.15} - 0.00216\right)\right) \tag{4.17}$$

Obtaining:

$$k = 0.15\,\mathrm{s}^{-1} \tag{4.18}$$

Then we obtain the Frequency Pre-Factor A from the Arrhenius equation:

$$k = A \cdot \exp\left(\frac{-E_a}{RT}\right) \tag{4.19}$$

Rearranging the equation to solve for A:

$$A = \frac{k}{\exp\left(\frac{-E_a}{RT}\right)} \tag{4.20}$$

where:

$k = 0.15\,\mathrm{s}^{-1}$

$E_a = 71\,\mathrm{kJ/mol} = 71000\,\mathrm{J/mol}$

$T = 463.15\,\mathrm{K}$

$R = 8.314\,\mathrm{J/mol \cdot K}$

Getting:

$$A = 5.5 \times 10^7\,\mathrm{s}^{-1} \tag{4.21}$$

To improve the accuracy of our results we assumed that the debromination ratio is equal to the diffusion into the sample. To simplify the model we assume that the reaction between the alkali and the fire retardant is instantaneous and there are no other limitations

First, debromination percentage is normalized to represent the jump frequency k. Then the potential barrier height δE is derived from the Arrhenius equation:

$$k = F_p \cdot e^{-\frac{\delta E}{k_B T}} \tag{4.22}$$

Then:

$$\ln(k) = \ln(F_p) - \frac{\delta E}{k_B T} \tag{4.23}$$

Rearranging for δE:

$$\delta E = -k_B T \cdot (\ln(k) - \ln(F_p)) \tag{4.24}$$

where:

δE: Potential barrier height (Joules),

k_B: Boltzmann constant (1.38×10^{-23} J/K),

T: Temperature in Kelvin ($T = T_C + 273.15$),

k: Normalized jump frequency,

F_p: Frequency pre-factor (s^{-1}).

Once the mathematical frame for the calculations is defined, we use a python program to run all our samples to calculate the Jump Frequency, the Potential barrier height, and the Diffusion coefficient (Table 4.5). For such calculation we had to stimate some parameters such as: Pre-factor for the concentration term ($beta = 1.0 \times 10^{-9}$m), Polymer concentration ($c = 1$ (dimensionless)) and, Model parameter for polymer concentration ($nu = 0.5$). Future work can explore different parameters and define wich ones fits best with the experimental data.

Table 4.5 Summary of diffusion parameters for each debromination experiment. DB=debromination, JF= Jump Frequency, δE= Potential barrier height, D= Diffusion coefficient

Code	T (K)	Time (s)	DB (%)	JF (s^{-1})	δE (J)	D ($mm^2\,s^{-1}$)
DBE-1	475.15	14400	79.9	4.63e+07	1.13e-21	4.63e-05
DBE-2	503.15	14400	91.3	4.63e+07	1.20e-21	4.63e-05
DBE-3	480.15	28800	87.3	2.31e+07	5.73e-21	2.31e-05
DBE-4	505.15	14400	95.3	4.63e+07	1.20e-21	4.63e-05
DBE-5	479.15	14400	75.6	4.63e+07	1.14e-21	4.63e-05
DBE-6	483.15	14400	99.4	4.63e+07	1.15e-21	4.63e-05
DBE-7	498.15	6000	97.8	1.11e+08	-4.83e-21	1.11e-04
DBE-8	433.15	86400	46.6	7.72e+06	1.17e-20	7.72e-06
DBE-9	433.15	86400	60.3	7.72e+06	1.17e-20	7.72e-06
DBE-10	461.15	43200	67.7	1.54e+07	8.09e-21	1.54e-05
DBE-11	475.15	43200	75.4	1.54e+07	8.33e-21	1.54e-05
DBE-12	458.15	14400	29.3	4.63e+07	1.09e-21	4.63e-05
DBE-13	456.15	14400	4.0	4.63e+07	1.08e-21	4.63e-05
DBE-14	448.15	14400	4.3	4.63e+07	1.07e-21	4.63e-05
FDBE-1	463.15	120	99.97	5.56e+09	-2.95e-20	5.56e-03
FDBE-2	463.15	120	99.79	5.56e+09	-2.95e-20	5.56e-03
FDBE-3	463.15	300	98.81	2.22e+09	-2.36e-20	2.22e-03
FDBE-4	293.15	86400	12.3	7.72e+06	7.95e-21	7.72e-06

4.4 Material and methods

4.4.1 Brominated PS/HIPS

PS and HIPS with brominated fire retardant additives from electronic waste recovered at Polytechnique Montreal. We classified the pieces and labeled them regarding resin and fire retardant additive. Most of the HIPS came from used printer toner manufactured by Hewlett Packard. The pure polystyrene used as reference was bought from Sigma Aldrich and virgin HIPS was provided by Lavergne Group INC.

Figure 4.12 An example of used Br-HIPS origin collected, before grinding it to pieces of about 3 mm.

4.4.2 Analytical methods

An EDXRF Epsylon4 from Malvern Panalytical and Brucker S1 TITAN Handheld XRF determined the bromine content in the samples and in the solvent. A PerkinElmer Spectrum 65 FTIR evaluated the samples before and after reaction to determine if the polymer structure was altered during the experiment by observing changes in the absorbance peaks. The wave numbers ranged from 500 cm^{-1} to 4000 cm^{-1} with a measurement interval of 2 cm^{-1} and 4 accumulations. A TGA Q500 V6.7 was used for the thermogravimetrical analysis under nitrogen atmosphere. The temperature ramp for analysis was 30 °C min^{-1} up to 150 °C followed by a 5 min hold to stabilize the oven temperature, then 5 °C min^{-1} until 650 °C, followed by a final ramp of 10 °C min^{-1} up to 800 °C. Once the temperature reached 800 °C the instrument substituted the nitrogen for air to decompose the char and recover any remaining minerals. Glass transition properties were studied using a DSC Q20 from TA Instruments.

4.4.3 Experimental design

Initially, the end-of-life brominated high impact polystyrene was recovered from the local electronic waste collection system. This polymeric waste was sorted and separated according to resin and coding. We measured the Br content with the XRF instruments and characterized the sample with an FTIR, TGA, and DSC to ensure that the chemical characteristics corresponded with the manufacturer code and to detect possible impurities or cross contamination. Once the polymer was cataloged, it was dried and stored.

The reaction media consisted of either ethylene glycol (EG) or triethylene glycol (TEG) with either sodium hydroxide or potassium hydroxide as the debromination solute (extractant, 0.5 M to 2 M). The reaction was carried out in stirring flasks with temperature control, and a reflux column. On one occasion we coupled the flask to an on-line mass spectrometer. Together with solvent and extractant, the screening experimental design comprised reaction time (5 min, 4 h, 8 h, 12 h, and 24 h), temperature (160 °C to 230 °C), agitation (with or without), and pellet size to explore the prominent factors that impacted reaction rates and estimate process efficacy. We assumed that the Br was evenly distributed throughout. Temperature control became problematic to achieve the 230 °C set temperature due to heat losses. TEG has a higher boiling point than ethylene glycol so most of the experiments were conducted it but an equal number of experiments were conducted with NaOH and KOH.

The test conditions were chosen to extract from 20 % to 80 % of the Br, but with as little as 5 min, >99 % of the Br left the polymer matrix. Because the extraction rates in the pellets were much longer, internal diffusion through the matrix was the rate limiting step.

The objective of the work was to maintain the chemical integrity so that the polymer could be mechanically recycled after the treatment. However, all the conditions applied to debrominate the samples are well know aging factors. [165] At the end of each test, the sample was dried for at least 8 h at 40 °C and then analyzed to determine its bromine content and its chemical integrity with TGA, DSC and FTIR.

The primary variable is the percent extraction—conversion—of Br (not the brominated compound as the XRF only detects elements) (Table 4.2). The XRF recorded the % Br before the test and after and we also analyzed the liquid phase after each test to close a mass balance.

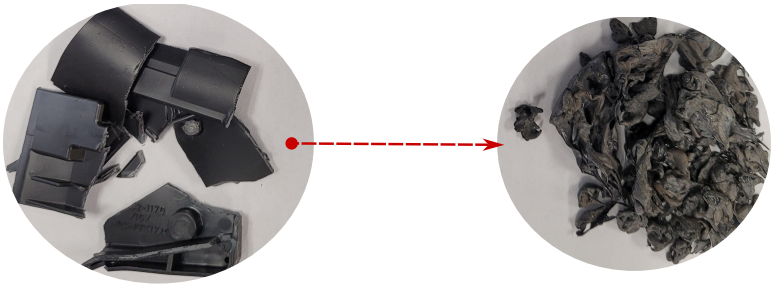

Figure 4.13 Left: Cut pellets from Fig. 4.12 before treatment (60 mm chuncks). Right: Pellets after treatment

Pellet morphology turned out to be a factor that has the greatest impact on extraction rate: we tested both pellets 60 mm (Figure 4.13) and fibres that were 5 mm long and as low as 60 µm in diameter.

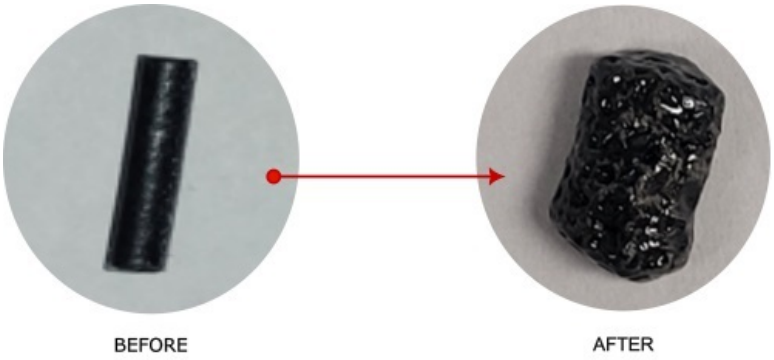

Figure 4.14 Left: Extruded filament from Fig. 4.12 before treatment. Right: Pellets after treatment. The cut filament shown was 3 mm diameter, 8 mm long, and weighed 0.064 g.

All tests with filaments were conducted with 25 mm of solvent: Even at 5 min conversion exceeded 99 %. KOH versus NaOH and TEG versus EG were also varied but because the conversion was so, the tests were incapable of differentiating between the contribution of these factors. The final factor was 4 levels of stirring rate: 400 rpm, 300 rpm, 100 rpm and no stirring. Seven tests were completed with 1 g of HIPS 50 mL of solvent, while 4 tests were conducted with 25 g of HIPS and either 100 mL or 500 mL of solvent. Interestingly, at high temperature with no stirring the solvent/caustic extracted more than 90 % of the Br. In the tests with 25 g or 100 g of HIPS, conversion was lower than expectation and this was likely due to the agglomerates formed during the test, which would introduce an external mass transfer resistance.

4.5 Conclusions

A solvothermal treatment removes more than 90 % of bromine from commercial WEEE HIPS: $T > 150\,^{\circ}\mathrm{C}$, KOH or NaOH and $t > 2\,\mathrm{h}$ for bulky pieces and $t < 5\,\mathrm{min}$ for filaments. High boiling point solvents, like ethylene glycol or triethylene glycol, disolve the alkali and operate at temperatures high enough to accelerate the kinetics. A drawback of this treatment is the apparent damage to the polybutadiene fraction of HIPS, leaving polystyrene polymer. Chemical properties of this dibrominated HIPS remain consistent with the virgin PS as confirmed with DSC, TGA and FTIR measurements. The treatment also partially removes any Sb_2O_3, which is a synergistic compound added with the brominated fire retardants; this compound is recovered with the solvent.

The efficacy of the treatment is limited by the solvent diffusion and thus the temperature: the debromination reaction rate is much great above $200\,^{\circ}\mathrm{C}$ (about two times greater than the glass transition temperature) but the limitation is the solvent volatility, which could be moderated by operating a higher pressure. However, the upper limit on temperature is the melting point of PS at $270\,^{\circ}\mathrm{C}$. Due to the nature of polymers the transition phase does not occur at one temperature, but is instead progressive. Logically, operating as close as possible to the melting point is optimal as it maximizes the debromination kinetics. Another limitation encountered, is that when treating more than 10 g of polymer, ball-shaped agglomerates form, which reduces the debromination rate as the diffusion path to the solution is longer. Polymer filaments and small pellets debrominate in the matter of minutes rather than hours. The difference between NaOH and KOH is statistically insignificant but requires a more extensive series of test to confirm this finding. With respect to safety, KOH that reacts to form KBr, which is less toxic than NaBr.

The screening design used in this work considered many factors like temperature, polymer morphology, solvent, solute, and time. A full-factorial statistical design would be required to better characterize how each factor affects the debromination rate. However, here, with the screening design, a kinetic model has identified the major factors that limit reaction rates. The critical factor for scale-up will be to maximize the surface area of the polymer matrix to the solvent and alkali. Bulk samples take hours to treat versus minutes for filaments. Furthermore, ensuring an adequate mixing between the solvent and polymer will be the second most critical parameter, particularly to avoid any aggolmeration that will reduce the reaction rates.

CHAPTER 5 ARTICLE 3: ALKALINE SOLVOTHERMAL DEBROMINATION OF COMMERCIAL BROMINATED ACRYLONITRILE BUTADIENE STYRENE (ABS)

Mario Ferreiro Gonzalez, Fernanda Cabañas-Gac, Gregory S. Patience

Article to be published in Chemical Engineering Journal Advances, Submitted: 13 July 2025

5.1 Acrylonitrile-butadiene-styrene (ABS) is one of the most common thermoplastics and for decades brominated fire retardants (BFR) were the primary compound added to comply with fire safety regulations in electronic and electrical polymeric components. BFRs require low concentrations to be effective, are stable up to 250 °C (sufficient for thermoplastic process such as injection moulding), and polymer compatibility (easy addition). However, their hazardous nature and persistence sparked concerns about their use. which limits the possibility of recycling them Nowadays, most of them are banned or have limitations on their applications and concentration Here, we report an alkaline solvothermal treatment to debrominate commercial ABS from end-of-life devices (up to 97 %. The process operates between 160 °C to 190 °C with ethylene-glycol as solvent and KOH as extraction agents (1 M). It removes 95 % of the Br in 4 h above 160 °C and 97 % at $T = 160$ °C and 24 h. FTIR spectroscopy confirms that 30 % of the acrylonitrile reacts to form acrylic acid in the most aggressive conditions. Curiously, the T_g increases by up to 10 °C, which might improve the mechanical properties of the polymer

5.1.1 keywords

Fire retardants, Polymers, Recycling, Solvothermal treatment, Alkali debromination, ABS, Brominated fire retardants.

5.2 Introduction

According to the reports of Plastics Europe in 2023 90 % of the world plastics were fossil-based, and 9 % of the recycled were mechanically recycled. The global plastic market by 2023 was 414 Mt but the recycling market was only 37 Mt. In Europe, the situation for recycled plastic was a little better compared with the global situation: The mass of pre-consumer and post-consumer mechanically recycled plastics reached 10 Mt, which was 19 % of the total produced. Recycled acrylonitrile-butadiene-styrene (ABS) accounts for less than 0.8 Mt of the total. More polyethylene (in all of its density variants) and polypropylene are recycled but they are the highest volume plastics. Most of the plastic recycled originated from packaging and construction at 39 % and 23 %, respectively. Logically, single plastics typical of packaging and construction are much easier to short and recycle since they lack additives, are present in high volumes, and their life-time is short. Regarding the waste electrical and electronic equipment (WEEE or e-waste) trend from 2018 to 2022 in Europe, recycling went up by 33 %, energy recovery by 11 %, and land-filling by 20 %. This illustrates the progress achieved in recycling but demonstrates that waste management falls short of approaching the zero waste goal [166].

In Canada, the fraction of WEEE accounts for 7 % of all plastic waste. Taking into account that roughly 50 % of the plastic is non-durable (lifetime $\geq$ 1 year), WEEE waste would account for roughly 14 % of the durable plastic waste .[167] WEEE plastics are considered hard-to-recycle polymers and the hard competition with virgin resins means that most of it is sent to landfill instead recycling facilities.

The promise of chemical recycling has yet to be realized as it trails mechanical recycling and accounts for 0.1 % of the 20 % recycled plastic in Europe. [166]. In the US, the situation comparable, with the additional challenge that pyrolysis and waste-to-energy are often considered as chemical recycling. These processes are also facing criticism from ecologists and anti-plastic groups. [168] While these groups could be considered bias, the reality is that chemical recycling is currently less developed to tackle plastic pollution.

Brominated fire retardants (BFRs) are organobrominated compounds that were developed to meet fire safety regulations passed in the 1960s. Because of their efficacy, compatibility, and low cost BFRs became they main fire-proofing additive for WEEE growing steadily beyond 2010. [169] The Michigan Chemical Corporation were the first to introduce polybrominated bisphenols (PBBs) to the market in 1970 as fire retardants for polymers.[170]

BFRs are incorporated either with the monomer, as an additive to the polymer, or as a reactant with the polymer chain. Brominated monomers link to polymer monomers and are

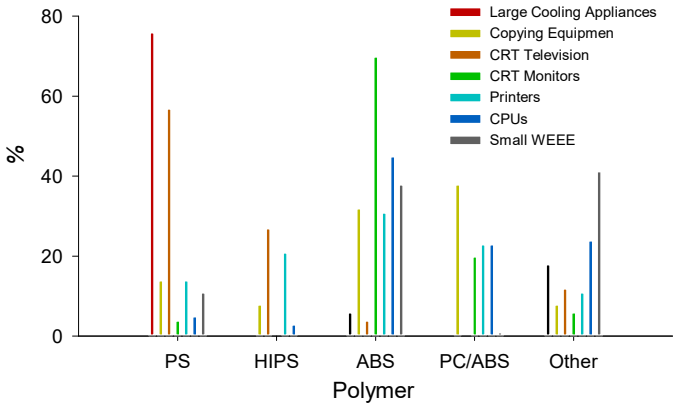

Figure 5.1 Polymers distribution on different WEEE shorted in a study carried in Portugal. Although the graph represents the percent of each polymer found, small WEEE and printers are the ones with larger amounts of plastic for weight unit. [12]

then blended with the polymer matrix or incorporated in the polymerization step. BFRs additives are blended with the polymer resin or in the online process. Reactive BFRs bond chemically to the polymer chain.[39, 169, 171]

Polybrominated biphenyls (PBBs), polybrominated diphenyl ethers (PBDEs), and tetrabromobisphenol A (TBBPA) dominate the market. Brominated compounds are synthesized by replacing 3 to 10 H atoms with Br,5.2. Commercially, each compound will have a range of Br atoms rather than a single composition. Industry has endeavoured to reduce PBBs in post-consumer plastics due to environmental concerns and the PBB episode in Michigan (1973) when the Michigan Chemical Corporation mistakenly shipped PBB instead of magnesium oxide, an animal food additive. This mix-up poisoned live-stock, especially cows, and subsequently tainted the milk supply and resulted in a severe intoxication to humans, leading to its phase out in 1974. [170] Hexabromocyclododecane (HBCD or HBCDD) which has 16 stereo-isomeres poses a challenge to study its toxicity and pharmacokinetics. [172] Due to its environmental persistence and toxicity HBCD was banned from most applications with the exception of polystyrene foams for construction. Ironically,in 2000 HBCD was the main BFR produced. [173]

When heated antimony oxide Sb_2O_3 reacts with BFR to from a metal halide, which inhibits flame propagation better than BFRs alone.[26, 37] This combination requires less BFR to achieve the same performance without this Sb synergistic compound.

WEEE plastic contains 30 % ABS, 30 % high impact polystyrene (HIPS), 30 % polypropylene

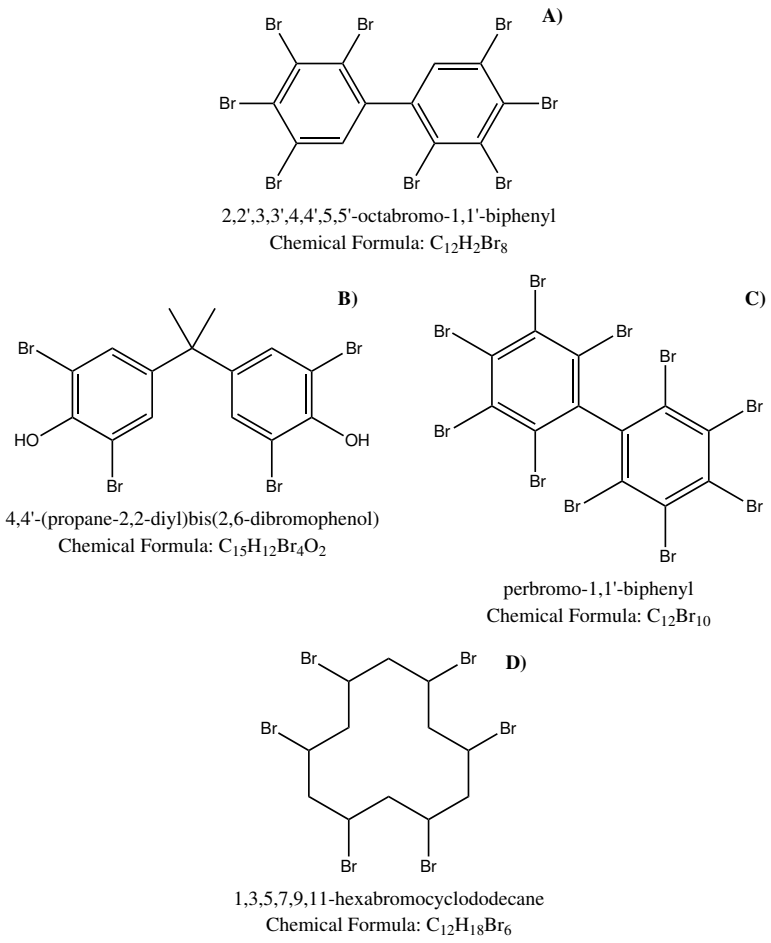

Figure 5.2 Examples of BFRs most representative structures.

(PP), and 10 % polycarbonate (PC) (Figure 5.1) from which at least 40 % is brominated. Hence bromine free ABS represents a tremendous potential for recycle while minimizing the risk of contamination. [174–177]

Occasionally WEEE is pre-sorted manually to obtain a fairly pure stream of a resin type, which is then separated based on density. Industry applies density separation to partition polymers but also isolate brominated fractions from the non-brominated fraction sin the same polymer type. However, the presence of BFRs can disrupt the density separation and force companies to to implement methods based on spectroscopy to separate the polymeric fractions. A problem that is accentuated since often these resins are not labelled as containing BFRs. [12, 178]

BFRs not only pose a health threat due to their toxicity and prevalence, they also limit the polymer recyclability. In 2018, China banned imports to plastic waste and so countries sought other ports to dump this waste. Up until 2025, Malaysia accepted this waste but then

began to refuse waste except to countries that obey the Basel Action Network, which would exclude all of the California plastic waste. New regulations restrict them to concentrations less than $500\,\mu g\,g^{-1}$ but even these materials must be pretreated to them before a pyrolysis, combustion, or gasification step, which are the main processes to treat WEEE. Even these tighter restrictions limit the availability of ABS as feedstock to recycle or reuse. [174]

Rather than thermal treatments, treating ABS plastic and maintaining the physical properties (as close to virgin as possible), would minimize the landfill burden. The additional challenge is to maintain the properties while stripping the polymer of brominated compounds. Studies of the mechanically reprocessing effects on ABS suggest that the polybutadiene fraction is the most susceptible to external stresses (due to chain scissions and crosslinking). This means that the SAN (styrene–acrylonitrile copolymer) fraction of the chain remains unchanged during the process, and thus the polybutadiene degradation primarily affects the impact strength, while the tensile modulus and strength remain essentially unchanged. Temperature and number of processing cycles are the two variables that affect the PB (polybutadiene) fraction the most. While the cycles number is a total value, temperatures up to 190 °C appear to be the less damaging. [179–183]

To best characterize the research related to thermal stability of ABS we queried the Web of Science bibliographic database (WOS) with the following keyword combinations: "ABS AND flame" OR "ABS AND fire". We then excluded articles with ammonium bisulfate as a keyword, which left 735 articles. The first one was published in 1938 and only another 6 prior 1990 were indexed by WOS. Since 2010 it has indexed 40 articles per year on average. The five most prolific scientific categories in terms of publishing are: polymer science (242 articles), multidisciplinary materials science (110), environmental sciences (83), energy & fuels (68), and chemical engineering (64). The 10 journals that published the most articles were *Polymer Degradation and Stability* (58), *Journal of Applied Polymer Science* (45), *Journal of Thermal Analysis And Calorimetry* (16), *Fire and Materials* (15), *Journal of Analytical And Applied Pyrolysis* (11), *Journal of Hazardous Materials* (11), *Polymers* (11), *Journal of Vinyl & Additive Technology* (10), *Journal of Fire Sciences* (9), and *Polymer Composites* (9).

VOSViewer, an open access program that identifies trends in bibliometric data, grouped the 100 most often mentioned keywords into 4 clusters. The red cluster, with 37 keywords (nodes in Figure 5.3) is centred around thermal degradation with 185 articles that mention it as a keyword, pyrolysis (53 articles), brominated retardant (45), and waste electrical and electronic equipment (WEEE—44). Flame (fire) retardant (FR) is the most prominent keyword of the green cluster with 278 articles. Polycarbonate (PC—68) and mechanism (mech—47) are two other frequent keywords of this cluster. The blue cluster includes ABS (219), me-

chanical properties (92), flammability (86), and propylene (63) with a total of 23 of the 100 keywords. Finally, in the yellow cluster, nanocomposite appears most often with 78 articles followed by thermal stability (66), and polymer (63).

Considering that flame retardancy in ABS has been such a huge commercial success for decades, it is somewhat surprising how little research has been dedicated to the subject before 1990. The push to recycle ABS is also a more recent preoccupation as more countries restrict importing WEEE, and in particular, brominated plastics.

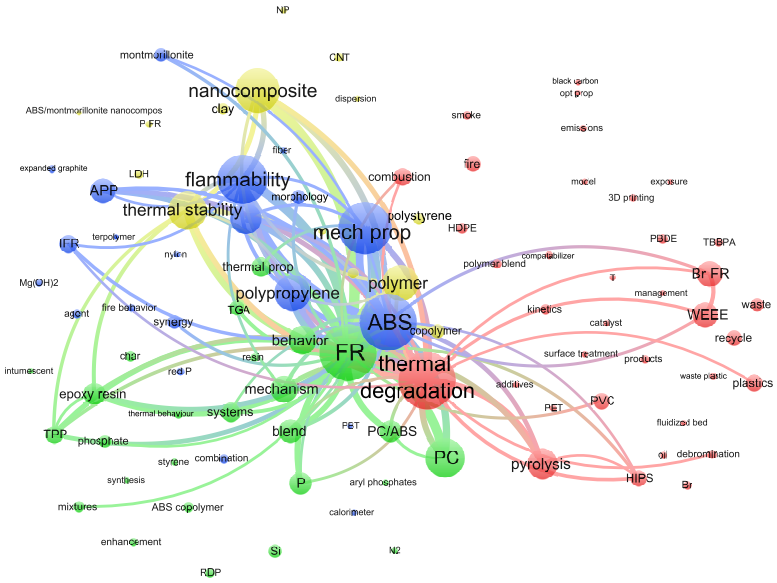

Figure 5.3 VOSViewer bibliographic map of keywords related to ABS and flame (fire) retardants.[9, 13] Node size correlates with the number of articles except for fire retardant (FR) ABS, and thermal degradation that were rescaled to 100 to reduce overlap with other keywords. The smallest nodes represent keywords that appear in 9 articles. Abbreviations: APP—ammonium polyphosphat, Br FR—brominated flame retardant, CNT—carbon nanotube, HDPE—high density polyethylene, HIPS—high impact polystyrene, IFR—intumescent flame retardant, LDH—layered double hydroxide, NP—nanoparticle, P—phosphorous, PBDE—polybrominated diphenyl ethers, PBT—poly(butylene terephthalate, PC—polycarbonate, PET—polyethylene terephthalate, PMMA—poly(methyl methacrylate), RDP—Resorcinol bis(diphenyl phosphate), T—temperature, TBBPA—tetrabromobisphenol A, TGA—thermgravimetric analysis, TPP—triphenyl phosphate, and WEEE—waste electrical and electronic equipment.

5.3 Material and methods

5.3.1 Brominated ABS

We recovered our brominated plastic samples from a WEEE collection point at Polytechnique Montreal, in order to match the most real life conditions. The plastic was sorted, labelled and stored for later treatment. Most of the HIPS came from used printer toner manufactured by Hewlett Packard. The pure ABS used as reference was provided by Lavergne Group INC.

Figure 5.4 ABS samples collected from the Polytechnique collection point.

5.3.2 Analytical methods

An EDXRF Epsylon4 from Malvern Panalytical and Brucker S1 TITAN Handheld determined the bromine content (and other elemental components) both in the samples and in the solvent. A PerkinElmer Spectrum 65 FTIR evaluated the samples before and after reaction to identify changes to the polymer chain and other changes induced by the treatment. The wave numbers ranged from $500\,\mathrm{cm}^{-1}$ to $4000\,\mathrm{cm}^{-1}$ with a measurement interval of $2\,\mathrm{cm}^{-1}$ and 4 accumulations. The thermogravimetric analysis was made with a TGA Q500 V6.7 under a nitrogen atmosphere. The parameters used were: A temperature ramp of $30\,^{\circ}\mathrm{C\,min}^{-1}$ up to $150\,^{\circ}\mathrm{C}$ followed by a 5 min hold to stabilize the oven temperature, then $5\,^{\circ}\mathrm{C\,min}^{-1}$ until $650\,^{\circ}\mathrm{C}$, followed by a final ramp of $10\,^{\circ}\mathrm{C\,min}^{-1}$ up to $800\,^{\circ}\mathrm{C}$. Once the temperature reached $800\,^{\circ}\mathrm{C}$ the instrument substituted the nitrogen for air to decompose the char and recover any remaining minerals. An Agilent 6880 GCMS characterized the solvent after reaction while, a DSC Q20 from TA Instruments was used to measure the glass transition temperature.

5.3.3 Experimental design

Once the polymer was analyzed, it was dried and stored to be used on the debromination process. The reaction media was ethylene glycol and the debromination reactant was potassium hydroxide $1\,\mathrm{mg\,kg}^{-1}$. (We also tested sodium hydroxide but it had a greater tendency to degrade the polymer properties.) The reaction was carried out in a stirred flask with temperature control, coupled with a reflux column.

We executed an experimental design comprising reaction time, t (from 1 min to 24 h), temperature, T (160-190 °C), and sample mass (from 1-50 g) to evaluate the kinetics and process efficacy. The objective of the work was to maintain the chemical integrity so that the polymer could be mechanically recycled after the treatment, However, all the conditions applied to debrominate the samples are well know ageing factors. The objective of the work was to maintain the chemical integrity so that the polymer could be mechanically recycled after the treatment, Thus, address any possible polymer damage is key. At the end of a test, the polymer was extracted dried for at least 8 h at 40 °C to be further studied to determine the debromination ratio and its chemical integrity with TGA, DSC and FTIR.

5.4 Results and discussion

A known possible undesirable side-effect of the treatment is the denitrification of the ABS acrylonitrile group.[14, 184] The combination of polyethylene glycol and hydroxides removes nitrogen form the ABS and NaOH is more aggressive than KOH, which was confirmed by a scouting experiment we conducted. Furthermore Du et al. (2011)[14] reported that denitrification rates were higher above 160 °C, setting a theoretical reference temperature for our experiments. However, they added glycol/hydroxide mixture to a solution of ABS dissolved in other solvents. This further increased denitrification rates as the combination of multiple solvents was more aggressive.

The concentrations of Br (1000 µg g^{-1}) and Sb (900 µg g^{-1}) in the solvent after the treatment, demonstrating that the treatment effectively extracts them from the plastic in agreement with previous studies.[172]

To account for the contribution of each factor to the extent Br was extracted from the sample, X, we assumed a completely backmixed reactor model with a first order reaction rate, $-r_{\mathrm{Br}} = kC_{\mathrm{Br}}$, where k is the rate constant, t is time, and V is volume:

$$\frac{\mathrm{d}C_{\mathrm{Br}}}{\mathrm{d}t} = -r_{C_{\mathrm{Br}}} = kC_{\mathrm{Br}} \tag{5.1}$$

$$X = 1 - \exp\left(-kt\right) \tag{5.2}$$

where the reference temperature, T_{o}, is 150 °C

$$k = 1.7 \exp\left[\frac{110\ 000}{R}\left(\frac{1}{T} - \frac{1}{T_{\mathrm{o}}}\right)\right] \tag{5.3}$$

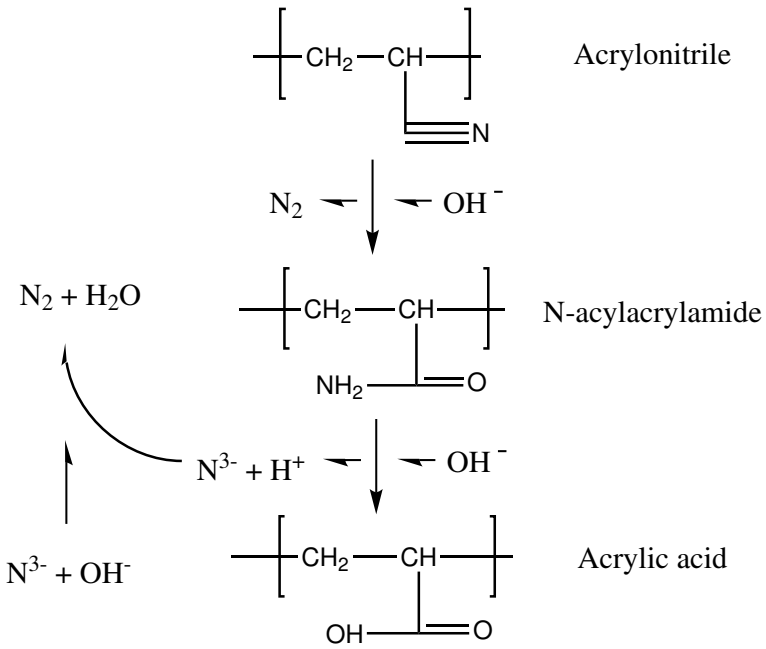

Figure 5.5 Denitrification pathway based on the literature and our proposal for the nitrogen elimination.[14]

The experimental plan considered time and temperature and we tested extraction rates with 1 g of ABS in a 50 mL flask and 50 g in a 200 mL. We first regressed the data with the 1 g of ABS and the simple model accounted for 94 % of the data for the tests with 1 g of catalyst (Figure 5.6). However, we excluded the data point at 0.5 h (red triangle in Figure 5.6) for which the extraction rate was significantly higher than expectation based on the model. Experimentally we rationalized excluding the data because it took at least 0.5 h to reach a steady operating condition and thus assigning a $t = 0$ h is particularly problematic for short time periods as the Br reacts. The extraction rate with 50 g of ABS (black squares in Figure 5.6) was lower than expectation and this was due to the agglomeration of the plastic, which restricts contact between the reactants.

FTIR

Fourier transform infrared spectroscopy (FTIR) determined when the treatment induced changes to the polymeric chain, particularly the peak at 2235 cm^{-1} related to the C≡N nitrile group (Figure 5.8).

By comparing a couple of peaks in each spectrum, we determine how much it denitrifies (Figure 5.9) [185]. We normalize the heights with respect to the peak at 1451 cm^{-1} for CH_2 scissoring that we assume is invariant.

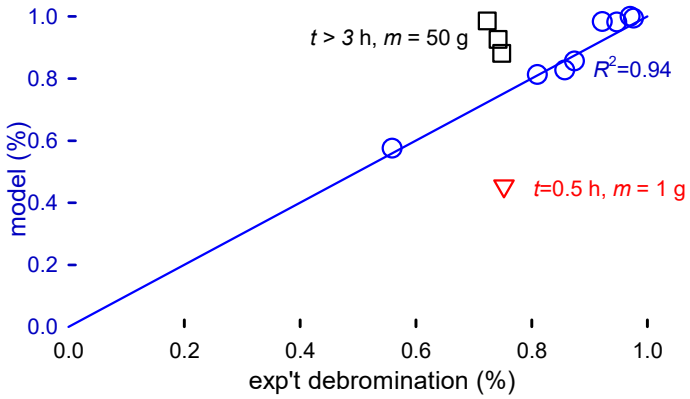

Figure 5.6 Parity plot of the model vs experimental data for the extent of bromine extracted from the ABS.

$$\text{Ratio}_{\text{ABS-FR17}} = \frac{A_{1451}}{A_{2232}} = \frac{0.0392}{0.0096} = 4.1 \tag{5.4}$$

$$\text{Ratio}_{\text{ABS}-160\,^{\circ}\text{C}} = \frac{A_{1451}}{A_{2232}} = \frac{0.0283}{0.0102} = 2.8 \tag{5.5}$$

$$\text{Ratio}_{\text{ABS}-170\,^{\circ}\text{C}} = \frac{A_{1451}}{A_{2232}} = \frac{0.0497}{0.0163} = 3.0 \tag{5.6}$$

$$\text{Ratio}_{\text{ABS}-193\,^{\circ}\text{C}} = \frac{A_{1451}}{A_{2232}} = \frac{0.0472}{0.0165} = 2.9 \tag{5.7}$$

With this data we estimate the degree of conversion (α) assuming that ABS-FR17 (prior treatment) is at 100 % and so the ratio represents how much it denitrifies.

- ABS-160 °C = (α_{160}) = 100-(2.8*100/4.1)= 32 %
- ABS-170 °C = (α_{170}) = 100-(3.0*100/4.1)= 27 %
- ABS-193 °C = (α_{193}) = 100-(2.9*100/4.1)= 29 %

Surprisingly, the denitrification process is reasonably independent of temperature as only about 1/3 denitrifies at 160 °C and 193 °C. On the contrary, debromination depended on temperature: 55.9, 85 and 97 % at 160, 170 and 193 °C, respectively.

Additionally, the FTIR spectra shows the increase of intensity of the peaks 1675 cm^{-1} corresponding to N-acylacrylamide $-CO-NH_2$ and 1705 cm^{-1} for acrylic acid $-COOH$ with

Table 5.1 Representative debromination results in 50 mL for 1 g experiments, 200 mL for 50 g experiments, of ethylene glycol (EG) and 1 M KOH.

Code	Mass g	T °C	t min	DB %	error %
ABS-1	1.03	160	1440	98	1
ABS-2	1.15	160	240	56	1
ABS-3	1.11	170	240	86	1
ABS-4	1.10	193	240	97	1
ABS-5	1.08	182	240	95	1
ABS-6	1.17	185	30	75	1
ABS-7	1.21	190	60	81	1
ABS-8	1.21	186	90	87	1
ABS-9	1.15	193	120	92	1
ABS-10	51.1	177	180	75	1
ABS-11	50.1	180	180	74	1
ABS-12	49.9	182	240	72	1

higher intensity in sample from the test at 190 °C. These findings align with the denitrification pathway reported by Du et al. [14]

TGA and DCS

The TGA results (Figure 5.10) of the brominated ABS in WEEE has a clear pattern of a polymer addition with brominated fire retardant (BFR) plus its synergist agent (Sb_2O_3). Antimony trioxide (Sb_2O_3) induces an earlier decomposition offset due to its interaction with the BFR, in concordance with our findings of our previous work (for brominated high impact polystyrene) and the literature.[53, 151, 172] After this initial decomposition step, the polymer decomposed following a typical ABS pattern (red curve in Figure 5.10).

Figure 5.10 shows other differences between a virgin plastic and its WEEE counterpart, which is related to the residue after the polymer decomposition. This final residue consists primarily in the mineral fillers and occasionally a carbon char (graphitization) that is formed during the decomposition in nitrogen. Aromatic groups are the main drivers of this type of graphitization. When the polymer is heated in nitrogen, the weakest bonds break — the bonds between the aromatic groups and the chain — rather than the aromatic groups. Benzene groups then form bonds until they reach a graphite-like structure. [186] Switching nitrogen for oxygen, at the end of the N_2, is a quick method to determine the nature of the graphite (organic or inorganic), since the carbon-based compounds combust. Virgin ABS,

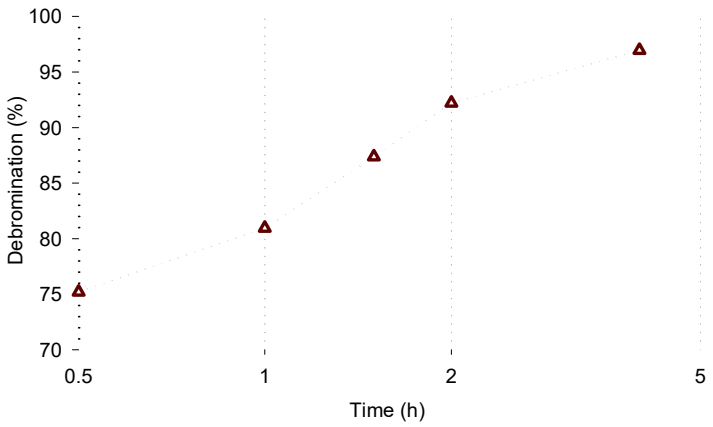

Figure 5.7 Debromination evolution over time(ABS-FR,KOH $1\,\mathrm{mg\,kg^{-1}}$, 190 °C, 1 g). The missing data for the 3 h is a result that we had data at 4 h previously and the debromination ratio from 2 h to 4 h was less than a 4 % when comparing the best results, we decided that this point will not uncover relevant information. Instead we focused on studying other parameters.

however, forms no residue in nitrogen indicating that there is no graphitization. Yet, TGA experiments of commercial ABS produces a residue in both nitrogen ($\leq 0.1\,\mathrm{g\,g^{-1}}$) and air ($\leq 0.05\,\mathrm{g\,g^{-1}}$). Additives like plasticizer, pigments and even the backbone of the fire retardant are likely to graphitize or induce it. The 5 % residue remaining after the air treatment is consistent with the mass of inorganic compounds added to commercial plastic like titanium oxide, which is a white pigment and UV stabilizer.[33] The functional carboxyl group of the acrylic acid is a known cross-linking agent at 200 °C or under UV exposition. [187–189] This cross-linking could explain the apparent graphitization in the TGA tests, and that it is more prominent with longer or harsher conditions (Figure 5.11).

The conditions that debrominated most samples 180 °C, 4 h, 180 °C, 24 h and 193 °C, 4 h of Figure 5.11) have an additional decomposition step as evidenced by change in the shape of the curve (shoulder) starting at 430 °C, which indicates that the treatment affects the polymer's structure as the shoulder is absent in the virgin ABS or the brominated ABS (Figure 5.10. The lack of major changes on the FTIR spectra from the treated samples suggest that this new step is related to the denitrification process and the inclusion of acrylic and N-acylacrylamide groups onto the polymer chain.

Higher temperatures and time, modifies the curve indicating that more acrylic acid groups react to form acrylic acid or N-acylacrylamide, which agrees with the FTIR estimates concerning denitrification. Additionally, the last decomposition pattern has a similar curve as

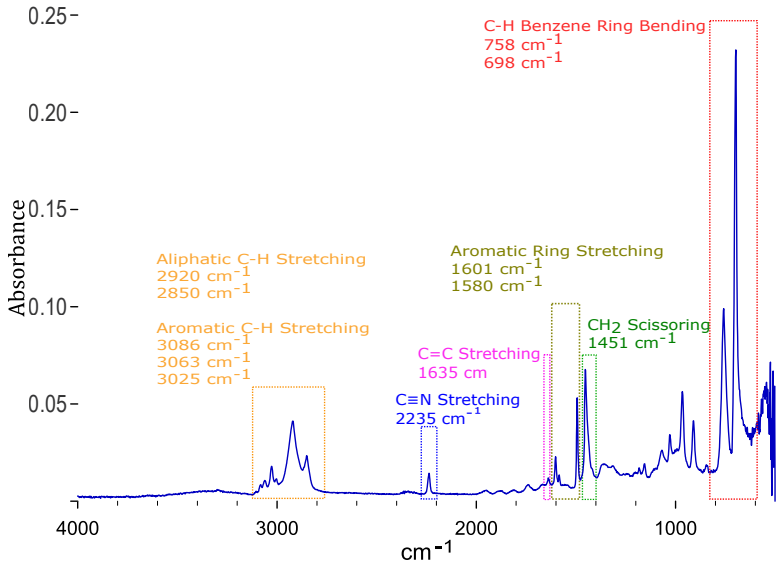

Figure 5.8 FTIR spectra of virgin ABS, with main peaks description.

the one reported for poly(isopropy1acrylate), or as decarboxylation step for the poly-acrylic acid. [190, 191] Acrylic acid reacts the ethylene glycol to form this compound. [192] Yet, decarboxylation seems the most plausible explanation as the FTIR spectra remains essentially the same.

Differential scanning calorimetry (DSC) detects changes in the glass transition temperature (T_g) and polymer thermodynamics (Table 5.2). [159] An increase of the T_g corresponds to an increased stability due to new inter-molecular bonds created by $-OH$ radicals form the denitrification and from the debrominated backbone of the BFRs. These radicals create hydrogen bonds between the radicals phenol groups, which in turn reduces the polymers enthalpy and thus increase the energy needed for the phase change. [159, 193]

We analyzed the following samples:

- ABS-FR: ABS from Lavergne feedstock (end-of-life plastic for recycle) who discarded due to its high Br content. Serial number (SN): MRG2900M-MPS2973-1-KP-05

- ABS-LV: Recycled ABS from Lavergne production. SN: S029-04-S4348 BTE 75

- ABS-DB-LV: 20 g ABS-FR from Lavergne treated with EG NaOH 2 M at 180 °C for 20 h (ABS-DB-LV03).

- ABS-5: (ABS-FR) treated with EG KOH 1 M at 180 °C for 4 h

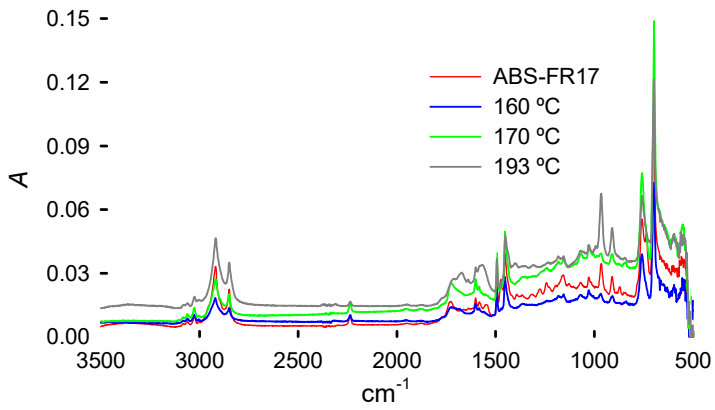

Figure 5.9 FTIR Spectra comparing the peak changes to the ABS after a treatment of 4 h at different temperatures. Table 5.1 shows the debromination ratio for each sample.

- ABS-12: (ABS-FR) treated with EG KOH 1 M 182 °C for 4 h

* ABS-5 and ABS-12 are batches from the same material, just different amount of polymer (1 g vs 50 g)

Table 5.2 DSC analysis of glass transition temperature (T_g) and bromine content for ABS samples, including untreated and treated variants.

Sample	T_g (°C)	Br (µg g^{-1})
ABS-Virgin [3]	103.0/105	0
ABS-FR	103.7	100000
ABS-LV	105.0	1881
ABS-DB-LV	112.5	252
ABS-5	113.9	8500
ABS-12	107.4	36000

Glass transition temperature vs. degree of conversion

As a first approach, we assume a linear relationship between T_g and the degree of conversion (α) derived from the relative intensities of the FTIR spectra.

$$T_g = T_{g,initial} + \alpha\,(T_{g,max} - T_{g,initial}) \tag{5.8}$$

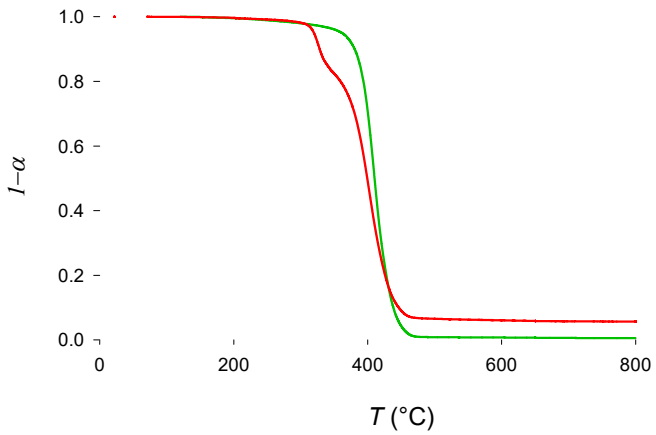

Figure 5.10 TGA thermograms from a sample of ABS virgin (green) and the ABS-FR (red) collected at the WEEE deposit of Polytechnique Montréal

Given:

$$T_{\mathrm{g,initial}} = 103.0\,^{\circ}\mathrm{C}, \quad T_{\mathrm{g,initial}} = 113.9\,^{\circ}\mathrm{C at} \alpha = 0.30 \tag{5.9}$$

Solving for $T_{\mathrm{g,max}}$:

$$113.9 = 103.0 + 0.30\,(T_{\mathrm{g,max}} - 103.0) \tag{5.10}$$

$$10.9 = 0.30\,(T_{\mathrm{g,max}} - 103.0) \tag{5.11}$$

$$T_{\mathrm{g,max}} = \frac{10.9}{0.30} + 103.0 \approx 139.3\,^{\circ}\mathrm{C} \tag{5.12}$$

To estimate the degree of conversion, once $T_{\mathrm{g,max}}$ is known, α for any measured T_{g} is:

$$\alpha = \frac{T_{\mathrm{g}} - T_{\mathrm{g,initial}}}{T_{\mathrm{g,max}} - T_{\mathrm{g,initial}}} \tag{5.13}$$

Example: For $T_{\mathrm{g}} = 112.5\,^{\circ}\mathrm{C}$ (ABS-12):

$$\alpha = \frac{107.4 - 103.0}{139.3 - 103.0} = \frac{4.4}{36.3} \approx 0.12 \tag{5.14}$$

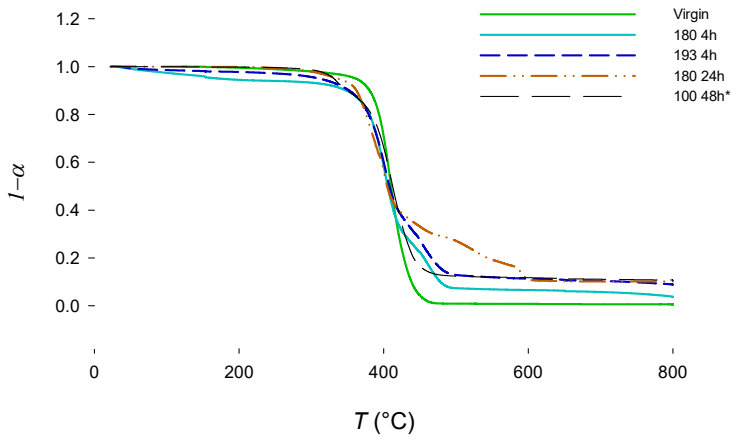

Figure 5.11 TGA results of different test to compare the ABS virgin, three representative treatments (with the highest debromination ratio) and a sample from a treatment of 24h at 100 °C proving that there is a lower threshold where denitrification does not occur. Unfortunately, debromination is limited as well.

Couchman's Equation

The glass transition temperature of a polymer mixture is given by [194]:

$$\ln T_{\mathrm{g}} = \frac{w_1 \Delta C_{p1} \ln T_{g1} + w_2 \Delta C_{p2} \ln T_{g2}}{w_1 \Delta C_{p1} + w_2 \Delta C_{p2}} \tag{5.15}$$

where:

- T_{g} is the glass transition temperature of the blend or modified polymer (in Kelvin),
- w_1 and w_2 are the mass fractions of the two components,
- ΔC_{p1} and ΔC_{p2} are the changes in specific heat capacity at T_{g1} and T_{g2},
- T_{g1} and T_{g2} are the glass transition temperatures of the pure components.

Table 5.3 shows the results of the linear extrapolation (from the DSC data) and the values obtained by Couchman's approach. The use of Couchman's expression is due to its general better fit to experimental data when studying polymers mixtures. [194, 195]

Both, the extrapolated T_{g} and that calculated from Couchman's expression begin to diverge at $\alpha > 0.6$,

Table 5.3 Glass transition temperatures (T_g) of modified ABS systems as a function of degree of conversion (α), estimated using Couchman's equation and linear extrapolation between 103.0 °C and 139.3 °C.

α	T_g Couchman °C	T_g Linear °C	ΔT_g °C
0.00	103.0	103.0	0.0
0.10	107.0	106.6	0.4
0.20	110.8	110.3	0.5
0.30	114.5	114.0	0.5
0.40	118.0	117.7	0.3
0.50	121.3	121.5	–0.2
0.60	124.4	125.2	–0.8
0.70	127.3	128.9	–1.6
0.80	130.0	132.6	–2.6
0.90	132.6	136.4	–3.8
1.00	135.0	139.3	–4.3

Table 5.4 T_g and chemical structure of related polymers [3]

Polymer	T_g (°C)	**Repeating Unit**
ASA (Poly(acrylonitrile-co-styrene-co-acrylate))	103–127	$[-CH_2-CH(CN)-]_x$ $[-CH_2-CH(Ph)-]_y$ $[-CH_2-CH(COOR)-]_z$
PAA (Poly(acrylic acid))	105 °C	$[-CH_2-CH(COOH)-]_n$
MABS (Poly(methyl methacrylate-co-acrylonitrile-co-butadiene-co-styrene))	107 °C	$[-CH_2-C(CH_3)(COOCH_3)-]_w$ $[-CH_2-CH(CN)-]_x$ $[-CH_2-CH=CH-CH_2-]_y$ $[-CH_2-CH(Ph)-]_z$
MBS (Poly(styrene-co-butadiene-co-methyl methacrylate))	−30 °C	$[-CH_2-CH(Ph)-]_x$ $[-CH_2-CH=CH-CH_2-]_y$ $[-CH_2-C(CH_3)(COOCH_3)-]_z$

GCMS

After treatment, the reaction media (EG) was analyzed using a GCMS to detect traces of by-products and/or solvent degradation. Due to the high pH of the solvent and the viscosity of the ethylene glycol the sample was diluted using acetone with prior its analysis. The GCMS detected only two peak corresponding to the acetone and ethylene glycol, with other minor components from column leaching (Figure 5.12)

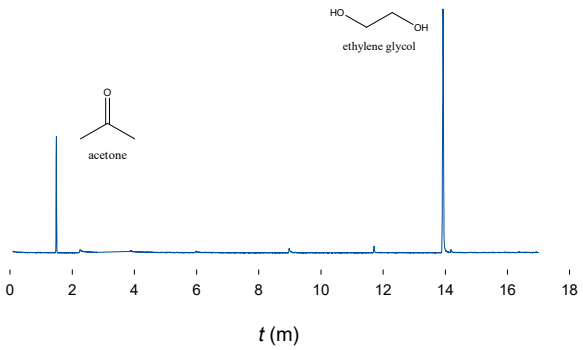

Figure 5.12 GCMS peaks of the solvent used for the debromination of ABS-7 (81 % debromination). Acetone was used to reduce viscosity and pH of the solution in order to protect the instrument's column.

These results indicate that the fire retardant backbone remains inside the polymer. However, when cleaning and trimming the GCMS column later the GCMS detected styrene residue. This is consistent with the observed breakage of the polymer in some tests. Although the concentration was very low, it is clear that some of the polymer chains crack.

5.5 Conclusions

A solvothermal treatment with ethylene glycol as a solvent and KOH as a reactant removes more than 95 % of the bromine content from commercial ABS. KOH denitrifies the acrylonitrile groups less than NaOH but denitrification reached 30 % in the most aggressive conditions ($T > 180\,°C$) Controlling reaction conditions—temperature and KOH concentration—limits the denitrification but requires longer reaction times 24 h to achieve the same debromination rate. Based on our previous experience treating high impact polystyrene, it is possible to

overcome the time limitation by increasing the surface contact, mainly by treating thin (up to 1 mm) filaments.

Even though the treatment induces denitrification of the ABS, this is not necessarily an undesirable outcome. We know that mechanical recycling, and all its related processes (grinding, extrusion etc. basically anything than does not imply a de-polymerization and re-polymerization) will damage a polymer's chain. The presence of the carboxyl groups, however, can improve the mechanical properties of the ABS, making it more resilient to mechanical recycling and thus demanding less virgin polymer down stream. Furthermore, the presence of these carboxyl groups could enhance the compatibility with other polymers and additives. Yet, it is important to control the level of denitrification to avoid losing the properties associated to the acrylonitrile group. Acrylonitrile-styrene-acrylate (ASA) is manufactured by grafting styrene acrylonitrile monomer (SAN) into butyl acrylate rubber cores. Thus, the polymeric chain is radically different to the one obtained by our process where the acrylonitrile is replaced by a acrylic acid group, implying that the different groups are in the same polymeric chain and not grafted onto it.

The process we report in this works demonstrate the possibility of removing bromine from ABS with a small denitrification. The absence of organic compounds on the solvent mean that the fire retardant backbone either stays on the polymer as an "additive" or is incorporated to its structure by cross-linking. Unfortunately, the nature of these backbone are similar to the polymers, and thus FTIR is of limited value to follow the progression of the reaction. The polymer thermal behaviour changes based on TGA and DCS, but are inconsequential as the the basic properties of the thermoplastic are the same or even improved. Further research on the mechanical aspects, compatibility and fine-tuning of the debromination vs denitrification are desirable to fully characterize the reaction and the process.

CHAPTER 6 CONCLUSION

6.1 General Discussion

The incorporation of brominated fire retardants in end-of-life polymers to comply with fire regulations limits the recyclability of EEE plastics due to new environmental regulations and health concerns. However, brominated polymers represent up to 20% of the EEE plastics released to the market. A process to remove these harmful BFRs from polymers, will increase plastic recycling objectives and open a significant feedstock that is currently out of reach.

Currently, there is a growing effort to find ways to access this feedstock, primarily through energy valorization. Additionally, there are some chemical recycling initiatives, but most of them are costly and difficult to implement in traditional recycling industries. The already difficult competition from virgin plastic resins (which are cheaper and chemically intact), means that any debromination process to be implemented industrially must be cost-effective and as simple as possible to be industrially feasible.

This PhD research project focuses on the development of an industrial process able to remove the brominated compounds from the plastics while keeping polymer properties acceptable for recycling. In addition, since this project is developed in an industrial partnership, keeping it within the interests and capabilities of our industrial partner is a requirement.

The first part involved finding an analytical method to effectively determine the bromine content within the plastics. While there are several techniques, such as inductively coupled plasma analysis (ICP), gas chromatography–mass spectrometry (GC–MS), or ion chromatography (IC), that can perform such a determination, they require access to the equipment, specific sample preparation, and sample destruction. We decided to use X-ray fluorescence, a tool already available industrially for screening and in the industrial setting. We demonstrated the capabilities of this technique for bromine determination, and we validated the results using neutron activation analysis (NAA), an instrument used to certify chemical standards. We proved that the XRF is a reliable tool and that our results are trustworthy, and at the same time, we provided the theoretical and experimental framework for this tool, with special focus on the plastic industry. The high energy (up to 50 keV) of XRF spectrometers, with the also high fluorescence energies of Br 11 to 13 keV and Sb 26 to 29 keV ensures an analysis depth of centimeters. Matrix effect and other constraints of these analytical methods are overcome either by the in-built software or with proper calibration and sample preparation.

After validating the XRF as an analytical tool for our research, we set a screening experimental design to study the solvothermal treatment as a tool to debrominated HIPS and ABS. We decided to focus on these two polymers since they are the two main components of WEEE plastics, and they share a styrenic base. The process was carried out in a batch reactor, treating commercial end-of-life HIPS and ABS. Ethylene glycol and triethylene glycol as solvents and reaction media. Sodium and potassium hydroxide were selected as alkali reagents. Volume, temperature, time, plastic dimensions, and alkali concentration as reaction conditions (variables). We initially demonstrate the solvothermal treatment successfully debrominated HIPS at temperatures of 190 °C and a reaction time of 24 h. We identified temperature and kinetic factors as major drivers for the reaction. Both parameters are, logically, correlated with higher temperatures improving the kinetics of the reaction. However, the shape and quantity (in a batch reactor) determined the reaction rate due to agglomeration effects (Figure 6.1).

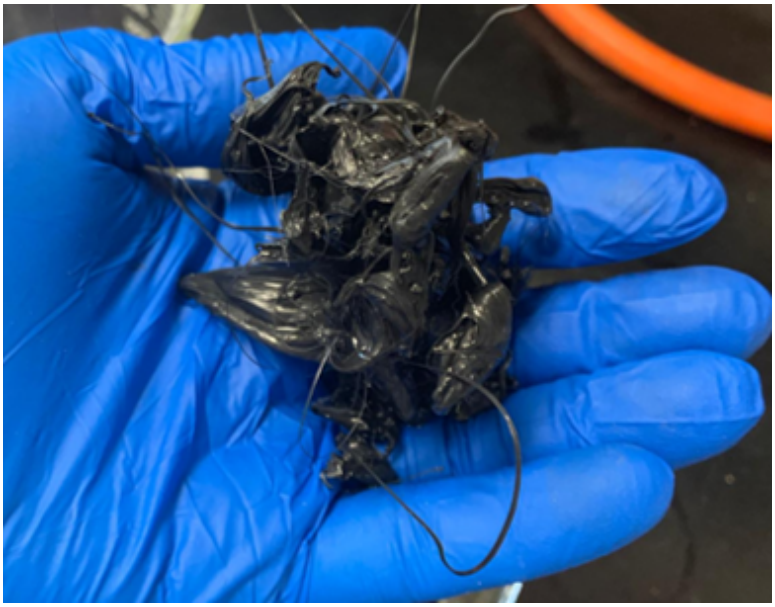

Figure 6.1 Agglomeration effect of large quantities. Due to the temperature, the polymer tends to agglomerate, forming agglomerates that make the kinetics difficult by reducing the surface contact with the solvent.

To increase the surface contact and improve the kinetics, we extruded the HIPS polymer into filament shape. With diameters of around 1 mm we achieved a debromination superior to 99% in less than 5 min at 190 °C. When studying the polymer properties to determine its internal integrity, we observed a change in FTIR spectra related to polybutadiene. While we did not find any organic compounds on the GC-MS studies of the solvent, this indicates that there are internal changes in the polybutadiene fraction that do not affect the thermal

properties of the polymer. Finally, we developed an initial kinetic model, based on our research and data obtaining that the reaction follows a power-law kinetics expression, in which temperature, polymer shape (chunks vs filaments), and time are the main parameters governing the reaction.

The third and last part consisted of studying the debromination performance and effects on ABS polymer (with the same batch reactor). Since ABS denitrification was a known possible side effect of this reaction, we decided to focus on mild conditions (Ethylene glycol, max temp of 190 °C and KOH instead NaOH due to its lower denitrification power). Debromination of 99% was achieved in 4 h at 190 °C and in 24 h at 160 °C. Based on the FTIR spectra, denitrification appears to remain at 30% regardless of the temperature. This is believed due to the limited chemically available nitrite groups of the polymer, while most of the groups could be protected by the rest of the polymeric matrix impeding its reaction with the alkali. The kinetic model for the ABS has a reduced number of variables compared with the one for HIPS. Followed a linear model where temperature and time were the main variables. It is, however, expected that the shape of the poly will affect the debromination rates. As the denitrification appears to be fairly constant we decided that there is no base for a kinetic modeling of this process and therefore to focus on debromination solely. In this case, the ABS undergoes significant internal changes affecting its thermal decomposition, showing this decomposition stage in the TGA spectra starting at approximately 450 °C. Additionally, we proved the denitrification effect and its substitution by a N-Acrylamide and acrylic acid increases the glass transition temperature, T_g (the higher the conversion to acrylic acid, the higher T_g).

6.2 Conclusion

As WEEE production continues to rise, while recovery and recycling lag behind, alternative solutions are needed. Mechanical recycling remains the primary method for processing plastic waste, when excluding energy recovery. However, the presence of brominated fire retardants in WEEE significantly limits its recyclability. A method capable of removing bromine, thereby enabling these plastics to undergo mechanical recycling without the challenges of chemical recycling, would be a groundbreaking development.

This PhD research aims to develop a sustainable and economical process that complements existing mechanical recycling methods. Initially, we established analytical methodologies and capabilities to ensure accurate and reliable measurements. We characterized the target polymers, Acrylonitrile Butadiene Styrene (ABS) and High Impact Polystyrene (HIPS), properties to detect any possible degradation and to determine their elemental composition. Our

findings demonstrated that XRF can accurately determine bromine concentrations, and our results are backed by alternative techniques such as neutron activation analysis, a technique that is used to certify analytical standards.

A solvothermal treatment with ethylene glycol (EG) and triethylene glycol (TEG) as media was coupled with KOH and NaOH as reagents. Our results prove that temperature and diffusion are the main variables affecting debromination. Ultimately, they are both interconnected, with higher temperatures incrementing diffusion coefficients, especially above the glass transition temperature of the polymer when interchain space and molecule freedom increase. We proved that the shape and size of the sample, logically, play a significant role in the kinetics. By converting the polymer (HIPS in this case) into filaments with diameters of less than 3 mm, we can achieve 99 % debromination in 2 min at 190 °C. For HIPS, we established that temperatures around 230 °C are the most effective to debrominate the plastic in a shorter time for pieces of about 1 mm^2, with agitation. These conditions removed 99.4% of the bromine in 240 min. For HIPS polymer, KOH and NaOH appear to be equally efficient. The alkali concentrations ranging from 0.5 to 2 M did not show any impact on the debromination performance, but we always kept it stoichiometrically rich compared with the Br present in the polymer, seeking to keep any possible equilibrium displaced towards debromination according to the principle of Le Chatelier.

Treating ABS presents other challenges than HIPS/PS. While the latter resists the treatment with only the polybutadiene fraction of HIPS being affected, an alkaline solvothermal treatment will attack the nitrile group, producing a denitrification. At 190 °C and 240 min we removed 98% of the bromine in the plastic. At 160 °C it required 1440 min to achieve a similar factor. KOH is preferred to NaOH due to its lower denitrification capabilities, while keeping the same debromination effect. This is likely due to the debromination mechanism, where the debromination is a reductive reaction with H from the glycolate salt and not a nucleophilic substitution reaction of Br by OH. These findings are supported by the fact that FTIR does not detect any clear peak for OH in the HIPS treatment. FTIR analysis of debrominated ABS in turn shows a peak for the acrylic group, proving that the OH will replace the N on the nitrile group in a two-step reaction. Finally, we detected that with harsh or longer treatment times, the TGA result show a tail when indicating a change in the internal polymeric structure. Our interpretation is that the debromination and denitrification induce the crosslinking and other reactions inducing a graphitization of some parts of the ABS during its thermal decomposition.

While denitrification of ABS is a non-desirable side effect, it might be an unexpected ally. Having a small percentage of carboxylic groups can enhance mechanochemical properties,

while keeping ABS- virgin properties. These groups can also protect this polymer from further degradation in the later mechanical reprocessing step.

We report the successful debromination of both ABS and HIPS end-of-life polymers with an alkaline solvothermal treatment. The treatment produced a limited impact in the ABS, via denitrification, but both polymers kept their main thermochemical properties largely unaltered. ABS treatment conditions must be mild to avoid larger denitrification and further polymer crosslinking (when this is undesirable). No by-products were detected in the solvent, only Br and Sb, suggesting that the BFR backbone remains inside the polymer, probably undergoing some crosslinking with the polymer chain.

6.3 Summary of Works

This PhD project aims to develop a new process to remove bromine from WEEE plastics, specifically ABS and HIPS.

With the interests of our industrial partner in mind, and after a thorough review of the state of the art in debromination processes, we selected a solvothermal treatment as the most promising alternative.

In the first step, we worked on the Br determination in the polymers. The analytical methods at our disposal were not very efficient or, due to the nature of the process selected, not adequate for the current setup of the equipment (GC-MS, HPLC, IC...). In collaboration with the Lavergne group, we were provided with an XRF Brucker S1 TITAN Handheld (later, we will get an EDXRF Epsylon4 from Malvern Panalytical, thanks to a grant we won to acquire such equipment, unique at Polytechnique and one of the few in Montreal) to analyze the bromine content. After receiving the proper training to legally use the instrument, we started working on the validation of this tool to accurately measure the bromine content. By using RoHS standards and a comparative analysis from the NAA, we ensured the results' trustworthiness. While these initial steps took place, we started collecting plastic pieces from Polytechnique's WEEE collection facility. The plastics were separated by type according to their resin code, and then analyzed with FTIR, TGA, DSC, and XRF to ensure the plastic type, initial characteristics, and bromine content. These parts without bromine were discarded or used in a side experiments, such as dissolution, separation, and purification.

After validating the reliability of our analytical equipment and establishing methods for XRF, FTIR, TGA, and DSC, we initiated debromination experiments. These experiments focused on treating HIPS (from 1-50 g) using ethylene glycol (EG) or triethylene glycol (TEG) combined with sodium hydroxide or potassium hydroxide as the debromination solute (extrac-

tant, 0.5 M to 2 M). Reactions were conducted in stirring flasks equipped with temperature control and a reflux column. In one instance, the flask was connected to an on-line mass spectrometer. The experimental design included variables such as reaction time (5 min, 4 h, 8 h, 12 h, and 24 h), temperature (160 °C to 230 °C), agitation (with or without), and pellet size to filament in order to identify key factors influencing reaction rates and process efficacy. We assumed uniform distribution of bromine throughout the polymer. Achieving the 230 °C set temperature proved challenging due to heat losses (this was challenging, especially for the high-temperature experiments, forcing us to develop techniques to maintain and control the temperature to ensure stable and repeatable conditions). While TEG's higher boiling point made it the preferred solvent, an equal number of experiments were conducted with NaOH and KOH. For the pellet size of the polymer, we used cut pieces of about 1 mm thickness with diferent sizes but keeping them around 3 mm^2. Some of the HIPS were extruded to obtain a filament of different diameters ranging from below 1 mm to 3 mm. These filaments were cut to a defined length and debrominated. After the debromination experiments, all the polymers were washed and analyzed again to find the bromination ratio and any possible change in the polymer's properties. Outside the lab, we developed two small Python programs to calculate diffusion parameters, activation energy from TGA data, and statistical analysis of the results (on SigmaPro).

The third phase of the project was to study the solvothermal debromination of ABS, a polymer that could be affected by denitrification under the conditions of the experiment. Once the polymer was analyzed, it was dried and stored for use in the debromination process. The reaction medium was ethylene glycol, and the debromination reactant was potassium hydroxide 1 $mg\,kg^{-1}$. EG has lower denitrification capabilities, and since we wanted to keep the temperature below 200 °C, the use of TEG was unnecessary. (Sodium hydroxide was also tested, but it showed a greater tendency to degrade the polymer properties and induced higher denitrification.) An experimental design was executed, comprising reaction time, t (from 1 min to 24 h), temperature, T (160-190 °C), and sample mass (from 1-50 g), to evaluate the kinetics and process efficacy. However, all the conditions applied to debrominate the samples are well-known aging factors. At the end of a test, the polymer was extracted and dried for at least 8 h at 40 °C to be further studied to determine the debromination ratio and its chemical integrity using TGA, DSC, and FTIR. Further work with the raw data from FTIR, TGA, and DSC data was used to determine changes in the ABS chains and denitrification levels. Finally, we performed a statistical analysis of the data. Parallel to the three main phases, we carried out several experiments to study possible improvements to the process. Although most of them were not successful enough to be incorporated into the main research findings, they did provide some insights.

- We built a microwave reactor to try to improve heating of the solvent media so the debromination could be more efficient. We did not succeed with it, despite the literature supporting this method. We also tried unsuccessfully a microwave-assisted debromination with solvents. A main cause might be the lack of power of the microwave to induce enough heat into an open system.

- We carried out dry and wet (using ethylene glycol and NaOH) debromination experiments in a planetary ball mill. We tried iron powder as a catalyst in an attempt to increase debromination. We could not reach any significant debromination from these experiments, but it is also to be noted that this ball mill is not adequate for this process, and more importantly, we tried with our standard plastic pieces without micronizing them prior to the experiment.

- Additionally, we experimented with low-toxicity solvents (mostly acetone and p-cymene) to attempt basic separations. While we tested several solvents and managed to study dissolving the polymers, we were unable to separate basic additives such as pigments. This indicates that solvent separation is more complex when working with polymeric matrices.

- We developed a direct extrusion system to heat up the filament just before the solvothermal treatment with the intention to drastically reduce the debromination times and in an attempt to use water rather than EG or TEG. This could not be completed due to the pandemic outbreak and changes within our technical support team. However, it sparked the declaration of invention attached to this thesis.

6.4 Limitations

The main limitation in its current experiment is the inability to treat large quantities of plastics. When adding large amounts and high temperatures, the plastics agglomerate, significantly reducing the surface area while increasing the diffusion depth, resulting in a dramatic reduction of the debromination. Additionally, another significant limitation is the already discussed denitrification of the ABS, which forces limitations on the conditions and could potentially limit the efficiency of the process.

6.5 Future Research

While the solvothermal debromination technique here proposed demonstrates to be an efficient debromination method, further research is recommendable. Here I propose some

research lines that I think I would like to pursue if I had the chance, and thus these are what I feel should be the future research:

- The diffusion mechanisms and boundaries of polymers in their glass transition temperature could result in a better understanding of the process, allowing for setting better conditions to achieve debromination more effectively and with lower impact on the polymer.
- Partnering with other teams carrying CFD simulations could potentially increase our knowledge of the internal mechanisms governing that pseudo-liquid phase of amorphous polymers.
- Further characterization of the solvent media during the reaction. Defining more precisely the alkali content of the reaction can potentially lead to an online reaction control through pH and conductivity monitoring. For that, it is needed to fully understand the reactions taking place between the alkali, solvent, polymer, and polymer's additives.
- Further research on microwave and mechanically assisted debromination. Regardless of our unsuccessful attempt, I still think that more efficient forms of conveying energy to the system could reduce reaction times and improve efficiency.
- A deep characterization of the debrominated ABS to completely understand what is happening within the polymeric chain, such as crosslinking, measuring a difference in van der Waals forces, hydrogen bonds, etc. This will help us to characterize the impact of the carboxylic groups on the polymer.
- A full study on mechanical and chemical resistance (to acids, bases, oxidative stress, etc.) properties of the polymers after debromination, with special focus on the ABS.

REFERENCES

[1] C. P. Baldé, R. Kuehr, T. Yamamoto, R. McDonald, E. D'Angelo, S. Althaf, G. Bel, O. Deubzer, E. Fernandez-Cubillo, V. Forti, V. Gray, S. Herat, S. Honda, G. Iattoni, D. S. Khetriwal, V. L. di Cortemiglia, Y. Lobuntsova, I. Nnorom, N. Pralat, and M. Wagner, "The global e-waste monitor 2024," Geneva/Bonn, 2024, fourth edition of the Global E-waste Monitor. [Online]. Available: https://ewastemonitor.info/wp-content/uploads/2024/03/GEM_2024_18-03_web_page_per_page_web.pdf

[2] P. Wäger, H. Böni, A. Buser, L. Morf, M. Schluep, and M. Streicher, "Recycling of plastics from waste electrical and electronic equipment (weee)—tentative results of a swiss study," *Proceedings of the R*, vol. 9, 2009.

[3] G. Wypych, *PS polystyrene*, 2nd ed. Toronto: ChemTec Publishing, 2016, pp. 560–566.

[4] "Regulation (eu) 2019/1021 of the european parliament and of the council of 20 june 2019 on persistent organic pollutants (recast)," https://eur-lex.europa.eu/legal-content/EN/TXT/?uri=CELEX:32019R1021, 2019, official Journal of the European Union, L 169, 25.6.2019, pp. 45–77.

[5] European Commission, "Waste statistics-electrical and electronic equipment, https://ec.europa.eu/eurostat/statistics-explained, accessed on 01/20/2024," 2024.

[6] G. Grause, J. D. Fonseca, H. Tanaka, T. Bhaskar, T. Kameda, and T. Yoshioka, "A novel process for the removal of bromine from styrene polymers containing brominated flame retardant," *Polymer Degradation and Stability*, vol. 112, pp. 86–93, 2015.

[7] N. Braidy, A. Béchu, J. C. de Souza Terra, and G. S. Patience, "Experimental methods in chemical engineering: Transmission electron microscopy—tem," *The Canadian Journal of Chemical Engineering*, vol. 98, no. 3, pp. 628–641, 2020.

[8] R. Klockenkämper and A. von Bohlen, "Worldwide distribution of total reflection x-ray fluorescence instrumentation and its different fields of application: A survey," *Spectrochimica Acta Part B: Atomic Spectroscopy*, vol. 99, pp. 133–137, 2014.

[9] N. J. van Eck, L. Waltman, R. Dekker, and J. van den Berg, "A comparison of two techniques for bibliometric mapping: Multidimensional scaling and vos," *Journal of the American Society for Information Science and Technology*, vol. 61, no. 12, pp. 2405–2416, 2010.

[10] Clarivate Analytics, "Web of Science™ Core Collection http://apps.webofknowledge.com (accessed: May 2024)," 2024.

[11] R. Geyer, J. R. Jambeck, and K. L. Law, "Production, uses, and fate of all plastics ever made," *Science Advanvances*, vol. 3, no. 7, p. 5, 2017.

[12] G. Martinho, A. Pires, L. Saaiva, and R. Ribeiro, "Composition of plastics from waste electrical and electronic equipment (weee) by direct sampling," *Waste Management*, vol. 32, no. 6, pp. 1213–1217, 2012.

[13] Clarivate Analytics, "Web of Science™ Core Collection http://apps.webofknowledge.com (accessed: March 2025)," 2025.

[14] A.-K. Du, Q. Zhou, Z.-B. Wen, J.-W. Yang, J. M. N. van Kasteren, and Y.-Z. Wang, "Denitrogenation of acrylonitrile–butadiene–styrene copolymers using polyethylene glycol/hydroxides," *Polymer Degradation and Stability*, vol. 96, no. 5, pp. 870–874, 2011.

[15] D. Feldman, "Polymer history," *Designed Monomers and Polymers*, vol. 11, no. 1, pp. 1–15, 2008.

[16] C. Cohen, "The early history of chemical engineering: a reassessment," *The British Journal for the History of Science*, vol. 29, no. 2, 1996.

[17] C. Richard, S. H. Thompson, C. J. Swan, C. J. Moore, and F. S. vom Saal, "Our plastic age," *Philosophical Transactions of the Royal Society B: Biological Sciences*, vol. 364, pp. 1973–1976, 2009.

[18] "Standard for flammability of plastic materials for parts in devices and appliances," Tech. Rep. UL 94, 2021.

[19] "Fire hazard testing – part 2–10: Glow-wire test and guidance," Tech. Rep. IEC 60695-2-10, 2020.

[20] "Fire hazard testing – part 2–12: Glow-wire flammability index (gwfi)," Tech. Rep. EN 60695-2-12 (ISO 1210), 2002.

[21] "Fire hazard testing – part 11–5: Test flames – 50 w horizontal and vertical methods," Tech. Rep. IEC 60695-11-5, 2014.

[22] "Tests on electric and optical fibre cables under fire conditions – part 1–2: Vertical flame propagation for single insulated wires or cables," Tech. Rep. IEC 60332-1-2, 2019.

[23] "Measurement of smoke density of materials used in electrical equipment – part 2: Test method and requirements," Tech. Rep. EN 61034-2, 2005.

[24] "Standard test method for rate of burning and/or extent and time of burning of plastics in a horizontal position," Tech. Rep. ASTM D635, 2018.

[25] Global Market Insights, Inc., "Bromine derivatives market size, share and forecast, 2024–2032," Industry report, 2024. [Online]. Available: https://www.gminsights.com/industry-analysis/bromine-flame-retardant-market

[26] R. Renner, "What fate for brominated fire retardants?" *Environmental Science & Technology*, vol. 34, no. 9, pp. 222A–226A, 2000.

[27] J. B. P. Soares, "Top 15 articles published in the cjce in 2024," *The Canadian Journal of Chemical Engineering*, vol. 103, no. 2, pp. 488–491, 2025.

[28] R. Porta, "Anthropocene, the plastic age and future perspectives," *FEBS Open Bio*, vol. 11, no. 4, pp. 948–953, 2021.

[29] A. Buekens and J. Yang, "Recycling of weee plastics: a review," *Journal of Material Cycles and Waste Management*, vol. 16, no. 3, pp. 415–434, 2014.

[30] E. Stenvall, S. Tostar, A. Boldizar, M. R. S. Foreman, and K. Möller, "An analysis of the composition and metal contamination of plastics from waste electrical and electronic equipment (weee)," *Waste Management*, vol. 33, no. 4, pp. 915–922, 2013.

[31] "Ti-Pure™ Titanium Dioxide (TiO2) by Chemours, Trusted Partner for Coatings, Plastics, Laminates and Paper," Product overview and applications page, The Chemours Company, 2025. [Online]. Available: https://www.tipure.com/en/

[32] H. Nawaz, M. Umar, R. Maryam, I. Nawaz, H. Razzaq, T. Malik, and X. Liu, "Polymer nanocomposites based on tio2 as a reinforcing agent: An overview," *Advanced Engineering Materials*, vol. 24, no. 11, p. 2200844, 2022.

[33] C. DeArmitt, "23 - functional fillers for plastics," in *Applied Plastics Engineering Handbook (Second Edition)*, second edition ed., ser. Plastics Design Library, M. Kutz, Ed. William Andrew Publishing, 2017, pp. 517–532.

[34] A. Alonso, M. Lázaro, D. Lázaro, and D. Alvear, "Thermal characterization of acrylonitrile butadiene styrene-abs obtained with different manufacturing processes," *Journal of Thermal Analysis and Calorimetry*, vol. 148, no. 20, pp. 10 557–10 572, 2023.

[35] A. Agirre, M. Aguirre, and J. R. Leiza, "Characterization of grafting properties of abs latexes: Atr-ftir vs nmr spectroscopy," *Polymer*, vol. 253, p. 124997, 2022.

[36] Z. Yu, Y. Li, Z. Zhao, C. Wang, J. Yang, C. Zhang, Z. Li, and Y. Wang, "Effect of rubber types on synthesis, morphology, and properties of abs resins," *Polymer Engineering and Science*, vol. 49, no. 11, pp. 2249–2256, 2009.

[37] G. Camino, L. Costa, and M. Luda di Cortemiglia, "Overview of fire retardant mechanisms," *Polymer Degradation and Stability*, vol. 3, no. 2, pp. 131–154, 1991.

[38] J. Green, "An overview of the fire retardant chemicals industry, past—present—future," *Fire and Materials*, vol. 19, no. 5, pp. 197–204, 1995.

[39] P. Das, Q. Zeng, A. Leybros, J.-C. P. Gabriel, C. Y. Tay, and J.-M. Lee, "Enhanced extraction of brominated flame retardants from e-waste plastics," *Chemical Engineering Journal*, vol. 469, p. 144126, 2023.

[40] M. L. di Cortemiglia, G. Camino, L. Costa, P. Roma, and A. Rossi, "Mechanism of action and pyrolysis of brominated fire retardants in acrylonitrile-butadiene-styrene polymers," *Journal of Analytical and Applied Pyrolysis*, vol. 11, pp. 511–526, 1987.

[41] J. Kaspersma, C. Doumen, S. Munro, and A.-M. Prins, "Fire retardant mechanism of aliphatic bromine compounds in polystyrene and polypropylene," *Polymer Degradation and Stability*, vol. 77, no. 2, pp. 325–331, 2002.

[42] E. Canada, "Risk management strategy for polybrominated diphenyl ethers (pbdes)," https://publications.gc.ca/collections/collection_2014/ec/En14-115-2010-eng.pdf, 2010, chemicals Sectors Directorate, Environmental Stewardship Branch, Final Revised: August 2010.

[43] P. Hennebert and M. Filella, "Weee plastic sorting for bromine essential to enforce eu regulation," *Waste Management*, vol. 71, pp. 390–399, 2018.

[44] M. Sharkey, M. A.-E. Abdallah, D. S. Drage, S. Harrad, and H. Berresheim, "Portable x-ray fluorescence for the detection of pop-bfrs in waste plastics," *Science of the Total Environment*, vol. 639, pp. 49–57, 2018.

[45] B. Beccagutti, L. Cafiero, M. Pietrantonio, S. Pucciarmati, R. Tuffi, and S. V. Ciprioti, "Characterization of some real mixed plastics from weee: A focus on chlorine and bromine determination by different analytical methods," *Sustainability*, vol. 8, no. 11, p. 1107, 2016.

[46] M. Sharkey, D. Drage, S. Harrad, W. Stubbings, A. H. Rosa, M. Coggins, and H. Berresheim, "Pop-bfrs in consumer products: Evolution of the efficacy of xrf screening for legislative compliance over a 5-year interval and future trends," *Science of the Total Environment*, vol. 853, p. 158614, 2022.

[47] C. Chaine, A. S. Hursthouse, A. Jandric, B. McLean, I. McLellan, B. McMahon, J. McNulty, J. Miller, S. Salhofer, and E. Viza, "Optimized industrial sorting of weee plastics: Development of fast and robust h-xrf technique for hazardous components," *Case Studies in Chemical and Environmental Engineering*, vol. 7, p. 100292, 2023.

[48] A. Aldrian, A. Ledersteger, and R. Pomberger, "Monitoring of weee plastics in regards to brominated flame retardants using handheld xrf," *Waste Management*, vol. 36, pp. 297–304, 2015.

[49] M. Schlummer, J. Vogelsang, D. Fiedler, L. Gruber, and G. Wolz, "Rapid identification of ps foam wastes containing hbcdd or its alternative polyfr by x-ray fluorescence spectroscopy (xrf)," *Waste Management and Research*, vol. 33, pp. 662–670, 2015.

[50] C. Gallen, A. Banks, S. Brandsma, C. Baduel, P. Thai, G. Eaglesham, A. Heffernan, P. Leonards, P. Bainton, and J. F. Mueller, "Towards development of a rapid and effective non-destructive testing strategy to identify brominated flame retardants in the plastics of consumer products," *Science of The Total Environment*, vol. 491-492, pp. 255–265, 2014, halogenated Persistent Organic Pollutants (Dioxin2013, Daegu/Korea).

[51] M. Blazsó, Z. Czégény, and C. Csoma, "Pyrolysis and debromination of flame retarded polymers of electronic scrap studied by analytical pyrolysis," *Journal of Analytical and Applied Pyrolysis*, vol. 64, no. 2, pp. 249–261, 2002.

[52] J. Scheirs and W. Kaminsky, *Feedstock recycling and pyrolysis of waste plastics*. Chichester, UK; Hoboken, NJ: J. Wiley & Sons, 2006.

[53] E. Jakab, M. Uddin, T. Bhaskar, and Y. Sakata, "Thermal decomposition of flame-retarded high-impact polystyrene," *Journal of Analytical and Applied Pyrolysis*, vol. 68–69, pp. 83–99, 2003, pyrolysis 2002 Conference issue.

[54] P. Shaohong, H. Yan, C. Lieqiang, X. Mingquan, H. Huajie, L. Chao, and L. Liubin, "Controlled pyrolysis of waste tv housing plastic added brominated flame retardants," in *2011 International Conference on Computer Distributed Control and Intelligent Environmental Monitoring*. IEEE, 2011, pp. 2023–2026.

[55] T. Bhaskar, T. Matsui, M. A. Uddin, J. Kaneko, A. Muto, and Y. Sakata, "Effect of sb2o3 in brominated heating impact polystyrene (hips-br) on thermal degradation and debromination by iron oxide carbon composite catalyst (fe-c)," *Applied Catalysis B: Environmental*, vol. 43, no. 3, pp. 229–241, 2003.

[56] T. Gamse and R. Marr, "Removal of flame retardants from electronic waste materials using supercritical co2-extraction," *Chemie Ingenieur Technik*, vol. 73, no. 6, pp. 590–590, 2001.

[57] J. Onwudili and P. Williams, "Degradation of brominated flame-retarded plastics (Br-ABS and Br-HIPS) in supercritical water," *Journal of Supercritical Fluids*, vol. 49, pp. 356–368, 2009.

[58] A. M. Altwaiq, M. Wolf, and R. V. Eldik, "Extraction of brominated flame retardants from polymeric waste material using different solvents and supercritical carbon dioxide," *Analytica Chimica Acta*, vol. 491, no. 1, pp. 111–123, 2003.

[59] F. Vilaplana, P. Karlsson, A. Ribes-Greus, P. Ivarsson, and S. Karlsson, "Analysis of brominated flame retardants in styrenic polymers: comparison of the extraction efficiency of ultrasonication, microwave-assisted extraction and pressurised liquid extraction," *Journal of Chromatography A*, vol. 1196, pp. 139–146, 2008.

[60] T. Bhaskar, A. Hosokawa, A. Muto, Y. Tsukahara, T. Yamauchi, and Y. Wada, "Enhanced debromination of brominated flame retardant plastics under microwave irradiation," *Green Chemistry*, vol. 10, no. 7, pp. 739–742, 2008.

[61] C.-C. Zhang and F.-S. Zhang, "Removal of brominated flame retardant from electrical and electronic waste plastic by solvothermal technique," *Journal of Hazardous Materials*, vol. 221, pp. 193–198, 2012.

[62] T. Kameda, Y. Fukuda, K.-S. Park, G. Grause, and T. Yoshioka, "Efficient dehalogenation of automobile shredder residue in naoh/ethylene glycol using a ball mill," *Chemosphere*, vol. 74, no. 2, pp. 287–292, 2009.

[63] H. Gilman, D. L. Esmay, and R. K. Ingham, "Aromatic reductive debromination with a glycol-alkali mixture," *Journal of the American Chemical Society*, vol. 73, no. 1, pp. 470–471, 1951.

[64] Q. Zhou, J. W. Yang, A. K. Du, Y. Z. Wang, and J. M. N. V. Kasteren, "Fuel oil from acrylonitrile-butadiene-styrene copolymers using a tandem peg-enhanced

denitrogenation-pyrolysis method," *AIChE Journal*, vol. 55, no. 12, pp. 3294–3297, 2009.

[65] A. B. Martins and R. M. C. Santana, "Effect of carboxylic acids as compatibilizer agent on mechanical properties of thermoplastic starch and polypropylene blends," *Carbohydrate Polymers*, vol. 135, pp. 79–85, 2016.

[66] T.-Y. Guo, J.-C. Liu, M.-D. Song, and B.-H. Zhang, "Effects of carboxyl group on the ambient self-crosslinkable polyacrylate latices," *Journal of Applied Polymer Science*, vol. 104, no. 6, pp. 3948–3953, 2007.

[67] C. Berti, V. Bonora, M. Colonna, N. Lotti, and L. Sisti, "Effect of carboxyl end groups content on the thermal and electrical properties of poly (propylene terephthalate)," *European Polymer Journal*, vol. 39, no. 8, pp. 1595–1601, 2003.

[68] A. W. Coats and J. P. Redfern, "Kinetic parameters from thermogravimetric data," *Nature*, vol. 201, no. 4914, pp. 68–69, 1964.

[69] S. Gopalakrishnan and R. Sujatha, "Comparative thermoanalytical studies of polyurethanes using coats-redfern, broido and horowitz-metzger methods," *Pelagia Research Library*, 2011.

[70] A. S. Panchbhai, "Wilhelm conrad röntgen and the discovery of x-rays: Revisited after centennial," *Journal of Indian Academy of Oral Medicine and Radiology*, vol. 27, no. 1, pp. 90–95, 2015.

[71] A. Iglesias-Juez, G. L. Chiarello, G. S. Patience, and M. O. Guerrero-Pérez, "Experimental methods in chemical engineering: X-ray absorption spectroscopy—xas, xanes, exafs," *The Canadian Journal of Chemical Engineering*, vol. 100, no. 1, pp. 3–22, 2022.

[72] J. Z. Buchwald and A. Warwick, *Histories of the Electron: The Birth of Microphysics*. MIT Press, 2004.

[73] I. W. Griffiths, "Jj thomson—the centenary of his discovery of the electron and of his invention of mass spectrometry," *Rapid Communications in Mass Spectrometry*, vol. 11, no. 1, pp. 2–16, 1997.

[74] C. G. Barkla, "Dublin philos. mag," *J. Sci*, vol. 22, p. 396, 1911.

[75] F. A. T. Furfari and J. E. Brittain, "History: William d. coolidge and ductile tungsten," *IEEE Industry Applications Magazine*, vol. 10, no. 5, pp. 9–10, 2004.

[76] R. G. Egdell and E. Bruton, "Henry moseley, x-ray spectroscopy and the periodic table," *Philosophical Transactions of the Royal Society A*, vol. 378, no. 2180, p. 20190302, 2020.

[77] H. G. J. Moseley and C. G. Darwin, "London, edinburgh, dublin philos. mag," *J. Sci*, vol. 26, no. 156, pp. 1024–1034, 1913.

[78] D. Coster and R. de L. Kronig, "New type of auger effect and its influence on the x-ray spectrum," *Physica*, vol. 2, no. 1–12, pp. 13–24, 1935.

[79] R. Glocker and H. Schreiber, "Quantitative röntgenspektralanalyse mit kalterregung des spektrums," *Annalen der Physik*, vol. 390, no. 8, pp. 1089–1102, 1928.

[80] J. Lefebvre, F. Galli, C. L. Bianchi, G. S. Patience, and D. C. Boffito, "Experimental methods in chemical engineering: X-ray photoelectron spectroscopy-xps," *The Canadian Journal of Chemical Engineering*, vol. 97, no. 10, pp. 2588–2593, 2019.

[81] H. Khan, A. S. Yerramilli, A. D'Oliveira, T. L. Alford, D. C. Boffito, and G. S. Patience, "Experimental methods in chemical engineering: X-ray diffraction spectroscopy—xrd," *The Canadian Journal of Chemical Engineering*, vol. 98, no. 6, pp. 1255–1266, 2020.

[82] M. O. Guerrero-Pérez and G. S. Patience, "Experimental methods in chemical engineering: Fourier transform infrared spectroscopy—ftir," *The Canadian Journal of Chemical Engineering*, vol. 98, no. 1, pp. 25–33, 2020.

[83] G. S. Patience, "Experimental methods in chemical engineering: Preface," *The Canadian Journal of Chemical Engineering*, vol. 96, no. 11, pp. 2312–2316, 2018.

[84] R. V. Murphy, H. Maharaj, J. Lachapelle, and P. K. Yuen, *Operator of Portable X-Ray Fluorescence Analyzers (XRF) Certification Information and Examination Preparation, 4th ed.* Nepean, Canada: Natural Canada Resources, 2017.

[85] A. M. W. Hunt, *The Oxford handbook of archaeological ceramic analysis*. Oxford University Press, 2017.

[86] J. H. Hubbell and S. M. Seltzer, "Tables of x-ray mass attenuation coefficients and mass energy-absorption coefficients 1 kev to 20 mev for elements z= 1 to 92 and 48 additional substances of dosimetric interest," National Inst. of Standards and Technology-PL, Gaithersburg, MD, Tech. Rep., 1995.

[87] B. Beckhoff, B. Kanngießer, N. Langhoff, R. Wedell, and H. Wolff, *Handbook of practical X-ray fluorescence analysis*. Springer Science & Business Media, 2007.

[88] H. Nikjoo *et al.*, "Auger electron transport calculations in biological matter," International Atomic Energy Agency, International Nuclear Data Committee ..., Tech. Rep., 2013.

[89] W. D. Coolidge, "X-ray tube," US Patent 1,946,312, 1934.

[90] K. Ono, T. Sakuma, and H. Takahashi, "X-ray tube," US Patent 4,730,353, 1988.

[91] D. S. Lee and T. C. T. Jr, "X-ray tube," US Patent 5,008,918, 1991.

[92] J. M. Boone, T. R. Fewell, and R. J. Jennings, "Molybdenum, rhodium, and tungsten anode spectral models using interpolating polynomials with application to mammography," *Medical Physics*, vol. 24, no. 12, pp. 1863–1874, 1997.

[93] A. Gupta, "Total reflection x-ray fluorescence spectroscopy working principles," *International Journal of Core Engineering and Management*, 2014.

[94] E. T. Puusaari, "Us patent 7,203,283," Patent, 2007.

[95] J. M. Guthrie and J. R. Ferguson, "Archaeometry laboratory at the university of missouri research reactor," https://archaeometry.missouri.edu/xrf_technical.html, 2012, accessed: April 2023.

[96] N. Broll, "Quantitative x-ray fluorescence analysis. theory and practice of the fundamental coefficient method," *X-Ray Spectrometry*, vol. 15, no. 4, pp. 271–285, 1986.

[97] M. West, A. T. Ellis, P. J. Potts, C. Streli, C. Vanhoof, and P. Wobrauschek, "2016 atomic spectrometry update–a review of advances in x-ray fluorescence spectrometry and its applications," *Journal of Analytical Atomic Spectrometry*, vol. 31, no. 9, pp. 1706–1755, 2016.

[98] V. Vaiano, M. Matarangolo, J. J. Murcia, H. Rojas, J. A. Navío, and M. C. Hidalgo, "Enhanced photocatalytic removal of phenol from aqueous solutions using zno modified with ag," *Applied Catalysis B: Environmental*, vol. 225, pp. 197–206, 2018.

[99] L. Zhao, Z. Zhang, Y. Li, X. Leng, T. Zhang, F. Yuan, X. Niu, and Y. Zhu, "Synthesis of Ce_aMnO_x hollow microsphere with hierarchical structure and its excellent catalytic performance for toluene combustion," *Applied Catalysis B: Environmental*, vol. 245, pp. 502–512, 2019.

[100] S. Khandaker, Y. Toyohara, G. C. Saha, M. R. Awual, and T. Kuba, "Development of synthetic zeolites from bio-slag for cesium adsorption: Kinetic, isotherm and thermodynamic studies," *Journal of Water Process Engineering*, vol. 33, p. 101055, 2020.

[101] Y. Liu, M. N. Banis, W. Xiao, R. Li, Z. Wang, K. R. Adair, S. Rousselot, P. Sauriol, M. Dollé, G. Liang *et al.*, "Visualization of the secondary phase in lifepo ingots with advanced mapping techniques," *The Canadian Journal of Chemical Engineering*, vol. 97, no. 8, pp. 2218–2223, 2019.

[102] L. Sun, X. Song, K. Li, C. Wang, X. Sun, P. Ning, and H. Huang, "Preparation of modified manganese slag slurry for removal of hydrogen sulphide and phosphine," *The Canadian Journal of Chemical Engineering*, vol. 98, no. 7, pp. 1534–1542, 2020.

[103] S. K. Utimura, S. J. Arevalo, C. G. A. Rosario, M. Q. Aguilar, J. A. S. Tenório, and D. C. R. Espinosa, "Bioleaching of metal from waste stream using a native strain of acidithiobacillus isolated from a coal mine drainage," *The Canadian Journal of Chemical Engineering*, vol. 97, no. 11, pp. 2920–2927, 2019.

[104] P. F. Nascimento, J. F. Sousa, J. A. Oliveira, R. D. Possa, L. S. Santos, F. C. Carvalho, J. A. Ruiz, M. M. Pedroza, and M. B. Bezerra, "Wood sawdust and sewage sludge pyrolysis chars for co2 adsorption using a magnetic suspension balance," *The Canadian Journal of Chemical Engineering*, vol. 95, no. 11, pp. 2148–2155, 2017.

[105] Q. Lian, Z. U. Ahmad, D. D. Gang, M. E. Zappi, D. L. B. Fortela, and R. Hernandez, "The effects of carbon disulfide driven functionalization on graphene oxide for enhanced pb (ii) adsorption: Investigation of adsorption mechanism," *Chemosphere*, vol. 248, p. 126078, 2020.

[106] Z. Liu, B. Deng, Q. Li, Y. Jin, Z. Liang, H. Yang, and M. Zhang, "Research on the mechanism of bed agglomeration and superheater fouling in cfb boiler fired pure petroleum coke," *The Canadian Journal of Chemical Engineering*, vol. 101, no. 5, pp. 2526–2536, 2023.

[107] C. Sheng, C. Duan, Y. Zhao, C. Zhou, and Y. Zhang, "Simulation and experimental research on coarse coal slime particles' separation in inclined tapered diameter separation bed," *The Canadian Journal of Chemical Engineering*, vol. 95, no. 11, pp. 2129–2141, 2017.

[108] L. Jia, P. Cheng, Y. Yu, S. hu Chen, C. xing Wang, L. He, H. tian Nie, J. cheng Wang, J. chun Zhang, and B. guo Fan, "Regeneration mechanism of a novel high-performance biochar mercury adsorbent directionally modified by multimetal multilayer loading," *Journal of Environmental Management*, vol. 326, p. 116790, 2023.

[109] A. Pitarch and I. Queralt, "Energy dispersive x-ray fluorescence analysis of ancient coins: The case of greek silver drachmae from the emporion site in spain," *Nuclear Instruments and Methods in Physics Research Section B: Beam Interactions with Materials and Atoms*, vol. 268, no. 10, pp. 1682–1685, 2010.

[110] A. Marucco, "Low-energy ed-xrf spectrometry application in gold assaying," *Nuclear Instruments and Methods in Physics Research Section B: Beam Interactions with Materials and Atoms*, vol. 213, pp. 486–490, 2004.

[111] I. Queralt, M. Ovejero, M. L. Carvalho, A. F. Marques, and J. M. Llabrés, "Quantitative determination of essential and trace element content of medicinal plants and their infusions by xrf and icp techniques," *X-Ray Spectrometry: An International Journal*, vol. 34, no. 3, pp. 213–217, 2005.

[112] K. G. McIntosh, D. Guimarães, M. J. Cusack, A. Vershinin, Z. W. Chen, K. Yang, and P. J. Parsons, "Evaluation of portable xrf instrumentation for assessing potential environmental exposure to toxic elements," *International Journal of Environmental Analytical Chemistry*, vol. 96, no. 1, pp. 15–37, 2016.

[113] A. G. Caporale, P. Adamo, F. Capozzi, G. Langella, F. Terribile, and S. Vingiani, "Monitoring metal pollution in soils using portable-xrf and conventional laboratory-based techniques: Evaluation of the performance and limitations according to metal properties and sources," *Science of the Total Environment*, vol. 643, pp. 516–526, 2018.

[114] M. S. Shackley, *X-ray fluorescence spectrometry (XRF) in geoarchaeology*. Springer Science and Business Media, 2010.

[115] E. I. Obiajunwa, D. A. Pelemo, S. A. Owolabi, M. K. Fasasi, and F. O. Johnson-Fatokun, "Characterisation of heavy metal pollutants of soils and sediments around a crude-oil production terminal using edxrf," *Nuclear Instruments and Methods in Physics Research Section B: Beam Interactions with Materials and Atoms*, vol. 194, no. 1, pp. 61–64, 2002.

[116] D. Bazin, E. Foy, S. Reguer, S. Rouzière, B. Fayard, H. Colboc, J.-P. Haymann, M. Daudon, and C. Mocuta, "The crucial contribution of x-ray fluorescence spectroscopy in medicine," *Comptes Rendus. Chimie*, vol. 25, no. S1, pp. 165–188, 2022.

[117] J. Hasikova, A. Sokolov, V. Titov, and A. Dirba, "On-line xrf analysis of phosphate materials at various stages of processing," *Procedia Engineering*, vol. 83, pp. 455–461, 2014.

[118] M. S. Shackley, "X-ray fluorescence (xrf): Applications in archaeology," in *Encyclopedia of global archaeology*. Springer, 2018, pp. 1–7.

[119] A. Kuczumow, Z. Rzączyńska, and M. Szewczak, "Matrix effects in the x-ray fluorescence method," *X-Ray Spectrometry*, vol. 11, no. 3, pp. 135–139, 1982.

[120] K. Norrish and B. W. Chappell, "X-ray fluorescence spectrometry," in *Physical Methods in Determinative Mineralogy*, J. Zussman, Ed. New York: Academic Press, 1977, pp. 201–272.

[121] A. Karathanasis and B. Hajek, "Elemental analysis by x-ray fluorescence spectroscopy," *Methods of Soil Analysis: Part 3 Chemical Methods*, vol. 5, pp. 161–223, 1996.

[122] M. Wang, Y. Gu, H. Lu, L. Ge, Q. Zhang, and G. Zeng, "Matrix effect correction method based on the main spectral parameters for rock samples in an in situ energy dispersive x-ray fluorescence analysis," *Spectrochimica Acta Part B: Atomic Spectroscopy*, vol. 193, p. 106438, 2022.

[123] B. L. Drake and B. L. MacDonald, *Advances in portable X-ray Fluorescence spectrometry: instrumentation, application and interpretation*. Royal Society of Chemistry, 2022.

[124] L. N. Rand, "Phd thesis," Ph.D. dissertation, Colorado School of Mines, Arthur Lakes Library (Illinois, CO), 2019.

[125] N. K. Aylikci, O. Oruc, E. Bahceci, A. Kahoul, T. Depci, and V. Aylikci, "Preparation of sample for x-ray fluorescence analysis," *X-Ray Fluorescence in Biological Sciences: Principles, Instrumentation, and Applications*, pp. 91–113, 2022.

[126] M. Nečemer, P. Kump, and M. Žvanut, "Application of energy dispersive x-ray fluorescence spectrometry for the characterization of plastic materials in synthetic polymer conservation work," *X-Ray Spectrometry*, vol. 41, no. 2, pp. 87–92, 2012.

[127] A. Otsuki, P. P. Gonçalves, C. Stieghorst, and Z. Révay, "Non-destructive characterization of mechanically processed waste printed circuit boards: X-ray fluorescence spectroscopy and prompt gamma activation analysis," *Journal of Composites Science*, vol. 3, no. 2, p. 54, 2019.

[128] A. N. Kadachi and M. A. Al-Eshaikh, "Limits of detection in xrf spectroscopy," *X-Ray Spectrometry*, vol. 41, no. 5, pp. 350–354, 2012.

[129] L. S. Birnbaum and D. F. Staskal, "Brominated flame retardants: cause for concern?" *Environmental health perspectives*, vol. 112, no. 1, pp. 9–17, 2004.

[130] U. E. P. Agency, "Toxic substances control act (tsca) chemical substance inventory: Revised inventory notice," https://www.epa.gov/tsca-inventory/abouttsca-chemical-substance-inventory, 2021, accessed: July 2021.

[131] S. of California Department of Toxic Substances Control, "Priority product work plan: 2018–2020," https://dtsc.ca.gov/wp-content/uploads/sites/31/2018/10/Final_2018-2020_Priority_Product_Work_Plan.pdf, 2017, accessed: July 2023.

[132] D. of Health and A. Care, "Decabromodiphenylethane regulatory action," https://www.industrialchemicals.gov.au/news-andnotices/decabromodiphenylethane-regulatoryaction, 2023, accessed: July 2023.

[133] ——, "Decabromodiphenylethane (decabde) and perfluorooctanoic acid (pfoa)-related compounds: Authorisation required," https://www.industrialchemicals.gov.au/news-andnotices/decabde-and-pfoa-related-compoundsauthorisation-required-21-july-2023, 2023, accessed: July 2023.

[134] C. P. Baldé, V. Forti, V. Gray, R. Kuehr, and P. Stegmann, *The Global E-waste Monitor 2017*. Bonn: United Nations University (UNU), International Telecommunication Union (ITU) & International Solid Waste Association (ISWA), 2017.

[135] M. A. Charitopoulou, K. G. Kalogiannis, A. A. Lappas, and D. S. Achilias, "Novel trends in the thermo-chemical recycling of plastics from weee containing brominated flame retardants," *Environmental Science and Pollution Research*, vol. 28, no. 42, pp. 59 190–59 213, 2021.

[136] G. Bonifazi, L. Fiore, C. Pelosi, and S. Serranti, "Evaluation of plastic packaging waste degradation in seawater and simulated solar radiation by spectroscopic techniques," *Polymer Degradation and Stability*, vol. 207, p. 110215, 2023.

[137] M. L. Hardy, "Regulatory status and environmental properties of brominated flame retardants undergoing risk assessment in the eu: Dbdpo, obdpo, pebdpo and hbcd," *Polymer Degradation and Stability*, vol. 64, no. 3, pp. 545–556, 1999.

[138] P. N. Breysse, "Toxicological profile for polybrominated biphenyls," Agency for Toxic Substances and Disease Registry (US), Atlanta, GA, Tech. Rep., 2004.

[139] L. Tange and D. Drohmann, "Waste electrical and electronic equipment plastics with brominated flame retardants — from legislation to separate treatment - thermal processes," *Polymer Degradation and Stability*, vol. 88, no. 1, pp. 35–40, 2005.

[140] S. Molyneux, A. A. Stec, and T. R. Hull, "The effect of gas phase flame retardants on fire effluent toxicity," *Polymer Degradation and Stability*, vol. 106, pp. 36–46, 2014.

[141] C. Ma, J. Yu, B. Wang, Z. Song, J. Xiang, S. Hu, S. Su, and L. Sun, "Chemical recycling of brominated flame retarded plastics from e-waste for clean fuels production: A review," *Renewable and Sustainable Energy Reviews*, vol. 61, pp. 433–450, 2016.

[142] A. Marongiu, G. Bozzano, M. Dente, E. Ranzi, and T. Faravelli, "Detailed kinetic modeling of pyrolysis of tetrabromobisphenol a," *Journal of Analytical and Applied Pyrolysis*, vol. 80, pp. 325–345, 2007.

[143] P. T. Williams and E. Slaney, "Analysis of products from the pyrolysis and liquefaction of single plastics and waste plastic mixtures," *Resources, Conservation and Recycling*, vol. 51, no. 4, pp. 754–769, 2007.

[144] M. Blazsó and Z. Czégény, "Catalytic destruction of brominated aromatic compounds studied in a catalyst microbed coupled to gas chromatography/mass spectrometry," *Journal of Chromatography A*, vol. 1130, no. 1, pp. 91–96, 2006.

[145] Y. Shen, R. Zhao, J. Wang, X. Chen, X. Ge, and M. Chen, "Waste-to-energy: Dehalogenation of plastic-containing wastes," *Waste Management*, vol. 49, pp. 287–303, 2016.

[146] X. Yang, L. Sun, J. Xiang, S. Hu, and S. Su, "Pyrolysis and dehalogenation of plastics from waste electrical and electronic equipment (weee): A review," *Waste Management*, vol. 33, no. 2, pp. 462–473, 2013.

[147] M. Brebu, E. Jakab, and Y. Sakata, "Effect of flame retardants and Sb_2O_3 synergist on the thermal decomposition of high-impact polystyrene and on its debromination by ammonia treatment," *Journal of Analytical and Applied Pyrolysis*, vol. 79, no. 1–2, pp. 346–352, 2007.

[148] A. Grand and C. Wilkie, *Fire Retardancy of Polymeric Materials*. Boca Raton, Florida: CRC Press, 2000.

[149] M. Menéndez, J. Herguido, A. Bérard, and G. S. Patience, "Experimental methods in chemical engineering: Reactors—fluidized beds," *The Canadian Journal of Chemical Engineering*, vol. 97, no. 9, pp. 2383–2394, 2019.

[150] M. F. Gonzalez, N. Saadatkhah, and G. S. Patience, "Experimental methods in chemical engineering: X-ray fluorescence—xrf," *The Canadian Journal of Chemical Engineering*, vol. 102, no. 6, pp. 2004–2018, 2024.

[151] N. Saadatkhah, A. C. Garcia, S. Ackermann, P. Leclerc, M. Latifi, S. Samih, G. S. Patience, and J. Chaouki, "Experimental methods in chemical engineering: Thermogravimetric analysis—tga," *The Canadian Journal of Chemical Engineering*, vol. 98, no. 1, pp. 34–43, 2020.

[152] M. Alghamdi, M. A.-E. Abdallah, and S. Harrad, "The utility of x-ray fluorescence spectrometry as a tool for monitoring compliance with limits on concentrations of halogenated flame retardants in waste polymers: A critical review," *Emerging Contaminants*, vol. 8, pp. 9–20, 2022.

[153] A. Turner and K. R. Solman, "Analysis of the elemental composition of marine litter by field-portable-xrf," *Talanta*, vol. 159, pp. 262–271, 2016.

[154] A. Vesel, R. Zaplotnik, G. Primc, and M. Mozetič, "Evolution of surface functional groups and aromatic ring degradation upon treatment of polystyrene with hydroxyl radicals," *Polymer Degradation and Stability*, vol. 218, p. 110582, 2023.

[155] Y. Wang, C. Zou, Y. Ding, L. Duan, A. Zhou, S. Sun, and Y. Lu, "The mechanism of the influence of radiation heat flux on the combustion behavior of raw rubbers," *Polymer Degradation and Stability*, vol. 224, p. 110748, 2024.

[156] K. Antoš and J. Sedlář, "Influence of brominated flame retardant thermal decomposition products on hals," *Polymer Degradation and Stability*, vol. 90, no. 1, pp. 188–194, 2005.

[157] K. Bensalem, M. Eesaee, M. Hassanipour, S. Elkoun, E. David, K. Agbossou, and P. Nguyen-Tri, "Lifetime estimation models and degradation mechanisms of elastomeric materials: A critical review," *Polymer Degradation and Stability*, vol. 220, p. 110644, 2024.

[158] L. Wang, W. Cheng, X. Yang, R. Wang, R. Liu, Y. Zhu, Y. Yi, Y. Tang, and Z. Wang, "An atomic insight into reaction pathways and temperature effects in the degradation of polyethylene, polypropylene and polystyrene," *Polymer Degradation and Stability*, vol. 215, p. 110450, 2023.

[159] J.-P. Harvey, N. Saadatkhah, G. Dumont-Vandewinkel, S. L. G. Ackermann, and G. S. Patience, "Experimental methods in chemical engineering: Differential scanning

calorimetry—dsc," *The Canadian Journal of Chemical Engineering*, vol. 96, no. 12, pp. 2518–2525, 2018.

[160] J. P. Siregar, M. S. Salit, M. Z. A. Rahman, and K. Dahlan, "Thermogravimetric analysis (tga) and differential scanning calometric (dsc) analysis of pineapple leaf fibre (palf) reinforced high impact polystyrene (hips) composites," *Pertanika J Sci Technol*, vol. 1, no. 1, pp. 161–170, 2011.

[161] M. J. Turk, A. S. Ansari, W. B. Alston, G. S. Gahn, A. A. Frimer, and D. A. Scheiman, "Evaluation of the thermal oxidative stability of polyimides via tga techniques," *Journal of Polymer Science Part A: Polymer Chemistry*, vol. 37, no. 21, pp. 3943–3956, 1999.

[162] F. Sinfrônio, J. Santos, L. Pereira, A. Souza, M. C. ao, V. Jr, and V. M. Fonseca, "Kinetic of thermal degradation of low-density and high-density polyethylene by non-isothermal thermogravimetry," *Journal of Thermal Analysis and Calorimetry*, vol. 79, pp. 393–399, 2005.

[163] J. Brandsch, P. Mercea, and O. Piringer, *Modeling of Additive Diffusion Coefficients in Polyolefins*. Washington: American Chemical Society, 2000, ch. 4, pp. 27–36.

[164] J.-M. Petit, B. Roux, X. X. Zhu, and P. M. Macdonald, "A new physical model for the diffusion of solvents and solute probes in polymer solutions," *Macromolecules*, vol. 29, no. 18, pp. 6031–6036, 1996.

[165] A. Gupta, N. Kumar, and A. Sachdeva, "Factors affecting the ageing of polymer composite: A state of art," *Polymer Degradation and Stability*, vol. 221, p. 110670, 2024.

[166] "The circular economy for plastics – a european analysis 2024," 2024, accessed: 2025-02-25. [Online]. Available: https://plasticseurope.org/knowledge-hub/the-circular-economy-for-plastics-a-european-analysis-2024/

[167] Environment and C. C. Canada, *Economic Study of the Canadian Plastic Industry, Markets and Waste*. Gatineau, QC: Environment and Climate Change Canada, 2019.

[168] B. Plastics, "Chemical recycling: A dangerous deception," 2023, accessed: 2025-03-05. [Online]. Available: https://www.beyondplastics.org/publications/chemical-recycling

[169] M. Alaee, P. Arias, A. Sjödin, and Åke Bergman, "An overview of commercially used brominated flame retardants, their applications, their use patterns in different countries/regions and possible modes of release," *Environment International*, vol. 9, no. 6, pp. 683–689, 2003.

[170] G. F. Fries and R. D. Kimbrough, "The pbb episode in michigan: an overall appraisal," *CRC Critical Reviews in Toxicology*, vol. 16, no. 2, pp. 105–156, 1985.

[171] D. Yoffe, R. Frim, S. D. Ukeles, M. J. Dagani, H. J. Barda, T. J. Benya, and D. C. Sanders, *Bromine Compounds*. John Wiley & Sons, Ltd, 2013, pp. 1–31.

[172] M. F. Gonzalez, F. C. Gac, and G. S. Patience, "Alkaline solvothermal debromination of commercial brominated polystyrene," *Recycling*, vol. 10, no. 3, 2025.

[173] P. Arias, "Brominated flame retardants—an overview," in *Second International Workshop on Brominated Flame Retardants*, 2001, pp. 14–16.

[174] D. S. Achilias, M.-A. Charitopoulou, and S. V. Ciprioti, "Thermal and catalytic recycling of plastics from waste electrical and electronic equipment—challenges and perspectives," *Polymers*, vol. 16, no. 17, 2024.

[175] L. E. Peisino, A. L. Cappelletti, M. G. Gómez, R. Gaggino, B. B. Raggiotti, and J. R. Kreiker, "Recycled aggregates based on plastic waste from weee," in *Recycled Aggregates: Materials and Uses*, G. Saini, Ed. Nova Science Publishers, 2021.

[176] E. Maris, P. Botané, P. Wavrer, and D. Froelich, "Characterizing plastics originating from weee: A case study in france," *Minerals Engineering*, vol. 76, pp. 28–37, 2015, sustainable Minerals.

[177] V. Lahtela, H. Hamod, and T. Kärki, "Assessment of critical factors in waste electrical and electronic equipment (weee) plastics on the recyclability: A case study in finland," *Science of The Total Environment*, vol. 830, p. 155627, 2022.

[178] S. V. den Eynde, S. Waumans, T. Dimas, D. J. Díaz-Romero, I. Zaplana, and J. Peeters, "Evaluating the effectiveness of density-based sorting of plastics from weee and elvs," *Resources, Conservation and Recycling*, vol. 209, p. 107753, 2024.

[179] B. Xiaojuan, D. Isaac, and K. Smith, "Reprocessing acrylonitrile–butadiene–styrene plastics: Structure–property relationships," *Polymer Engineering and Science*, vol. 47, no. 2, pp. 120–130, 2007.

[180] M. Rahimi, M. Esfahanian, and M. Moradi, "Effect of reprocessing on shrinkage and mechanical properties of abs and investigating the proper blend of virgin and recycled abs in injection molding," *Journal of Materials Processing Technology*, vol. 214, no. 11, pp. 2359–2365, 2014.

[181] J. M. Pérez, J. L. Vilas, J. M. Laza, J. L. Abad, and L. M. León, "Effect of reprocessing and accelerated weathering on abs properties," *Journal of Polymers and the Environment*, vol. 18, pp. 71–78, 2010.

[182] R. Scaffaro, L. Botta, and G. D. Benedetto, "Physical properties of virgin-recycled abs blends: Effect of post-consumer content and of reprocessing cycles," *European Polymer Journal*, vol. 48, no. 3, pp. 637–648, 2012.

[183] X. Bai, P. Liang, M. Zhang, K. Song, Y. Li, D. Xu, and C. Hu, "Effects of reprocessing on acrylonitrile–butadiene–styrene and additives," *Journal of Polymers and the Environment*, vol. 30, pp. 1803–1819, 2022.

[184] E. N. Zil'berman, "The reactions of nitrile-containing polymers," *Russian Chemical Reviews*, vol. 55, no. 1, p. 39, 1986.

[185] W. Camacho and S. Karlsson, "NIR, DSC, and FTIR as quantitative methods for compositional analysis of blends of polymers obtained from recycled mixed plastic waste," *Polymer Engineering and Science*, vol. 41, no. 9, pp. 1626–1635, 2001.

[186] P. Patel, T. R. Hull, R. W. McCabe, D. Flath, J. Grasmeder, and M. Percy, "Mechanism of thermal decomposition of poly(ether ether ketone) (peek) from a review of decomposition studies," *Polymer Degradation and Stability*, vol. 95, no. 5, pp. 709–718, 2010.

[187] K. Kumeta, I. Nagashima, S. Matsui, and K. Mizoguchi, "Crosslinking reaction of poly(vinyl alcohol) with poly(acrylic acid) (paa) by heat treatment: Effect of neutralization of paa," *Journal of Applied Polymer Science*, vol. 90, no. 9, pp. 2420–2427, 2003.

[188] J. Santiago-Morales, G. Amariei, P. Letón, and R. Rosal, "Antimicrobial activity of poly(vinyl alcohol)-poly(acrylic acid) electrospun nanofibers," *Colloids and Surfaces B: Biointerfaces*, vol. 146, pp. 144–151, 2016.

[189] A. Gestos, P. G. Whitten, G. M. Spinks, and G. G. Wallace, "Crosslinking neat ultrathin films and nanofibres of ph-responsive poly(acrylic acid) by uv radiation," *Soft Matter*, vol. 6, pp. 1045–1052, 2010.

[190] N. Grassie and J. G. Speakman, "Thermal degradation of poly(alkyl acrylates). i. preliminary investigations," *Journal of Polymer Science Part A-1: Polymer Chemistry*, vol. 9, no. 4, pp. 919–929, 1971.

[191] M. Kumari, B. Gupta, and S. Ikram, "Characterization of n-isopropyl acrylamide/acrylic acid grafted polypropylene nonwoven fabric developed by radiation-induced graft polymerization," *Radiation Physics and Chemistry*, vol. 81, no. 11, pp. 1729–1735, 2012.

[192] C. Alkan, E. Günther, S. Hiebler, and M. Himpel, "Complexing blends of polyacrylic acid-polyethylene glycol and poly(ethylene-co-acrylic acid)-polyethylene glycol as shape stabilized phase change materials," *Energy Conversion and Management*, vol. 64, pp. 364–370, 2012, iREC 2011 The International Renewable Energy Congress.

[193] P. C. Painter, J. F. Graf, and M. M. Coleman, "Effect of hydrogen bonding on the enthalpy of mixing and the composition dependence of the glass transition temperature in polymer blends," *Macromolecules*, vol. 24, no. 20, pp. 5630–5638, Sep 1991.

[194] J. P. Pascault and R. J. J. Williams, "Relationships between glass transition temperature and conversion," *Polymer Bulletin*, vol. 24, no. 1, pp. 115–121, 1990.

[195] E. J. Mayhew, C. H. Neal, S.-Y. Lee, and S. J. Schmidt, "Glass transition prediction strategies based on the couchman-karasz equation in model confectionary systems," *Journal of Food Engineering*, vol. 214, pp. 287–302, 2017.

APPENDIX A DECLARATION OF INVENTION

USAGE OF BRCDT ONLY
Contact at BRCDT :
Contact at Univalor :
Contact inventor :
Date of 1st version :

REPORT OF INVENTION

DIV-1061

VAL# if applicable–

POLYTECHNIQUE MONTRÉAL
TECHNOLOGICAL UNIVERSITY

La This Report of Invention (ROI) is filed at the Office of Research (Bureau de la recherche et Centre de développement technologique (BRCDT)) as stated in the *Politique de propriété intellectuelle technologique («IP Policy»)* of École Polytechnique de Montréal. This ROI presents Research Results made by one or more researchers (solely or collectively referred as the «Inventors») of École Polytechnique, as defined in the IP Policy, who identify these results to be, but not limited to, a new technology, a new method of process, a new product or expertise, or any other innovative technology («Invention»).

Section A. Title of the Invention and key words (in English and in French)

Continuous process to remove bromine from styrenic thermoplastics (ABS and HIPS) *Debromination, HIPS, ABS, WEEE*
Procédé continu pour éliminer le brome des thermoplastiques styrènes (ABS et HIPS) *Débromation, HIPS, ABS, DEEE*

Section B. Summary

Please provide a **brief** description of the invention. Exhaustive description must be added in Appendix A.

Here I present a process and a technique to debrominate styrenic polymers. The process used a modification of an extrusion process to create the media for a chemical debromination, polymer and bromine recovery in a continuous operation.
All the consumables (polymer, solvent, reagent, and polymer) can be recovered and/or replaced in continuous ensuring a smooth operation.

Section C. Type of invention

Software ☐ Apparatus ☒ Product ☐ Process ☒ Methodology ☐

Other (description) _____

Section D: Publications and public disclosures

This Invention has been or will be published (as theses, scientific articles, presentations, poster sessions, private presentation, courses, conferences, or any other written or oral presentation) at these specific dates and places.

-
-
-
-
-

A copy of the publications, a bibliography and list of other disclosures, if any, are presented in Appendix D.

Section E1: Inventor(s)

*The term «**Inventor**» is defined by a person who has a significant inventorship over the Invention disclosed in this Form. For more clarity, the «**Inventor**» must have contributed in the definitive and practical proof of concept of the ideas sustaining this Invention. A person who has merely contributed as a financial provider or an adviser is not considered an **Inventor**.*
***The Inventor** has to write his personal address at the date of signature of this Form.*
***The name and addresses of Employers are the ones at the time of Research.*

INVENTORSHIP (TOTAL 100%)

Name :	MARIO	Surname :	FERREIRO GONZALEZ	90%
Address* :	Avenida de Europa 17, Portal 5, 1-1			
Citizenship :	Spanish	Tél (rés) :	+34647664239	
Employer**:	Polytechnique Montreal / Lavergne Group INC			
Département/Research Group :	Chemical Engineering			
Email :		Position :	PhD Candidate	
Tél (Off) :		Fax :		

Name :	GREGORY S.	Surname :	PATIENCE	10%
Address* :				
Citizenship :	Canadian	Tél (rés) :		
Employer**:	5567 Woodbury Ave Montreal, H3T 1S6			
Département/Research Group :	Chemical Engineering			
Email :	gregory-s.patience@polymtl.ca	Position :	Professor	
Tél (Off) :		Fax :		

Name :		Surname :		
Address* :				
Citizenship :		Tél (rés) :		
Employer**:				
Département/Research Group :				
Email :		Position :		
Tél (Off) :		Fax :		

Name :		Surname :		
Address* :				
Citizenship :		Tél (rés) :		
Employer**:				
Département/Research Group :				
Email :		Position :		
Tél (Off) :		Fax :		

Name :		Surname :		
Address* :				
Citizenship :		Tél (rés) :		
Employer**:				
Département/Research Group :				
Email :		Position :		
Tél (Off) :		Fax :		

Section E2 : Inventorship (for Sofware Source code only)

*The term «**Author**» is defined as someone who has participated in the writing of part or whole source code sustaining the Invention as described in this Form. An **author** can also be an **Inventor** and/or a **Collaborator**.*
***The Author** has to write his personal address at the date of signature of this Form.*
***The name and addresses of Employers are the ones at the time of Research.*

Name :		Surname :		***AUTHORSHIP (TOTAL 100%)***
Address* :				
Citizenship :		Tél (rés) :		
Employer**:				
Département/Research Group :				
Email :		Position :		
Tél (Off) :		Fax :		

Name :		Surname :		
Address* :				
Citizenship :		Tél (rés) :		
Employer**:				
Département/Research Group :				
Email :		Position :		
Tél (Off) :		Fax :		

Name :		Surname :		
Address* :				
Citizenship :		Tél (rés) :		
Employer**:				
Département/Research Group :				
Email :		Position :		
Tél (Off) :		Fax :		

Name :		Surname :		
Address* :				
Citizenship :		Tél (rés) :		
Employer**:				
Département/Research Group :				
Email :		Position :		
Tél (Off) :		Fax :		

Section E3 : Collaborators

*The term «**Collaborator**» is defined as the person who has contributed in the testing, validation, and/or implementation of the Invention described in this Form.*
***The Collaborator** has to write his personal address at the date of signature of this Form.*
***The name and addresses of Employers are the ones at the time of Research.*

Name:		Surname		Email :	
Address* :					
Employer**:					
Département/Research Group :					
Tél (bur) :		Fax :		Position :	
Details of the collaboration :					

Name:		Surname		Email :	
Address* :					
Employer**:					
Département/Research Group :					
Tél (bur) :		Fax :		Position :	
Details of the collaboration :					

Name:		Surname		Email :	
Address* :					
Employer**:					
Département/Research Group :					
Tél (bur) :		Fax :		Position :	
Details of the collaboration :					

Name:		Surname		Email :	
Address* :					
Employer**:					
Département/Research Group :					
Tél (bur) :		Fax :		Position :	
Details of the collaboration :					

Section E : Funding

Section E-1 : SOURCES OF FUNDING :

Grants, research Agreements or donations having contributed to the financing of this Invention (dates, sums, partners)

Polytechnique Montreal and Lavergne Group INC from September 2017 to May 2019

Polytechnique Montreal and Lavergne Group INC through a MITACS from May 2019 to December 2021
Sum of (120 000.00)

Section E-2 : INTELLECTUAL PROPERTY RIGHTS :

Polytechnique's and Third Party rights on the Invention:

Lavergne Group

SECTION E-3 : AGREEMENT INVOLVING THE INVENTION :

Please list all R&D agreements, service agreements, Confidentiality agreement and other agreement that involve to the Invention in whole or in part:

MITACS Accelerate Grant

Section F : Patents

A patent protection has been or will be filed for this invention:

Type of filing		Country		Date		# Appl.	
Application Name			Assignee				
Type of filing		Country		Date		# Appl.	
Application Name			Assignee				
Type of filing		Country		Date		# Appl.	
Application Name			Assignee				

INVENTOR'S DECLARATION

We, the Inventors and Authors, hereby acknowledge and warranty that we are the sole inventors and Authors of the above described Invention and that the information contained hereinafter, including information provided in all appendixes and attachments, is true and precise, and represents to the best of our knowledge, the complete information pertinent to the Invention.

We, the Inventors and Authors, herby agree that our names with the title of the Invention can be made available to École Polytechnique's scientific Community.

Name :	*Mario Ferreiro Gonzalez*		
Place	*Madrid*	Date	*20/03/2025*

Name:	*Gregory S Patience*		
Place	*Montreal*	Date	*20/03/2025*

Name:			
Place:		Date	

Name:			
Place:		Date	

Name:			
Place:		Date	

Name:			
Place:		Date	

APPENDIX A
COMPLETE DESCRIPTION OF INVENTION

Containing at least the following elements:

1. **Summary of Innovation (around 5 lines)**
   Continuous process to remove bromine from styrenic polymers (mainly HIPS and ABS). The invention uses a modified extrusion system to perform a chemical process to remove bromine without damaging the polymer. A system to recover in bromine in continuous is also implemented.

2. **Context of discovery and prior art**
   Brominated fire retardant is an increased environmental and health concern due to its toxicity and persistence. There are few debromination procedures, mostly at laboratory scale (pyrolysis, hydrothermal extraction…).
   Here we use our research to develop an industrial process that can remove bromine while keeping polymer properties, that it is economical feasible and easily scalable.

3. **Current research within the field of application of the Invention**
   The basic knowledge about the processes is described on our research and on the literature. However, there is not yet an industrial-ready solution other than a company that claims to be able to do it by solvolysis.

4. **Detailed description of Invention (important aspects, novel and original elements, etc …)**
   The process consists of introducing the pelletized polymer into a pseudo extrusion system where the polymer will enter in contact with an alkaline solution of ethylene glycol or triethylene glycol. This process will heat up the polymer (and solution) at a classical working temperature during the extrusion of thermoplastics (above glass transition temperature – below decomposition temperature). During this process the pellets first, and the filament after, will be in contact with the circulating solution, that thanks to the temperature and the high contact surface given by the filament size, will induce the debromination reaction in times of around 5 minutes. The solution is continuously filtered by a ion exchange membrane to recover inorganic bromine that can be recovered and valorized afterward.
   The exiting filament would undergo a drying process to remove the remaining solvent and recovered as filament, to be pelletized afterwards as it is done at the industry.
   This approach is new to the problem of brominated fire retardants. It represents a feasible solution, use mostly known equipment by any polymer recycling company and does not require the use of toxic or very hazardous chemicals. The only hazards are the temperature and the alkali salts (KOH or NaOH). Both the salts and the solvent are well known chemicals, inexpensive and widely used.

5. **Date et place of first proof of concept**
   There is small prove of concept by performing the debromination of filament pellets at the lab but the process it is only in a design stage.

6. **Advantages et limits of Invention over existing technology**

This process offers a continuous solution to remove brominated fire-retardant form styrene polymers from WEEE. It used a accessible equipment and reagents require low adaptation for traditional mechanical recycling companies. It could also externalize part of the process such as bromine recovery and solvent purification and removal. Thus, it does not require the installation of a full chemical facility, and it could be done using a moderate space. It uses nonhazardous chemicals

And it can be easily scaled.

As limitations, this process (so far) only serves to remove the brominated fire retardants from the styrenic polymers. We know thar some of the antimony trioxide is removed partially with the solvent but not as the bromine. Other additives and colorants remain on the polymer.

Another limitation is that when HIPS is treated most of the polybutadiene is degraded meaning that you get polystyrene rather than high impact polystyrene which might imply the need to add it again to the polymer.

7. **Stage of development of Invention (prototypes, demonstrations, tests, ongoing research, improvements, etc) : dates and places**

   The invention is ready to be tested on a pilot plant but there are no dates on it yet.

8. **Cited References (including known patents)**

APPENDIX B
GENERAL PURPOSE AND COMMERCIAL APPLICATIONS

Including but not limited to:

1. Possible commercial Application(s)

To remove BFR from styrenic polymers allowing a large feedstock of unrecyclable polymers to be recycled.
Reducing landfilling of polymers.

2. Possible commercial benefits

Allowing the use of a large feedstock currently unavailable to recycling companies due to the banned BFR presence.
It could improve the position and of the company due to its unique situation at the market.

3. Marketing approaches undertaken (including established contacts)

Collaboration with Lavergne Group as they would be the main beneficiaries.

4. Contact information of third parties presently or probably interested in marketing the invention.

N/A

5. Recommendations and suggestions regarding the commercial exploitation of the invention.
It would be important to create a pilot plant to prove the concept and to define the processing parameters.

APPENDIX C

CONFIDENTIALITY AGREEMENT AND ASSIGNMENT UNDERTAKING

IN CONSIDERATION of the present Report of Invention filed on this day by :

Mario Ferreiro Gonzalez

(hereinafter referred to as «Inventors» and «Authors»),

and related to the research and development work performed by themselves related to the technology referred as « ***Continuous process to remove bromine from styrenic thermoplastics (ABS and HIPS)*** » (hereinafter referred to as the « **Invention** »), The Corporation de l'École Polytechnique de Montréal (« **POLYTECHNIQUE** ») and Polyvalor, *société en commandite* ("**POLYVALOR**"), acting through its general partner Univalor Inc. (« **UNIVALOR** ») are authorized to evaluate or have evaluate some and all information regarding this Invention as agreed with all Parties.

The Inventors and Authors agree to communicate to POLYTECHNIQUE and UNIVALOR all the information related to the Invention required for its evaluation and commercialization, and all information related to the invention that POLYTECHNIQUE or UNIVALOR should require from time to time.

Aiming towards an optimal commercialization process, the Inventors and Authors agree, for a **period of (2) two years,** to maintain the Invention and all related information confidential, and not to transfer to third parties, all or in part, in any form, information related to the Invention without the written consent of POLYTECHNIQUE and UNIVALOR.

Should a public disclosure be required (scientific publication, symposium presentation, etc.), the inventors undertake to inform, as soon as possible, POLYTECHNIQUE (through the BRCDT) and UNIVALOR to initiate the necessary the intellectual property protection, such as the filing of a patent application.

If the invention results from NSERC's funding in whole or in part, a maximum (6) six month confidentiality period is applicable to comply with NSERC's Intellectual Property Policy.

POLYTECHNIQUE and UNIVALOR hereby agree, for a **period of (2) two years**, to use the received information for the sole purposes of evaluating the Invention and acting on a commercialization strategy in accordance with all the parties.

This information will not be used by POLYTECHNIQUE or UNIVALOR, or the Inventor and Author, with such matter that may negatively affect the commercial exploitation of the Invention, or UNIVALOR's rights or interests, its successors and assigns, or POLYTECHNIQUE, or the Inventors or any third party having rights or interests in or to this information.

However, the requirements of confidentiality shall not apply to information which:

a) Was already in the public domain or becomes publicly available through no breach of this Agreement by POLYTECHNIQUE or UNIVALOR;
b) Was lawfully received without any restriction on use or disclosure from a third party free to disclose such information to POLYTECHNIQUE or UNIVALOR; or,
c) Was in POLYTECHNIQUE or UNIVALOR's possession at the time of disclosure by the Inventors as shown by written evidence.

Assignment and collaboration undertaking. The Inventors and Authors hereby undertake to cooperate with POLYTECHNIQUE and POLYVALOR in order to enforce any right, any required assignment or any necessary measure to protect the assigned Invention or enforce any commercialization agreement involving the said intellectual Property.

IN WITNESS WHEREOF, the Inventors and Authors have executed this Agreement in the place and date indicated below.

Name Mario Ferreiro Gonzalez	Date	Name	Date
Name	Date	Name	Date
Name	Date	Name	Date

LA CORPORATION DE L'ÉCOLE POLYTECHNIQUE DE MONTRÉAL

Place *Montreal* Date

By *Olivier Grenier*
Director – Office of Research (BRCDT)

POLYVALOR, LIMITED PARTNERSHIP
Acting through its general partner **UNIVALOR INC.**, itself, herein acting through its general partner **UNIVALOR INC.**

Place *Montréal* Date

By *Jacques Simoneau, ing. PhD*
President and Managing Director

APPENDIX D

PUBLICATIONS AND PUBLIC DISCLOSURES (including draft)

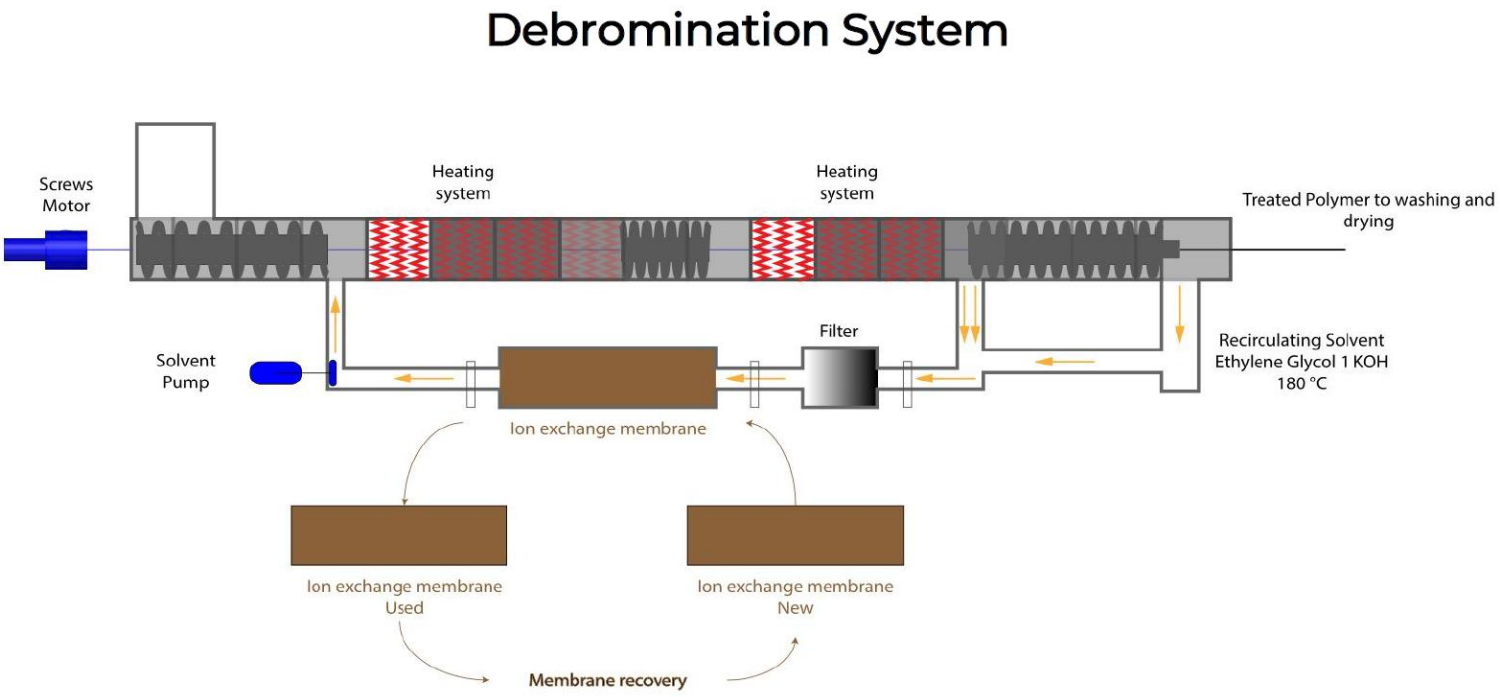

APPENDIX B A PROPOSED TREATMENT SYSTEM DEVELOPED FOR MECHANOCHEMICAL TREATMENT.

Debromination Plant Flow Chart

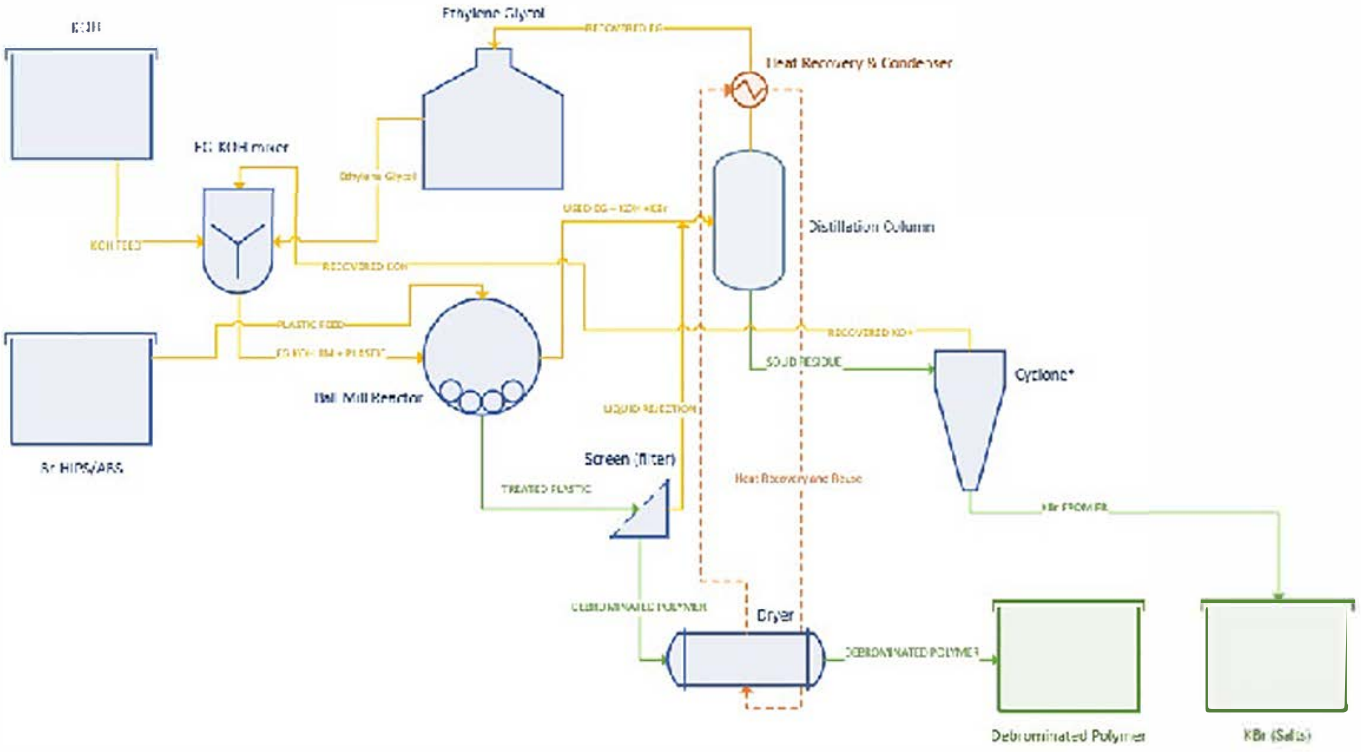

APPENDIX C A PROPOSED PRE-TREATMENT SYSTEM TO TREAT PC/ABS BLENDS.

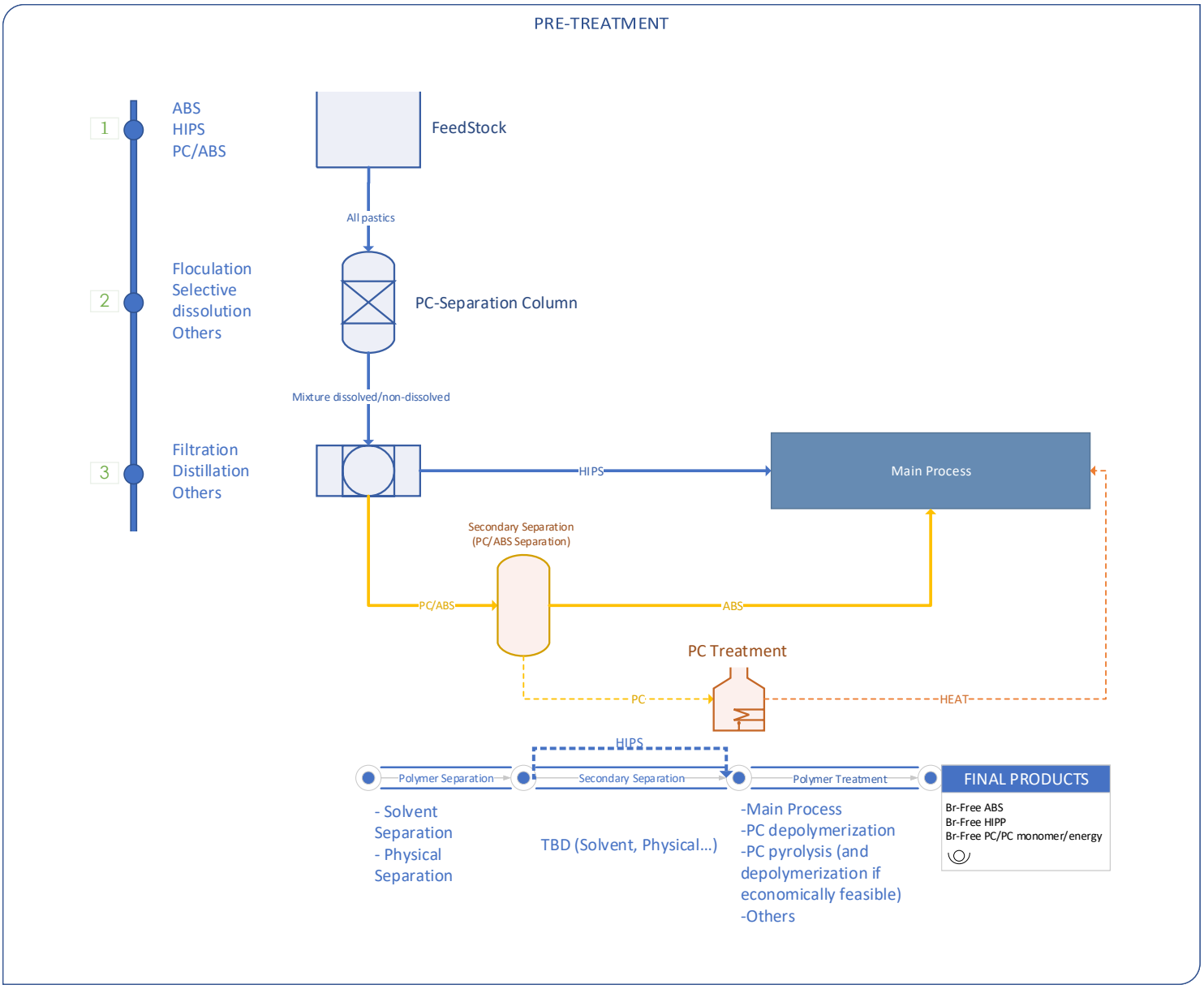
PRE-TREATMENT
1
ABS
HIPS
PC/ABS
FeedStock
All pastics
2
Floculation
Selective
dissolution
Others
PC-Separation Column
Mixture dissolved/non-dissolved
3
Filtration
Distillation
Others
HIPS
Main Process
Secondary Separation
(PC/ABS Separation)
PC/ABS
ABS
PC Treatment
PC
HEAT
HIPS
Polymer Separation
Secondary Separation
Polymer Treatment
FINAL PRODUCTS
Br-Free ABS
Br-Free HIPP
Br-Free PC/PC monomer/energy
- Solvent
Separation
- Physical
Separation
TBD (Solvent, Physical...)
-Main Process
-PC depolymerization
-PC pyrolysis (and
depolymerization if
economically feasible)
-Others